MICROFABRICATED PALLADIUM-BASED MEMBRANES FOR HYDROGEN SEPARATION

Tong Duy Hien

graduation committee

Chairman:
Prof. dr. W.H.M. Zijm

Secretary:

Prof. dr. W.H.M. Zijm	University of Twente
Promotors:	
Prof. dr. M.C. Elwenspoek	University of Twente
Prof. dr. ir. J.T.F. Keurentjes	University Eindhoven
Assistant promotor:	
Dr. ir. H.V. Jansen	University of Twente
Members:	
Prof. dr.ir. P. Enoksson	Chalmers University, Sweden
Prof. dr. J.C. Lodder	University of Twente
Prof. dr. ir. D.H.A. Blank	University of Twente
Dr. ir. J.G.E. Gardeniers	University of Twente
Dr. ir. C.J.M. van Rijn	Aquamarijn Microfiltarion B.V.

Acknowledgments

The research in this thesis was carried out at the group Transducers Science and Technology of the MESA$^+$ Research Institute at the University of Twente, Enschede, The Netherlands. This work was funded by the Dutch Technology Foundation (STW) under the project EST.4863.

Title: Microfabricated Palladium-based membranes for hydrogen separation
Author: Tong Duy Hien
Keywords: Microfabication, Palladium membrane, Hydrogen separation

ISBN90-365-2058-4.
Printed in the Netherlands

MICROFABRICATED PALLADIUM-BASED MEMBRANES FOR HYDROGEN SEPARATION

DISSERTATION

to obtain
the doctor's degree at the University of Twente,
on the authority of the rector magnificus,
prof. dr. F.A. van Vught,
on account of the decision of the Graduation Committee,
to be publicly defended
on Friday, June 4th 2004, at 16:45

by

Tong Duy Hien
born on January 30th, 1973
in Thai Binh, Vietnam

This doctoral dissertation is approved by promotors:

Prof. dr. M.C. Elwenspoek
Prof. dr. ir. J.T.F. Keurentjes

and assistant promoter

Dr. ir. H.V. Jansen

To my parents,
my brother and sister,
to Nhu and Quynh Anh

Contents

Chapter 1

Introduction

1.1. General introduction on palladium-based membranes

First investigations of the hydrogen absorption and diffusion through palladium (Pd) were carried out by Graham in 1866 [1]. Since then the Pd-based membranes have been studied extensively, especially in the last decade, due largely to their unique properties for applications involving hydrogen [2-38]. For example, Pd has very high hydrogen solubility, it absorbs 600 to 900 times its volume at room temperature, and its various alloys absorb comparable quantities [2,10]. This high solubility couples with its high diffusivity for hydrogen. Furthermore, Pd is chemical inert with oxygen at elevated temperature. These facts make that Pd has an unmatched potential in hydrogen-selective membranes for separation and purification, or as membrane reactors for (de) hydrogenation reactions [2-38].

The permeation of hydrogen through Pd involves several steps in series [2-3, 9-12]. These are, in order from the high partial pressure side to the low partial pressure side (Figure1.1);

1. molecular transport from the bulk gas to the gas layer adjacent to the surface,
2. dissociative adsorption onto the surface,
3. transition of atomic H from the surface into the bulk metal,
4. atomic diffusion through the bulk metal,
5. transition from the bulk metal to the surface on the low partial pressure side,
6. recombinative desorption from the surface, and
7. gas transport away from the surface to the bulk gas.

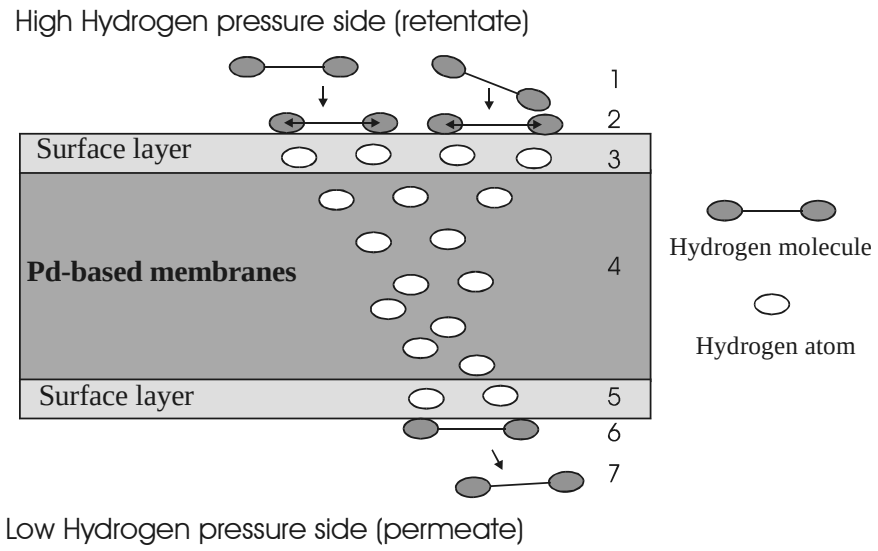

***Figure 1.1**: A mechanism of H_2 permeation through Pd-based films.*

The overall observed rate of permeation may be limited by one step if it is much slower than the others, or it may be governed by a combination of steps. Generally, to obtain high hydrogen separation flux, the Pd membranes are desired to be as thin as possible to speed up the diffusion step (step 1.4), while a clean membrane surface helps to speed up surface reactions (steps 1.2 and 1.6).

The use of pure Pd membranes, however, suffers from a transition from the α-phase (hydrogen-poor) to the β-phase (hydrogen-rich) at temperatures below 300 ^{o}C and pressures below 20 bars, which depends on the hydrogen concentration in the metal [3,6,9-11]. Since the lattice constant of the β-phase is 3% larger than that of the α-phase this transition leads to lattice strain and, consequently, after a few cycles to a distortion of the metal lattice, i.e. embrittlement. Alloying the Pd with Group 1b metals, especially with silver (Ag), reduces the problem of embrittlement and leads to an increase of the hydrogen permeability [3,6,9-11]. It has been explained that the increased resistance to embrittlement with face centered cubic lattice (f.c.c) alloys is attributed to the low diffusivity and high solubility of hydrogen in these alloys compared to f.c.c structured Pd [18,35]. In addition, alloying with several elements improves the chemical stability of the Pd membranes. Pure Pd

membranes are sensitive towards sulfur and chlorine, and also the chemical stability towards CO might be problematic. It has been reported that a CO concentration of only 0.2 vol-% gives a significant reduction in hydrogen flux [36,37]. The poisoning effects of gases, however, depend largely on the type of alloy, and can therefore be limited by choosing the right type of alloy for a specific gas mixture [26,27,34,38]. For instance Pd-Cu membrane is reported to have a high resistance against sulphur containing gases [26,27,34]. Among its alloys, Pd77-Ag23 at wt% has been the most commonly used, as it posses both high hydrogen permeation and high resistance to hydrogen embrittlement [9-11].

1.2. Current and future applications of hydrogen

Hydrogen has been extensively used in many industrial sectors e.g., petroleum refining, petrochemical and semiconductor, industrial material processing, and fuel cell [39-48]. The current hydrogen industry is not focused on the production or use of hydrogen as an energy carrier or a fuel for energy generation. Rather, for instance in the US hydrogen industry, the nine million tons of hydrogen produced each year are used mainly for chemicals, petroleum refining, metals and electronics [39,40,44]. The processes for making gasoline and diesel fuels, such as the breakdown of heavier crude oils and the removal of sulphur, are major users of hydrogen. The production of ammonia, used to make fertilizers, also consumes large amounts of hydrogen [39,40,44]. Therefore, hydrogen has been one of the real important industrial chemicals.

Moreover, the depletion of crude oil, natural gas and fossil fuel in combination with the stricter rules on environmental regulations have made hydrogen to be seriously considered as one of the alternative clean energy carriers in future [40,42-48]. In this scenario, hydrogen is produced from different resources and used to feed fuel cells to generate electricity. By using hydrogen as the energy carrier, people have expected to solve two major energy challenges that confront society today: (1) reducing dependence on petroleum and fossil resources, and (2) reducing greenhouse gas emissions as hydrogen fuel cells operate without producing emissions. Although there have been many technological and economical challenges that should be solved, ranging from production, storage, delivery to conversion etc. of hydrogen, it has been predicted that hydrogen will be used as one of the major energy carriers in coming decades [40,42,44,46]. Therefore, hydrogen not only has been one of

the real important industrial chemicals, but it may be an energy carrier for the future.

1.3. Hydrogen production and Pd-based membranes as hydrogen purifiers and membrane reactors

Although the most abundant element in the universe, on Earth hydrogen is mostly found chemically bonded. It must be produced from other compounds such as water, biomass, or fossil fuels [39,40]. Generally, chemical reactions are necessary to break hydrogen bonds in these compounds and release the hydrogen; in doing so a multi-component gas stream of hydrogen and several other gases is formed. To have hydrogen with high purity for the end-uses, the gas stream is then separated by several separation techniques like a pressure swing adsorption or using of porous and non-porous membranes [40]. Among the mentioned separation methods, separation and purification of hydrogen by means of dense Pd-based membranes are of great importance and interest, because the technology is able to provide high hydrogen separation flux with very high selectivity. Therefore, Pd-based membranes have been used as hydrogen purifiers to supply ultra-pure hydrogen for several applications like semiconductor and metal processing, or for the operation of the fuel cells since several decades [4,6,8-11,49,50]. For example, in 1964 Johnson Matthey developed a hydrogen purifier, which employed a thick (50-100 μm) Pd-Ag tube [49-50]. This relatively thick Pd-Ag membrane achieved a hydrogen permeance of 0.1 mol/m^2.s.bar at 500 ^oC.

Furthermore, there has been a growing interest in the industrial application of Pd-based membranes for hydrogen producing reactions in recent years. Extensive investigations have been conducted for the employment of Pd-based membranes for hydrogen removal to shift thermodynamic (equilibrium) limitations towards higher conversions, e.g. during dehydrogenation of hydrocarbons [51–56], steam reforming of methane [57–58] and the water-gas-shift reaction [59]. For instance, continuous hydrogen removal in a membrane reactor enabled 99.7% conversion of cyclohexane to benzene, compared to the closed-system equilibrium conversion of 18.7 % [55].

1.4. Conventional Pd-based membranes

The existing Pd-based membranes can be mainly classified into two types, according to the structure of membrane: (1) self-supporting Pd-based membranes, and (2) composite type structures composed of a thin selective layer deposited on porous supports.

Most self-supporting Pd-based membranes are commercially available in the forms of tubes or foils, fabricated by fine metallurgical methods. These membranes have an adequate mechanical strength and are available in the forms that are easily integrated into a separation set up. They are, however, relatively thick (50 μm or larger)[2,4-6,9,49-50], consequently reducing the hydrogen flux, which is inversely proportional to the thickness of the membrane. Besides the low flux, thick Pd membranes are too expensive for an economic use, in particular since the price of palladium has tremendously increased over the last few years. For practical use it is necessary to reduce the thickness of the palladium layer.

In the last decade, a substantial research effort has been carried out on achieving higher fluxes by depositing thin layers of Pd or Pd alloys on porous supports, such as ceramic or stainless steel, thus forming a so-called composite Pd membrane [10-13,18-28]. Generally, producing membranes as such is not too difficult, while the use of a thin Pd layer enhances the flux and reduces the membrane cost. However, to make sub-micron thick, defect-free separation membranes is very difficult, most probably due to the fact that the porous supports are seldom defect–free. The commercial available porous supports are likely to be supplied with imperfections e.g., particulates on the substrate, non-uniformities in pore size etc., which make the metal films could not cover up the supports completely, consequently leading to the membrane defects [18-22,27-28]. For instance, Roa et al. deposited 10μm Pd-Cu films on a porous γ-alumina (nominal pore sizes of 5-50 nm) and reported that their membranes were not defect-free due to the imperfections of the initial supports [27]. As the gas molecules are small, even only few defects with $\varnothing$>0.5μm.cm^{-2} of membrane surface significantly deteriorate the membrane selectivity.

In addition, to have an adequate mechanical strength, the used porous supports should be in relatively thick form, i.e. in the range of a few mm, which have a considerable high mass transfer resistance, influencing negatively the separation flux [12,28]. Furthermore, it has been observed that the thin films are often deposited on porous supports with an insufficient step coverage, i.e. the inner walls of the pores of the support are not well covered by the film [18-

19,22], leading to pinholes in the membranes that give rise to gas leakage. To prevent pinhole formation, the pore size of the top layer in the support should be reduced. It however means that the supports with even higher mass transfer resistance are used, leading to even lower separation flux.

Recently, using several very precise techniques to repair the surface of the commercially available supports [26,28], in combination with deposition methods with improved pore coverage [23-26], researchers have made thin membranes with a reasonably high selectivity for hydrogen. For instance, Nam et al. reported a selectivity of about 3000 for H_2 over N_2 for a less than 2 μm thick Pd-Cu membrane, which was deposited by a vacuum electrodeposition method on porous stainless steel [26]. However, the reported procedure to repair the substrate surface is rather complicated and time consuming, which may limit batch production of their methods.

To avoid the initial surface imperfections and film coverage problem, Bredesen and Klette deposited Pd alloy films on a bare silicon wafer with atomic surface roughness, then peeled-off and transferred the deposited films to other supports to form membranes [29]. However, perfect transfer is crucial to obtain defect-free, submicron thick membranes, which is not an easy task.

Generally, although there has been an extensive development in the field of membrane engineering in the last decades, a method to fabricate thin and defect-free Pd-based membranes (preferably sub-micron thick) on supports with a low mass transfer resistance is still very desirable.

1.5. Project description and objectives

Giving the above challenges, the goal of this project was to fabricate thin and defect-free Pd-based membranes. This is thought to be accomplished by using techniques of microfabrication technology [60-62]. In order to show their potential, the fabricated membranes are then used as hydrogen purifiers to get high quality hydrogen, and as membrane reactors for several dehydrogenation reactions.

The development and characterization of these microfabricated membranes require considerable effort, so a co-project was formed and carried out at two research groups: the Transducers Science and Technology Group of the University of Twente; and the Process Development Group of the University of Eindhoven. The project was mainly funded by the STW (Dutch

Technology Foundation), and several users like ABB LUMMUS GLOBAL INC., DSM and Aquamarijn contributed.

Using techniques of microfabrication technology to develop thin and defect-free Pd-based membranes was the main task of the research at the University of Twente. Also, the microfabricated membranes should be made in forms that are suitable for hydrogen permeation measurements performed at operation pressures as high as 1 bar and temperatures as high as 500 ^{o}C. The results of this development are described in this thesis.

In the mean time, the University of Eindhoven was responsible to build up a measurement environment where the hydrogen permeation flux and the hydrogen selectivity of the fabricated membranes are determined. Besides the membrane characterization, the University of Eindhoven combines the hydrogen permeation measurements with calculations to come to optimal membrane designs.

1.6. Thesis outline

In chapter 2, a new process is designed to make the Pd and Pd-Ag membranes directly on a <110> silicon wafer. Pd-Ag alloy films are synthesized by a dual sputtering technique, and membranes with thickness ranging from 700 to 1000 nm are made.

In chapter 3, we show that by using an extra support, a silicon nitride microsieve [63-65] on the <110> silicon wafer, allows fabrication of even thinner membranes; Pd and Pd-Ag membranes with thickness down to 100 nm are made. In addition, we also fabricate Pd-Cu membranes on the supporting microsieve.

The technology developed in chapter 3 is then utilized to fabricate an ultrathin silicon nitride membrane for creating a nanosieve membrane with nanopore sizes. A fabrication process of this nanosieve membrane is described in chapter 4. Note that although the developed nanosieve membrane can not be used for hydrogen separation, it has great potential applications in different sectors.

In chapter 5, a dual sputtering set-up is described that allows the synthesis of Pd-based alloy films with a high composition control; Pd-M (M = Ag and Cu) alloy films with an M content of 23 wt% are synthesized.

After fabrication at the University of Twente the membranes are sent to the Process Development Group, University of Eindhoven for characterization mainly with respect to the hydrogen permeation flux and the membrane selectivity. Because the membrane separation results are thoroughly described in the PhD thesis of the University of Eindhoven, the separation results are briefly reported in chapter 6. However, the advantages of microfabricated membranes used for hydrogen separation will be highlighted.

Finally, in chapter 7, conclusions are drawn and suggestions are made for further research on several aspects. Though not all of the project objectives were obtained, the first suggestion was made in the application of using the fabricated membranes to perform the dehydrogenation reactions. Then, other suggestions like producing a silver membrane for oxygen separation, using the nanosieve as a shadow mask for pattern transfer of nanodots, and making a nano-slit shadow mask for patterning nanowires are proposed.

1.7. References

[1] T. Graham, Philos. Trans. R. Soc., London, 156, 39 (1866).
[2] F.A. Lewis, “The Palladium Hydrogen System”, Academic Press (1967).
[3] F.A. Lewis, “Hydrogen in Palladium and Palladium Alloys”, Int. J. Hydrogen Energy, 21, 461 (1996).
[4] A.C. Markrides, M.A. Wright, D.N. Jewett, US Patent 3,350,846 (1967).
[5] R. Goto, “Purification of Hydrogen by Selective Osmosis with Palladium Alloy Membranes”, KagaKu KogaKu, 34, 381 (1970).
[6] A.G. Knapton, “Palladium Alloys for Hydrogen Diffusion Membranes”, Platinum Metal. Rev., 21, 44 (1977).
[7] G. Alefeld and J. Volkl (Eds), “Hydrogen in Metals”, Springer (1978).
[8] V.M. Gryaznov, “Hydrogen Permeable Palladium Membrane Catalysts. An Aid to the Efficient Production of Ultra Pure Chemical and Pharmaceuticals”, Platinum Metal. Rev., 30, 68 (1986).
[9] J. Shu, B.P.A. Grandjean, A. VanNeste, J. Kaliaguine, “Catalytic Palladium-Based Membrane Reactors: review”, Can. J. Chem. Eng., 69, 233 (1991).
[10] R. Hughes, “Composite Palladium Membranes for Catalytic Membrane Reactors”, Membr. Techno., 131, 9 (2001).

[11] R. Dittmeyer, V. Hollein and K. Daub, "Membrane Reactors for Hydrogenation and Dehydrogenation Processes Based on Supported Palladium", J. Mole. Catal. A., 173, 135 (2001).

[12] T.L. Ward and T. Dao, "Model of Hydrogen Permeation Behavior in Palladium Membranes", J. Membr. Sci., 153, 211(1999).

[13] J.P. Collins and J.D. Way, "Preparation and Characterization of a Composite Palladium-Ceramic Membrane", Ind. Eng. Chem. Res., 32, 3006 (1993).

[14] V.A. Goltsov, "Hydrogen Treatment (Processing) of Materials: Current Status and Prospects", J. Alloy. Comp., 293-295, 844 (1999).

[15] G.D. Berkheimer and R.E. Buxbaum, "Hydrogen Pumping with Palladium Membranes", J. Vac. Sci. Technol. A, 3, 412 (1985).

[16] R.E. Buxbaum and T.L. Marker, "Hydrogen Transport through Non-Porous Membranes of Palladium-Coated Niobium, Tantalum and Vanadium", J. Membr. Sci., 85, 29 (1993).

[17] R.E. Buxbaum, J.H. Park and D.L.Smith, "Hydrogen Transport and Embrittlement of Palladium Coated Vanadium Chromium Titanium Alloys", J. Nuclear Materials, 233-237, 510 (1996).

[18] V. Jayaraman and Y.S. Lin, "Synthesis and Hydrogen Permeation Properties of Ultrathin Palladium-Silver Alloy Membranes", J. Membr. Sci., 104, 251 (1995).

[19] B. McCool, G. Xomeritakis, Y.S. Lin, "Composition Control and Hydrogen Permeation Characteristics of Sputter Deposited Palladium-Silver Membranes", J. Membr. Sci., 161, 67 (1999).

[20] G. Xomeitakis and Y.S. Lin, "Fabrication of Thin Metallic Membranes by MOCVD and Sputtering", J. Mem. Sci., 133, 217 (1996).

[21] Xomeritakis, G., and Y.S. Lin, "CVD Synthesis and Gas Permeation Properties of Thin Palladium/Alumina membranes", AIChE. J., 44, 174 (1998).

[22] J.O. Brien, R. Hughes, J. Hisek, "Pd-Ag Membranes on Porous Alumina Substrates by Unbalanced Magnetron Sputtering", Surf. Coat. Technol., 142, 253 (2001).

[23] K.L. Yeung and A. Varma, "Novel Preparation Technique for Thin Metal–Ceramic Composite Membranes", AIChE J., 41 (9), 2131 (1995).

[24] L.Q. Wu, N. Xu, J. Shi, "Novel Method for Preparing Palladium Membranes by Photocatalytic Deposition", AIChE J., 46, 1075 (2000).

[25] S. Yan, H. Maeda, K. Kusakabe, S. Morooka, "Thin Palladium Membrane Formed in Support Pores by Metal-Organic Chemical Vapor Deposition Method and Application to Hydrogen Separation", Ind. Eng. Chem. Res., 33, 616 (1994).

[26] S.E. Nam and K.H. Lee, "Hydrogen Separation by Pd Alloy Composite Membrane: Introduction of Diffusion Barrier", J. Membr. Sci., 192, 177, (2001).

[27] F. Roa, J.D. Way., R.L. McCormick., S.N. Paglieri., "Preparation and Characterization of Pd-Cu Composite Membranes for Hydrogen Separation", J. Chem. Eng., 93, 11 (2003).

[28] A.J. Burggraaf, "Key Points in Understanding and Development of Ceramic Membranes", In Proc. ICIM 3, p.1 (1994).

[29] R. Bredesen and H. Klette, "Method of Manufacturing Thin Metal Membrane", US pattern 06086729.

[30] A.J. Frank, K.F. Jensen, M.A. Schmidt, "Palladium Based Membranes for Hydrogen Separation and Hydrogenation/Dehydrogenation", Proc. IEEE. MEMS 99, 382 (1999).

[31] S.V. Karnik, M.K. Hatalis and M.V. Kothare, "Towards a Palladium Micro-Membrane for the Water Gas Shift Reaction: Microfabrication Approach and Hydrogen Purification Results", J. Microelectromech. Syst., 1, 93 (2003).

[32] F.C. Gielens, H. D. Tong, C.J.M. Rijn, M.A.G. Vorstman, J.T.F. Keurentjes, "High-Flux Palladium-Silver Alloy Membranes Fabricated by Microsystem Technology", Desalination 147, 417 (2002).

[33] H.D. Tong, J.W. Ervin Berenschot, M.J. De Boer, J. G. E. Gardeniers, H. Wensink, H.V. Jansen, W. Nijdam, M.C. Elwenspoek, F.C. Gielens, and C.J.M. Rijn, "Microfabrication of Palladium–Silver Alloy Membranes for Hydrogen Separation", J. Microelectromech. Syst., 12, 622 (2003).

[34] H.T. Hoang, H.D. Tong, F.C. Gielens, H.V. Jansen, M.C. Elwenspoek, "Fabrication and Characterization of Dual Sputtered Pd–Cu Alloy Films for Hydrogen Separation Membranes", Materials Letters, 58, 525 (2004).

[35] J. Xu, "Hydrogen Permeation and Diffusion in Iron-Base Super Alloys", Acta Metal Mater., 41(5), 1455 (1993).

[36] F. Sakamoto, Y. Kinari, F.L. Chen, Y. Sakamoto, "Hydrogen Permeation through Palladium Alloy Membranes in Mixture Gases of 10% Nitrogen and Ammonia in the Hydrogen", Int J. Hydrogen Energy, 22, 369 (1997).

[37] F.L. Chen, Y. Kinari, Y. Nakayama, Y. Sakamoto, "Hydrogen Permeation through Palladium-Based Alloys Membranes in Mixtures of 10% Methane and Ethylene in the Hydrogen", Int J. Hydrogen Energy, 21, 555 (1996).

[38] H. Yoshida, S. Konishi, Y. Naruse, "Effects of Impurities on Hydrogen Permeability through Palladium Alloy membranes at Comparatively

High Pressures and Temperatures", J. Less-Common Metals, 89, 429 (1983).

[39] R. Ramachandran and R.K. Menon, "An Overview of Industrial Uses of Hydrogen", Int. J. Hydrogen Energy., 23, 593 (1998).

[40] United States Department of Energy, "A Review of the National Hydrogen Vision Meeting: A National Vision of America's Transition to a Hydrogen Economy- to 2030 and Beyond", Washington, DC, November 15-16, 2001.

[41] B.H.C. Steele and A. Heinzel, "Materials for Fuell–Cell Technology", Nature, 414, 338, (2001).

[42] Hoffmann, P., Tomorrow's Energy, The MIT Press (2001).

[43] M.S. Dresselhaus and I.L. Thomas, "Alternative Energy Technology", Nature, 414, 332 (2001).

[44] T.N. Veziroglu, "Hydrogen Energy System as a Permanent Solution to Global Energy-Environment Problems", Chem. Ind., 53, 383 (1999).

[45] D. Malakoff and F. Robert, " Bush Trades Hybrid for Hydrogen Model", Science, 295, 426 (2002).

[46] M. Schrope, "Which Way to Energy Utopia? ", Nature, 414, 682 (2001).

[47] Koppel, T., J. Reynolds, "A Fuel Cell Primer: the Promise and the Pitfalls", Review 4, (2000).

[48] R.B. Moore and V. Raman, "Hydrogen Infrastructure for Fuel Cell Transportation", Int. J. Hydrogen Energy, 23, 617 (1998).

[49] J.E. Philpott, "Hydrogen Diffusion Technology: Commercial Applications of Palladium Membranes", Platinum Metals Rev., 29, 12 (1985).

[50] J.E. Philpott, "The On-site Production of Hydrogen: A Mobile Generator for Meteorological and Industrial purposes", Platinum Metals Rev., 20, 110 (1975).

[51] Y. Yilidirim, E. Gobina, R. Hughes, "An Experimental Evaluation of High-Temperature Composite Membrane Systems for Propane Dehydrogenation", J. Membr. Sci., 135, 107 (1997).

[52] J.P. Collins, R.W. Schwartz, R. Sehgal, T.L. Ward, C.J. Brinker, G.P. Hagen, C.A. Udovich, "Catalytic Dehydrogenation of Propane in Hydrogen Permselective Membrane Reactors", Ind. Eng. Chem. Res., 35, 4398 (1996).

[53] J.K. Ali, E.J. Newson, D.W.T. Rippin, "Exceeding Equilibrium Conversion with a Catalytic Membrane Reactor for the Dehydrogenation of Methylcyclohexane", Chem. Eng. Sci., 49, 2129 (1994).

[54] S.I. Niwa, M. Eswaramoorthy, J. Nair, A. Raj, N. Itoh, H. Shoji, T. Namba, F. Mizukami, "A One-Step Conversion of Benzene to Phenol with a Palladium Membrane", Science, 295, 105 (2002).

[55] N. Toh, AIChe J., 33, 1576 (1987).

[56] H. Weyten, J. Luyten, K. Keizerb, L. Willems, R. Leysen, "Membrane Performance: The Key Issues for Dehydrogenation Reactions in a Catalytic Membrane Reactor", Catal. Today, 56, 3 (2000).

[57] T.H. Hsiung, D.D. Christman, E.J. Hunter, A.R. Homyak, "Methane Formation on H_2 Purification Using a Commercial Pd-Ag Membrane", AIChE. J., 45, 204 (1999).

[58] E. Kikuchi," Hydrogen-Permselective Membrane Reactors", CATTECH, 1, 67 (1997).

[59] S. Uemiya, N. Sato, H. Ando, E. Kikuchi, "The Water Gas Shift Reaction Assisted by a Palladium Membrane Reactor", Ind. Eng. Chem. Res., 30, 585 (1991).

[60] K.D. Wise and K. Najafi, "Microfabrication Techniques for Integrated Sensors and Microsystems", Science, 254, 1335 (1991).[61] M.C. Elwenspoek and H.V. Jansen, "Silicon Micromachining", Cambridge, 1999.

[62] M.J. Madou, "Fundamentals of Microfabrication: The Science of Miniaturization", CRC Press, 2002.

[63] C.J.M. van Rijn and M.C. Elwenspoek, "Micro Filtration Membrane Sieve with Silicon Micro Machining for Industrial and Biomedical Applications", Proc. IEEE MEMS95, 83 (1995).

[64] S. Kuiper, "Development and Application of Microsieves", Ph.D Thesis, University of Twente, 2000.

[65] C.J.M. van Rijn, "Nano and Micro Engineered Membrane Technology", Elsevier Science (2004).

Chapter 2

Palladium-based membranes on a <110> silicon wafer

Abstract

An innovative process for the microfabrication of Pd-based membranes (Pd and Pd-Ag) on a <110> silicon wafer is presented. Pd-Ag alloy films containing 23wt% Ag are prepared by a dual-sputtering from pure Pd and Ag targets. In the first step, deep grooves are KOH etched in one side of a <110> oriented silicon wafer, leaving membranes with a thickness of ca. 50 μm. After Pd alloy deposition on the unetched side, the silicon membranes are removed by etching, leaving Pd-Ag membranes. Membranes with a porosity, i.e. the ratio of effective separation area over the total area, of up to 20% may be fabricated. Anodic bonding of thick glass plates (containing powder blasted flow channels) to both sides of the silicon substrate is used to package the membranes and create a robust module. The mechanical strength of the membrane is found to be adequate, pressures of up to 3 bars at room temperature do not break the 1000 nm thick membrane. With 700 nm Pd-Ag membrane a high separation flux of ca. 3.6 mol H_2 /m^2.s is obtained with a minimal selectivity of 1500 for H_2 with respect to helium (He) at 723 K and 0.83 bars H_2 retentate pressure.

2.1. Introduction

As discussed in the previous chapter, the increased demand for hydrogen in recent years in many industrial applications, like petroleum refinement, petrochemical and semi-conductor processing and sustainable energy (fuel cells)[1-9] has led to a revival of interest in methods for separation and purification of hydrogen from gas mixtures. In particular, palladium (Pd)-based membranes have been extensively studied, due largely to their unmatched potential as hydrogen-selective membranes for gas separation and purification, or as membrane reactors for (de)hydrogenations [10-25]. In most cases, palladium is alloyed with silver (Ag) to overcome the well-known problem of hydrogen embrittlement [10-13]. Comprehensive review of Pd-based membranes and their applications has recently been provided by several authors [11-13].

Also, in the previous chapter we discussed that although there has been an extensive development in the field of a membrane engineering in the past decades [11-25], a development of new methods to fabricate thin and defect-free Pd-based membranes on supports with a low mass transfer resistance is still very desirable.

In the last decade, microfabrication techniques, originally developed for semiconductor technology [26-28], are increasingly used in different fields of chemistry and biotechnology [29-36]. By a combination of miniaturization with an integration of different components like sensors (temperature and flows), heaters, mixers, valves, pumps etc. into one system, microchemical devices and systems achieve many benefits and have capabilities exceeding those of conventional macroscopic system [29-36]. For instance, in addition to many already demonstrated chemical and biological analysis applications [31], microchemical systems are expected to have numerous advantages for chemical kinetics studies [30] or on-site toxic and hazardous chemical synthesis, and process development etc [32]. In all of the mentioned examples, [25-32] microchemical devices and systems are advantageous in large part simply because they are smaller and more compact – *a trend for process miniaturization* [33].

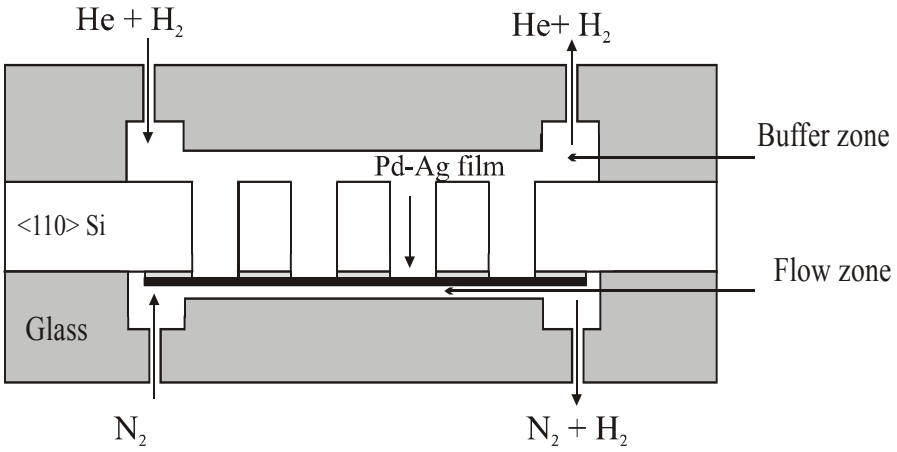

***Figure 2.1**: A cross-section of the separation membrane module.*

Moreover, researchers from the field of process engineering have realized that the advantages of microstructured components are not only limited to simple miniaturization, and a number of highly promising applications involving moderate and, in some cases, even large quantities of matter and energy have begun to emerge in the rapidly growing field of process intensification [33-34]. In this trend, microfabrication technology is not simply utilized to make devices smaller, but rather to make them better – *a trend for process intensification* [33-34].

In the last few years, it has been demonstrated that microfabrication technology offers a new approach for the fabrication of the thin and defect-free Pd-composite membranes [35-39]. Such thin films dramatically increase the achievable hydrogen flux as well as the selectivity of the membrane, and possibly decreasing the costs, if the batch fabrication possibilities of microfabrication technology can be exploited. In this new approach, the Pd alloy films are first deposited on a dense and smooth surface of previously microfabricated supports. Then, the supports are partially etched from their backside to create pathways to the Pd surface for the gases, thus forming the membranes. As the separation films are now deposited on a dense and smooth surface, the films can cover the support completely, leading to defect-free membranes later. Meanwhile the use of the microfabricated supports still allows fabricating very thin films. Also, the microfabricated supports can be made in the forms that have a rather low mass transfer resistance, leading to highly obtainable fluxes.

In this chapter, we present an innovative process for the microfabrication of Pd-Ag alloy membrane on a <110> silicon substrate. The performance with respect to mechanical strength, hydrogen flux and selectivity of the Pd-Ag membranes in such a module is characterized and will be discussed in detail in this chapter.

2.2. Microfabrication of membrane module

2.2.1. Palladium silver membranes on a <110> silicon wafer

A cross-section of the Pd-Ag membrane module is shown in Figure 2.1. It consists of a silicon wafer and two glass wafers. The sequence of process steps that is applied to achieve the membrane module is outlined in Figure 2.2. In brief, the sequence runs as follows: A 3 inch, double-side polished, <110>-oriented silicon wafer (<110>-Si) is coated with 1 μm of wet-thermal silicon dioxide (SiO_2), which is used as a protective layer during subsequent etching steps (Figure 2.2.a). To fabricate high-aspect-ratio features by anisotropic etching of <110>-Si, precise alignment of the features to the {111} planes is of critical importance. To reveal the {111} planes in the <110>-Si, fan-shaped structures (or "Wagon wheel") are first imprinted on the oxidised silicon wafer by standard photolithography (Figure 2.2.b), followed by a local removal of SiO_2 in a commercial buffered hydrofluoric acid (BHF) etch, and a short etch in a concentrated KOH solution. More details can be found in refs. [27,40-43].

Next, long narrow slits of 23 by 1500 μm are aligned to the revealed {111} planes and lithographically patterned using the steps mentioned above (Figure 2.2.c). A slit design as well as its orientation on the <110>-Si is depicted in Figure 2.3. A current membrane design consists of 1000 of such slits, which are divided into 8 ranges on a square area of 18 by 18 mm. The wafer is immersed in 25 % KOH solution at 75 ^{o}C to etch the silicon until ca. 50 μm of silicon is left at the bottom of the etched slits (Figure 2.2.d) As a result, an etched structure or a silicon support frame is created and shown in Figure 2.4.

Subsequently, a RCA cleaning procedure [27-28] is carried out, following a rinsing in DI water to remove KOH residual (and any other contamination) from the SiO_2 layer remaining at the flat side of the silicon frame. At this stage, alloy films of Pd77-Ag23 at wt% with thickness from 700 to 1000 nm are sputtered through a shadow mask on the flat side of the

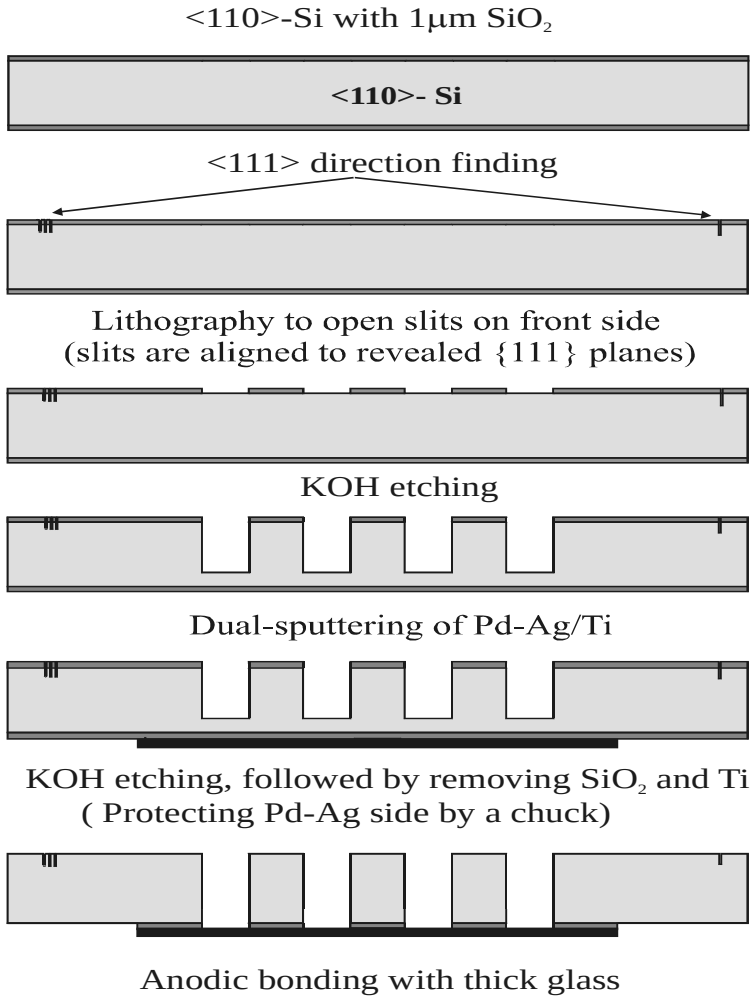

Figure 2.2*: Fabrication process of the Pd-Ag membrane module.*

etched silicon frame, using titanium (Ti) as an adhesion layer (Figure 2.2.e). The dual-sputtering procedure to deposit a homogenous Pd-Ag alloy film will be discussed in detail in chapter 5. Obviously, an advantage of this fabrication method is that *Pd and Pd-Ag films are deposited onto a flat and smooth surface, therewith avoiding possible step coverage problems that may arise during deposition on porous or patterned substrates*. Thus, very thin Pd or Pd-Ag films, potentially free of pinholes will be obtained.

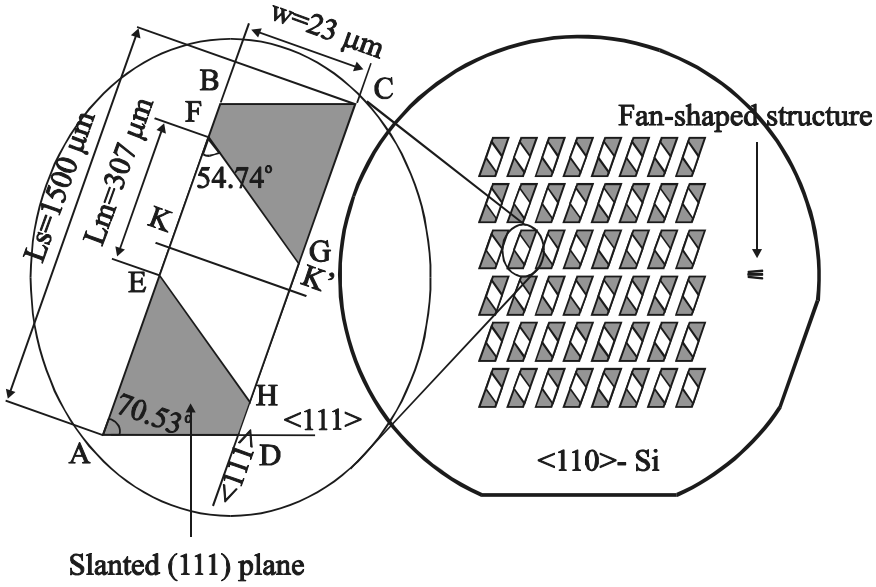

Figure 2.3*: Design of slits and its orientation on the <110>-Si (not in scale). ABCD is the shape of opened slit on silicon, while EFGH is an etched shape at the bottom. The two slanted {111} planes are shown in dark color.*

After alloy deposition, the concentrated KOH solution mentioned above is used to remove the remaining 50 µm of silicon in the trenches. Etching in KOH is continued until the SiO_2 layer is reached. Finally, this oxide layer and the Ti film are removed in BHF to uncover the back surface of the Pd-Ag membranes (Figure 2.2.f). It should be mentioned here that the BHF removes Ti, but does not affect Pd, Ag or Pd-Ag. A close up of the Pd-Ag membrane across one etched slit is depicted in Figure 2.5, while Figure 2.6 shows a top view of an array of long narrow etched slits on the silicon wafer. In Figure 2.6, the gray parts are unpatterned silicon, the black areas are oblique {111} planes appearing inside the etched slits, and the whitish parts are free Pd-Ag areas as seen through the etched slits. Using this silicon frame, Pd and Pd-Ag membranes with a thickness from 700 nm to 1000 nm are fabricated.

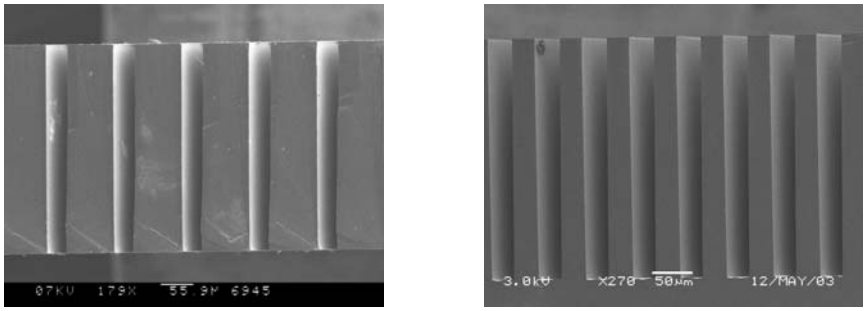

(a) (b)

Figure 2.4*: Narrow slits were etched in the <110>-Si wafer: (a) with a period of 90 µm; (b) with a period of 50µm.*

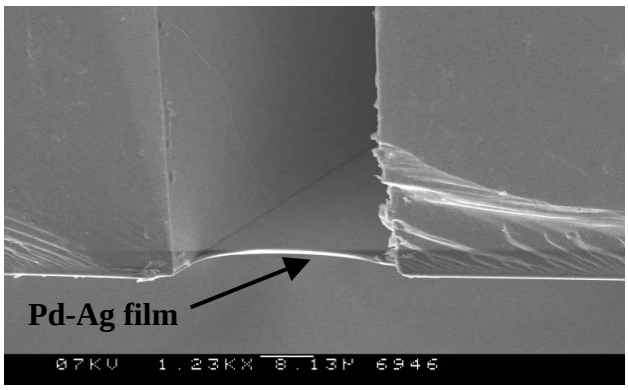

Figure 2.5*: Close up of cross-section of the Pd-Ag membrane.*

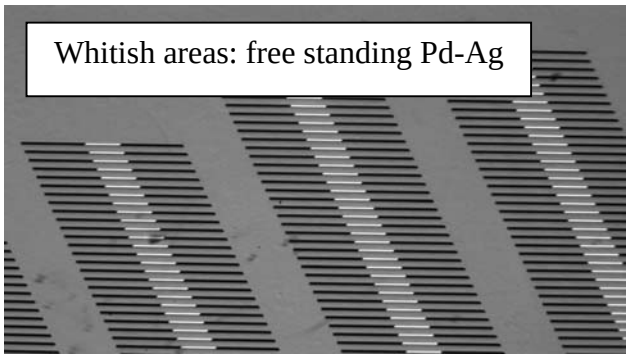

Figure 2.6*: Top view picture of free areas of Pd-Ag (whitish colour) on the Si wafer. The Pd-Ag layer is deposited on the other side of the Si wafer.*

2.2.2. Flow channels in glass by powder blasting

Like the silicon wafer, the 5 mm thick glass wafers (borosilicate from Schott Co.) need to be micromachined before these wafers are bonded. In a first step, holes are drilled through the glass wafers. These holes are needed for the gas connections after finishing the separation module. Afterwards, powder blasting is used to create a flow channel in the glass wafer. The method consists in directing particles with a high velocity towards a substrate, from which material will be removed by mechanical corrosion. Advantages of the method are: simplicity, low-cost and high etch rate [44].

The process steps used in powder blasting of thick glass plates are outlined in Figure 2.7. In brief, two glass wafers are covered with an Ordyl BF 410 photosensitive foil, which acts as a protective layer during powder blasting. After a photolithography process as described in [44], powder blasting is applied to obtain a 1 mm deep gas buffer zone on each of two glass wafers (see Figure 2.8). These buffer zones are used to distribute the flow uniformly over the membrane surface. Without them, most of the gas would flow along the center of the membrane, therewith limiting the effective working area of the membrane. A second powder blasting step is performed in order to create a 0.2 mm deep flow channel, which is connected to the peripheral equipment via holes previously drilled in the glass wafers. Figure 2.8 is a top view of the glass wafer with the drilled holes and flow channels.

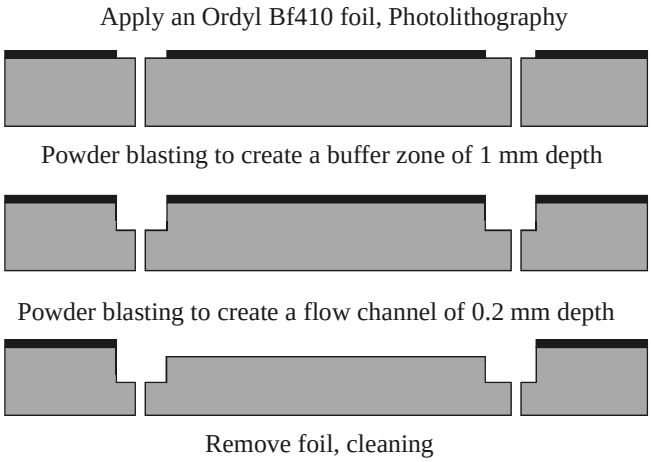

***Figure 2.7**: Process-outline of fabrication of flow channels by powder*

blasting.

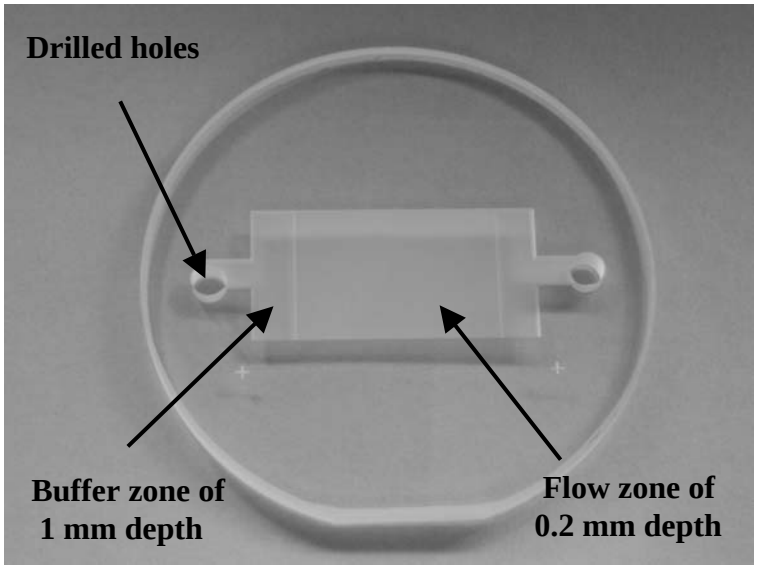

Figure 2.8*: Glass wafer with drilled holes and flow channels.*

2.2.3. Membrane packaging

In the last process step, the silicon wafer is bonded between the two thick glass wafers by a four-electrode anodic bonding technique (Figure 2.9)[27,38]. This process is performed in two steps, because adequate bonding requires that a positive electrical voltage has to be applied to the silicon and a negative voltage to the glass. The process resulted in a tight seal between each glass wafer and the silicon wafer. In this study, the anodic bonding is carried out in different environments like a normal air, nitrogen and vacuum with electrical voltages ranging from 1000 to 1500 volts. Bonding in nitrogen and vacuum environments may avoid the membranes to be contaminated or even oxidized.

However, there has been not much difference in separation results of the membranes bonded in these different environments, therefore we often do wafer bonding in the normal air. Note that before the bonding procedure, the silicon membrane and the glass wafers were cleaned in a fuming nitric acid (100 % HNO_3) for 15 minutes, followed by a rinsing in DI water.

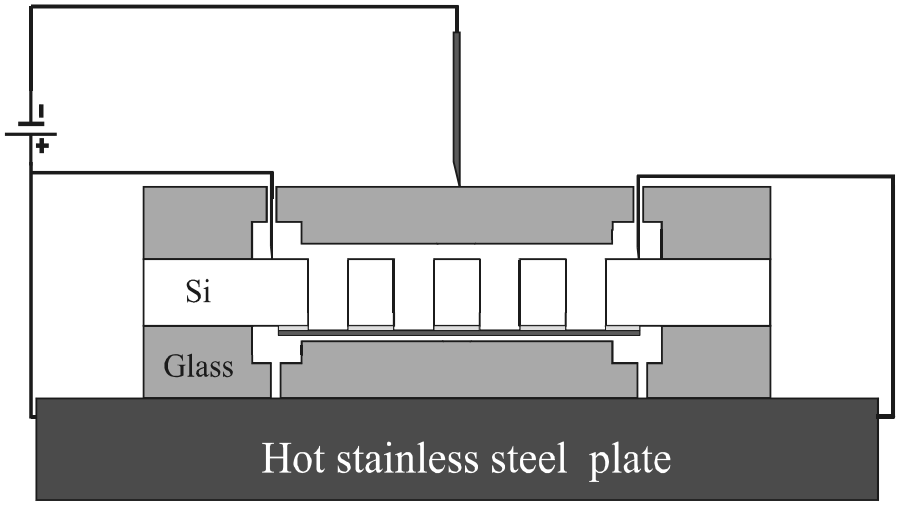

***Figure 2.9**: Four electrode anodic bonding setup for glass-silicon-glass packaging.*

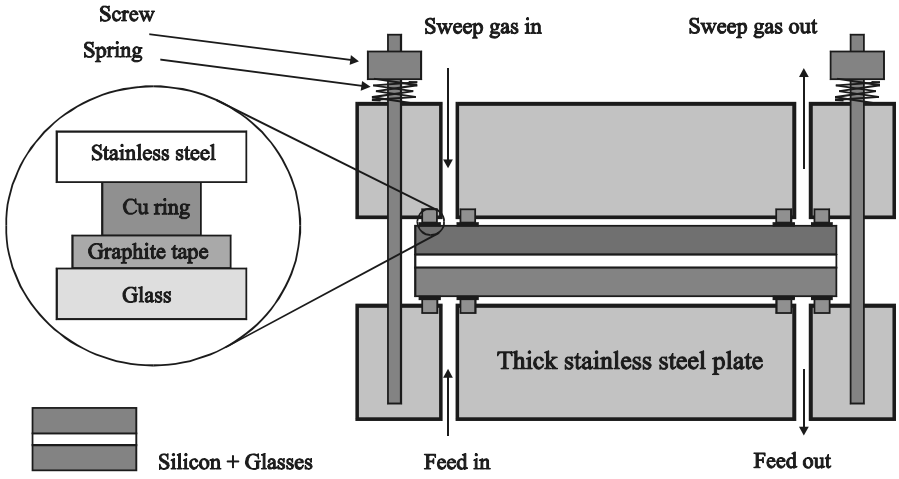

***Figure 2.10**: Membrane holder, the upper part can move up and down and is pressed to the lower part by screws and springs.*

The bonding process as it is performed here creates a membrane module, which is robust enough for practical use e.g., it can be integrated in a stainless steel membrane holder (see Figure 2.10) to have connections to a gas manifold and analysis equipment. In this membrane holder, high forces, exerted by screws, are needed to press membrane module and stainless steel plates tightly together, without leakage. In this set-up, flexible graphite rings are applied in between the holder and the membrane module to make a gastight connection.

Although not tested here, the bonding method discussed above may allow the construction of a larger module that consists of a large number of silicon wafers separated by glass plates. Such a module would be suitable for industrial applications where a high volume of hydrogen needs to be extracted from a gas mixture.

2.3. Microfabrication results and discussion

2.3.1. Membranes on <110> silicon wafer

Figure 2.4.a shows a SEM micrograph of the cross-section of several narrow parallel slits, etched in a 350μm thick <110>-Si and having a periodicity of 90 μm. More details on high-aspect-ratio etching in <110>-Si wafers can be found elsewhere [40-43,46].

From Figure 2.5 the width of the etched slit is estimated to be about 28 μm, while its initial width was defined by lithography to be 23 μm. This widening of the etched slit should be characterized exactly and taken into account during the design, for two main reasons: 1) a wider slit would imply a wider membrane, which would have a lower mechanical strength (membrane strength strongly depends on membrane width [47]), and 2) unexpected widening of the slits would make the determination of the total free membrane area, i.e. the separation area, difficult. Slit widening is due to a non-zero etch rate of the vertical {111} planes, and also depends on the accuracy of alignment of the mask patterns to the {111} planes (this factor was reduced to a minimum in our work by using the previously described fan-shaped pattern to find the exact {111} planes), but also on etching conditions [42-43]. In our work, the ratio of the etch rates of the {110} to the {111} planes is estimated to be about 140, which is comparable to data reported by Holke and Henderson [43].

These data can be used to calculate the substrate porosity, defined here as the relative area of the substrate that is available for hydrogen permeation. To define the hydrogen separation membrane area, the length of the free area (L_m) created by KOH etching of one slit through a {110} silicon substrate should be known (Figure 2.3). Using simple geometrical considerations, this length L_m is given by [40]:

$$L_m \sim L_s - 2\sqrt{3}\,t + \frac{3\sqrt{2}}{4}W \qquad (1)$$

with L_s the length and W the width of the opening slit, and t the thickness of silicon wafer. Applying equation (1) with L_s= 1500 μm, t = 350 μm and W = 28 μm, gives a length L_m of 317 μm. As a result, etching one slit per area of 1800 μm by 90 μm through a <110>-Si creates an effective separation area of 317 μm by 28 μm, leads to the membrane porosity of ca. 6%.

By making the slit broader (increasing w) or longer (increasing L_s) or using a thinner wafer (see equation 1) will give a larger effective area for hydrogen separation and will increase the porosity. However, as will be shown in the next section, the mechanical strength of the membranes strongly depends on their shortest dimension [47], therefore increasing their width (w) will result in weaker membranes. An alternative way to increase the porosity is to decrease the pitch of the slits. For instance, Figure 2.4.b shows the etched structure with a smaller periodicity of 50 μm. Putting all the above into an optimized design, a membrane consisting of slits of 3000 μm by 23 μm with a periodicity of 50 μm would give a membrane porosity of about 20%.

The porosity can be increased even further, by using Deep Reactive Ion Etching (DRIE) [45]. DRIE of silicon is not restricted by silicon {111} planes and therefore it is possible to achieve slits with $L_m = L_s$. However, with that method only one wafer at the time can be processed, while KOH etching allows a large number of wafers to be etched simultaneously.

2.3.2. Mechanical strength of the membrane

The mechanical strength of the membranes is an important aspect, as the hydrogen flux is driven by a (partial) pressure difference across the membrane. Predicting the mechanical strength of the membranes is however quite complicated, as it depends on various factors like membrane construction,

thickness and material properties (which for thin films may be difficult to estimate or measure). Therefore, the strength of membranes is normally determined experimentally. Nevertheless, a rough estimation of the strength is very valuable during the design phase, and therefore we started our work with an estimation of the strength of our microfabricated membranes based on the originally chosen design parameters width and length (defined by the lithographic process), thickness and (bulk) material properties.

As can be seen in Figure 2.1 and Figure 2.6, the microfabricated membrane module is composed of many smaller Pd-Ag membranes acting in parallel, of which a single one is formed by a Pd-Ag membrane spanning across one etched slit. It can safely be assumed that the mechanical strength of the silicon support that surrounds the Pd-Ag membranes is much higher than that of a single Pd-Ag membrane, therefore the strength of the whole membrane module will be mainly determined by that of a single membrane. Van Rijn et al. [47] derived an equation that can be used to estimate the maximum trans-membrane pressure $P_{\max}$ for a thin membrane of composed of a ductile material:

$$P_{\max} = 6.4\frac{t\sigma_{yield}^{3/2}}{WE^{1/2}} \qquad (2)$$

where t is the thickness of the membrane, W the width of the shortest side of the membrane, σ_{yield} the yield stress and E the Young's modulus of the membrane material. Several values of E and σ_{yield} for thick foils of Pd and Ag are given in Table 2.1 [48]. However, the values of E and σ_{yield} for sputtered Pd77-Ag23 wt% alloy film have not been reported yet. Besides that, the mechanical properties of thin films may differ for different deposition methods and conditions [49,50], so that film property data obtained from literature cannot be taken for granted. Very critical is the temperature at which the membrane will have to operate. In general, both E and σ_{yield} are temperature dependent and typically a higher temperature will lower σ_{yield}. If it is assumed that the material properties of an alloy can be interpolated from the properties of the individual metal elements, we arrive at a yield strength of 80 MPa and a Young's modulus of 112 GPa for the deposited Pd-Ag alloy film. Applying equation 2 for a 1000 nm thick Pd-Ag membrane spanning across a 28 μm wide slit, we find a $P_{\max}$ of 5 bars.

The rupture strength P_{break} of the Pd-Ag membrane is measured at room temperature in the set-up described by van Rijn et al. [47]. It is found that the

1000 nm thick Pd-Ag membranes broke at pressure differences of about 3 to 3.5 bars, which are close to the predicting value of 5 bars. Also, as was expected, the membranes that broke ruptured on the Pd-Ag membranes and not on the silicon support. Although the rupture strength of the membranes has not been measured at higher temperatures, the room temperature tests show that the microfabricated membrane is mechanically strong enough to operate under the desired pressure gradient.

Table 2.1*: Mechanical properties of Pd, Ag and the postulated data*

for the sputtered Pd-Ag alloy.

MATERIAL	σ_{YIELD} (MPA)	E (GPA)
Pd	35-205	121
Ag	172-330	83
Pd-Ag	80*	112*

** Postulated data for the sputtered Pd-Ag in this work*

2.4. Preliminary hydrogen permeation results

After fabrication at the Transducers Science and Technology Group of the University of Twente, the membranes were sent to the Process Development Group of the University of Eindhoven, for characterizing mainly with respect to the hydrogen permeation flux and the membrane selectivity. Because the separation results will be described in detail in chapter 6, the separation results are briefly presented here.

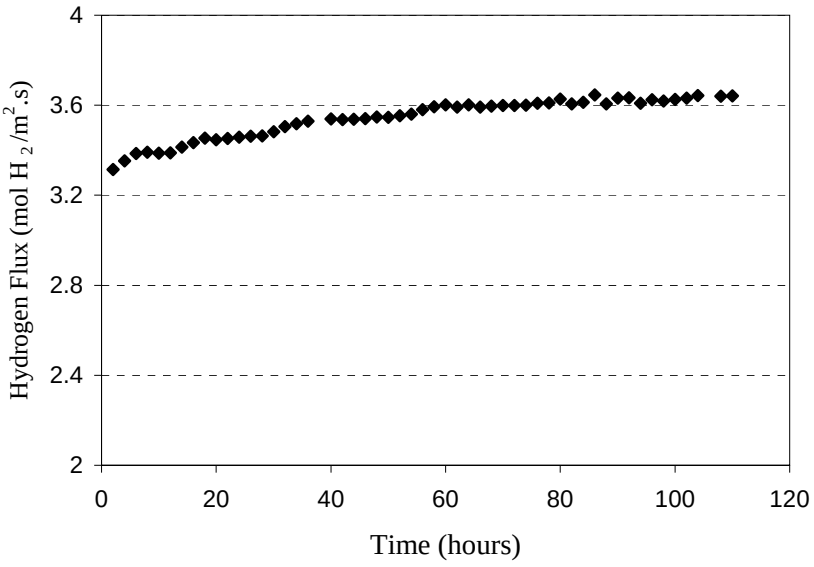

Figure 2.11*: Hydrogen flow rate through a 700 nm Pd-Ag alloy membrane as a function of time at temperature of 723 K, hydrogen pressure of 0.83 bars in retentate. Note that the temperature was at 673 K in hydrogen environment at t = 0 hr.*

2.4.1. Separation flux

The permeability of the membrane was determined for H_2 and helium (He) with an experimental setup shown in Figure 6.1 (chapter 6). The hydrogen flow rate through the 700 nm Pd-Ag membrane versus the duration of the experiment is given in Figure 2.11. The flux is defined as the molecular hydrogen flow through the membrane divided by the free Pd-Ag area (mol $H_2/m^2.s$). It should be noted that the measurement started when the membrane temperature was at 673 K, and hydrogen was already applied at the retentate. At a membrane temperature of 723 K and a hydrogen partial pressure of 0.83 bars at the retentate, a high hydrogen flux of 3.6 mol $H_2/m^2.s$ (or equivalent to 290.3 $m^3/m^2.h$) is measured. This flux is high in comparison to the reported fluxes from literature (see Table 6.2, chapter 6). The reasons for obtaining such high fluxes for the present membrane are;

1) the thin Pd-Ag membrane (700 nm) with high composition control and nanostructures is used.
2) most importantly, such a membrane has a very low resistance to the mass transfer, as virtually no support layer is present. The advantages of the microfabricated membranes using in a hydrogen separation will be discussed in more detail in chapter 6.

2.4.2. Membrane selectivity

Possible membrane leaks during the permeation experiment can be detected by measuring the He concentration at the permeate side. However, no He has been found during the experiments. Therefore, in order to calculate a minimum selectivity of H_2 over He, the detection limit of the gas chromatograph for He is used as the maximum He concentration. In this way, a minimal separation factor of 1500 for H_2 to He (or equivalent to about 4000 for H_2 to N_2) is calculated. This high selectivity indicates that the microfabricated membrane is most likely defect free. We believe that depositing the Pd-Ag separation layer on a very smooth and clean silicon oxide layer and preparing the membrane in a dust-poor clean room environment were the key points to get to this result.

2.5. Discussion and conclusions

Pd-Ag alloy membrane modules were micromachined and tested. KOH etching of <110>-Si was utilized to fabricate a supporting structure for a sputtered Pd-Ag film. The Pd-Ag layer was deposited by a dual sputtering, which is a powerful method to make thin alloy films with highly homogeneous composition. Anodic bonding of thick glass to silicon was used to package the membrane and create a robust module.

The membranes were found to have adequate mechanical strength; 1000 nm thick Pd-Ag membrane were capable of withstanding a pressure difference of 3 to 4 bars at room temperature. The microfabricated Pd-Ag membranes obtained a high permeation rate and high selectivity for hydrogen. Typical flow rates of 3.6 mol $H_2/m^2.s$ were measured at the hydrogen pressure of 0.83 bars at 723 K with a minimal selectivity of 1500 for H_2 to He.

In the author's opinion, the biggest advantage of the membrane process presented in this chapter is that it is a rather simple and low-cost process (Figure 2.2). For example, the membranes are fabricated by using a two-mask process.

In addition, this process utilizes only the wet etching of silicon (KOH) and the wet etching of SiO_2 (BHF) to create the membrane support. As the wet etching is cheap and easy for a batch production, the membrane may be produced at a low-cost. Furthermore, the membranes are able to withstand the expected pressure difference of several bars and achieved a high separation flux as well as a high selectivity (see separation result in chapter 6).

However, a main limitation of the membrane process development presented in this chapter is that it is very difficult to produce a very thin membrane - a membrane with a thickness of a few hundred of nm, while retaining a membrane mechanical strength. For instance, equation 2 predicts that a 500 nm thick Pd-Ag membrane (t = 0.5 μm) on the current support (W = 28 μm) is able to withstand a pressure difference of a couple of bars. In fact, mechanical strength tests (at a room temperature) show that this membrane broke at pressure differences of around 1.5 bars. Because the fabricated membrane should survive handling during the fabrication process and application, a fabrication of this thin but fairly week membrane is not desirable. Therefore, we only fabricated the membranes with the thickness down to 700 nm by using the current technology.

Alternatively, equation 2 suggests that by depositing a thin metal film on a support frame that has very narrow, through-wafer etched slits (very short W), we may produce the very thin membrane while retaining its mechanical strength. For example, a 300 nm thick membrane on a supporting frame consists of through-wafer etched slits of ca. 9 μm width may withstand a pressure difference of about 3 bars. Although this support frame may be created by KOH etching of very narrow slits through the <110>-Si wafer, utilizing a so-called very high aspect ratio etching procedure [27,40,43], its etching conditions are critical; especially the steps of finding {111} planes and then aligning the slits to them (Figures 2.2.a and 2.2.b) should be done very accurately [27,40,43]. As a consequence of a highly demanding accuracy during fabricating of such a supporting frame, the membrane process to make this thin (but strong) membrane would become very time consuming (and thus expensive). Thus, we have not tried to make the very thin membrane by using the membrane process present in this chapter. Also, Deep Reactive Ion Etching (DRIE) [45] may be used to create the mentioned silicon support for producing the very thin membrane. This technique however has a low wafer throughput, and therefore not being used in our work. Nevertheless, another new membrane process development that allows fabricating the very thin but strong membranes will be presented in chapter 3.

2.6. References

[1] R. Ramachandran and R.K. Menon, "An Overview of Industrial Uses of Hydrogen", Int. J. Hydrogen Energy., 23, 593 (1998).

[2] United States Department of Energy, "A Review of the National Hydrogen Vision Meeting: A National Vision of America's Transition to a Hydrogen Economy- to 2030 and Beyond" Washington, DC, November 15-16, 2001.

[3] Hoffmann, P., "Tomorrow's Energy", The MIT Press (2001).

[4] M.S. Dresselhaus and I.L. Thomas, "Alternative Energy Technology", Nature, 414, p.332 (2001).

[5] T.N. Veziroglu, "Hydrogen Energy System as a Permanent Solution to Global Energy-Environment Problems", Chem. Ind., 53, p.383 (1999).

[6] V.A. Goltsov, "Hydrogen Treatment (Processing) of Materials: Current Status and Prospects", J. Alloy. Comp., 293-295, 844 (1999).

[7] M. Schrope, "Which Way to Energy Utopia? ", Nature, 414, 682 (2001).

[8] Koppel, T., J. Reynolds, "A Fuel Cell Primer: the Promise and the Pitfalls", Review 4, (2000).

[9] R.B. Moore and V. Raman, "Hydrogen Infrastructure for Fuel Cell Transportation**",** Int. J. Hydrogen Energy, 23, 617 (1998).

[10] R. Hughes, "Composite Palladium Membranes for Catalytic Membrane Reactors", Membr. Techno., 131, 9 (2001).

[11] R. Dittmeyer, V. Hollein and K. Daub, "Membrane Reactors for Hydrogenation and Dehydrogenation Processes Based on Supported Palladium", J. Mole. Catal. A., 173, 135 (2001).

[12] J. Shu, B.P.A. Grandjean, A. VanNeste, J. Kaliaguine, "Catalytic Palladium-Based Membrane Reactors: review", Can. J. Chem. Eng., 69, 233 (1991).

[13] Y.S. Lin, "Microporous and Dense Inorganic Membrane: Current Status and Prospective", Sep. Pur. Techno., 25, 39 (2001).

[14] A.C. Markrides, M.A. Wright, D.N. Jewett, US Patent 3,350,846 (1967).

[15] R. Goto, "Purification of Hydrogen by Selective Osmosis with Palladium Alloy Membranes", KagaKu KogaKu, 34, 381 (1970).

[16] J.E. Philpott, "Hydrogen Diffusion Technology: Commercial Applications of Palladium Membranes", Platinum Metals Rev., 29, 12 (1985).

[17] T.L. Ward and T. Dao, "Model of Hydrogen Permeation Behavior in Palladium Membranes", J. Membr. Sci., 153, 211(1999).

[18] J.P. Collins and J.D. Way, "Preparation and Characterization of a Composite Palladium-Ceramic Membrane", Ind. Eng. Chem. Res., 32, 3006 (1993).

[19] J.P. Collins, R.W. Schwartz, R. Sehgal, T.L. Ward, C.J. Brinker, G.P. Hagen, C.A. Udovich, "Catalytic Dehydrogenation of Propane in Hydrogen Permselective Membrane Reactors", Ind. Eng. Chem. Res., 35, 4398 (1996).

[20] S.I. Niwa, M. Eswaramoorthy, J. Nair, A. Raj, N. Itoh, H. Shoji, T. Namba, F. Mizukami, "A One-Step Conversion of Benzene to Phenol with a Palladium Membrane", Science, 295, 105 (2002).

[21] J.O. Brien, R. Hughes, J. Hisek, "Pd-Ag Membranes on Porous Alumina Substrates by Unbalanced Magnetron Sputtering", Surf. Coat. Technol., 142, 253 (2001).

[22] S. Yan, H. Maeda, K. Kusakabe, S. Morooka, "Thin Palladium Membrane Formed in Support Pores by Metal-Organic Chemical Vapor Deposition Method and Application to Hydrogen Separation", Ind. Eng. Chem. Res., 33, 616 (1994).

[23] S.E. Nam and K.H. Lee, "Hydrogen Separation by Pd Alloy Composite Membrane: Introduction of Diffusion Barrier", J. Membr. Sci., 192, 177, (2001).

[24] A.J. Burggraaf, "Key Points in Understanding and Development of Ceramic Membranes", In Proc. ICIM 3, 1 (1994).

[25] F. Roa, J.D. Way., R.L. McCormick., S.N. Paglieri., "Preparation and Characterization of Pd-Cu Composite Membranes for Hydrogen Separation", J. Chem. Eng., 93, 11 (2003).

[26] K.D. Wise and K. Najafi, "Microfabrication Techniques for Integrated Sensors and Microsystems", Science, 254, 1335 (1991).

[27] M.C. Elwenspoek and H.V. Jansen, "Silicon Micromachining", Cambridge, 1999.

[28] M.J. Madou**, "**Fundamentals of Microfabrication: The Science of Miniaturization", CRC Press, 2002.

[29] M.U. Kopp, A.J. de Mello, A. Manz**, "**Chemical Amplification: Continuous-Flow PCR on a Chip", Science, 280, 1046 (1998).

[30] K.F. Jensen, "Chemical Kinetics: Smaller, Faster Chemistry", Nature, 393, 735 (1998).

[31] A.V. Berg, W. Olthuis , P. Bergveld, (eds), "Micro Total Analysis System," Kluwer Academic Press (2000).

[32] M. Matlosz, W. Ehrfeld, J.P. Baselt, (eds), "International Conference on Microreaction Technology 5,"(IMRET5), Springer (2001).

[33] M. Matlzosz, S. Rode, J.M. Commenge, "Microstructures for Smart Reactors: Precision Performance in Industrial Production", Proc. International Conference on Microreaction Technology 5 (IMRET5), 13, Springer (2001).

[34] C. Wille, V. Autze, H. Kim, U. Nickel, S. Oberbeck, T. Schwalbe, L. Unverdorben, "Progress in Transferring Microreactors from Lab into Production –an Example in the Field of Pigment Technology", Proc. International Conference on Microreaction Technology 6 (IMRET6), 7 (2002).

[35] A.J. Frank, K.F. Jensen, M.A. Schmidt, " Palladium Based Membranes for Hydrogen Separation and Hydrogenation/Dehydrogenation," Proc. IEEE. MEMS 99, 382 (1999).

[36] S.V. Karnik, M.K. Hatalis and M.V. Kothare, "Towards a Palladium Micro-Membrane for the Water Gas Shift Reaction: Microfabrication Approach and Hydrogen Purification Results", J. Microelectromech. Syst., 1, 93 (2003).

[37] F.C. Gielens, H. D. Tong, C.J.M. Rijn, M.A.G. Vorstman, J.T.F. Keurentjes, "High-flux Palladium-Silver Alloy Membranes Fabricated by Microsystem Technology", Desalination 147, 417 (2002).

[38] H.D. Tong, J.W. Ervin Berenschot, M.J. De Boer, J. G. E. Gardeniers, H. Wensink, H.V. Jansen, W. Nijdam, M.C. Elwenspoek, F.C. Gielens, and C.J.M. Rijn, "Microfabrication of Palladium–Silver Alloy Membranes for Hydrogen Separation", J. Microelectromech. Syst., 12, 622 (2003).

[39] H.T. Hoang, H.D. Tong, F.C. Gielens, H.V. Jansen, M.C. Elwenspoek, "Fabrication and Characterization of Dual Sputtered Pd–Cu Alloy Films for Hydrogen Separation Membranes", Materials Letters, 58, 525 (2004).

[40] D.L. Kendall, "Vertical Etching of Silicon at Very High Aspect Ratios", Rev. Instr. Sci., 9, 373 (1979).

[41] M. Vangbo and Y. Backlund, "Precise Mask Alignment to the Crystallographic Orientation of Silicon Wafers Using Wet Anisotropic Etching", J. Micromech. Microeng., 6, 279 (1996).

[42] P. Krasuse, E. Oermeier and W. Wehl,"Backshooter- a New Smart Micromachined Single –Chip Inkjet Printhead", Proc. IEEE. Transducer'95, 325 (1995).

[43] A. Holke and H.T. Henderson, "Ultra-deep Anisotropic Etching of (110) Silicon", J. Micromech. Microeng, 9, 51 (1999).

[44] H. Wensink, "Fabrication of Microstructures by Powder Blasting", PhD thesis, University of Twente (2002).

[45] M.J. De Boer, J.G.E. Gardeniers, H.V. Jansen, M.J. Gilde, G. Roelofs, J.N. Sasserath, and M.C. Elwenspoek, "Guidelines for Etching Silicon MEMS Structures Using Fluorine High Density Plasmas at Cryogenic Temperatures," J. Micromech. Syst., 11, 385 (2002).

[46] S. Kuiper, Development and Application of Microsieves, Ph.D thesis, University of Twente (2000).

[47] C.J.M. van Rijn, M. Wekken, W. Nijdam and M.C. Elwenspoek, " Deflection and Maximum Load of Microfiltration Membrane Sieves Made with Silicon Micromachining," J. Microelectromech. Syst., 6, 48 (1997).

[48] http://www.Goodfellow.com.

[49] M. Ohring, "The Material Science of Thin films", Academic Press (1992).

[50] J.L. Vossen and W. Kern, "Thin Film Processing II", Academic Press (1991).

Chapter 3

Palladium-based membranes on a supporting microsieve

Abstract

Very thin, strong and defect-free palladium-based membranes (Pd, Pd-Ag, Pd-Cu) are fabricated on a supporting microsieve by using techniques of microfabrication technology. The microfabricated membrane obtains high separation fluxes of up to 4 mol H_2 /m^2.s with a minimal selectivity of 1500 for hydrogen over helium (H_2/He) at 723 K and 0.83 bars H_2 retentate pressure. Furthermore, the present technology can be used to fabricate other kinds of ultrathin but strong and defect-free membranes to setup new applications.

3.1. Introduction

In chapter 2, we presented the relatively simple process to make Pd and Pd-Ag alloy membranes directly on <110>-Si substrates; the membranes with thickness down to 700 nm were successfully fabricated and tested. Because this process development is simple, it may produce the membranes at low-cost. However, as discussed in the previous chapter, its main limitation is that it is difficult to fabricate very thin membranes for higher hydrogen separation fluxes - membranes with a thickness in the range of a few hundred of nm, while retaining the membrane mechanical strength. Therefore, in this chapter we present another membrane fabrication procedure that allows us to make the desired membranes. Instead of holding the metal films by the <110>-Si support with a limitation of making a very small support size (the slit size), the thin metal films are now supported by a microsieve with micron-sized pores. This allows the fabrication of thin but strong membranes. The membranes are fabricated by using microfabrication techniques like thin film sputter deposition, KOH etching of silicon, and dry etching of silicon nitride, and anodic wafer bonding [1-3]. The microfabrication, the membrane performance with respect to hydrogen separation, and selectivity are presented and discussed.

3.2. Microfabrication of membrane module

3.2.1. Microfabication of membrane on a supporting microsieve

A cross-section of the Pd-Ag membrane module is shown in Figure 3.1. A Pd-Ag membrane is microfabricated on a supporting microsieve on a <110> silicon wafer (<110>-Si), then sandwiched between two thick glass wafers to form a membrane module.
The process steps to come to the Pd-Ag membrane are shown in Figure 3.2, and are as follows: a 4 inch, double side polished <110>-Si is coated with 0.2 μm of wet-thermal silicon dioxide (SiO_2) and 1 μm of low-stress silicon-rich silicon nitride (SiN) by means of low-pressure chemical vapour deposition (LPCVD) [4]. Parallelogram-shaped structures of 600 by 2600 μm are aligned and imprinted on the backside of the wafer by standard photolithography, followed by a dry (CHF_3 + O_2) etching of the SiN and wet etching of the oxide layer, using a buffered hydrofluoric acid (BHF) (Figure 3.2.a).

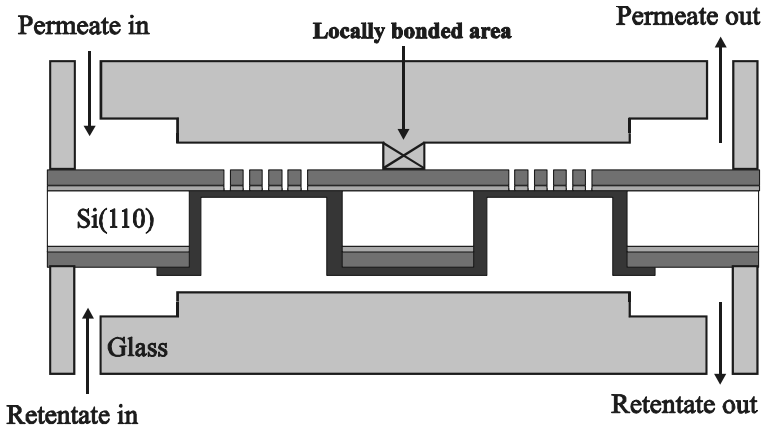

***Figure 3.1**: Cross-section of the separation membrane module; only two Pd-Ag membrane/microsieve segments are drawn for an illustration.*

The wafer is immersed in 25% KOH solution at 75 ^{o}C to etch the silicon until the SiO_2 layer is reached, thus forming an array of suspended bilayer SiN/SiO_2 membranes (Figure 3.2.b). Afterwards, standard lithography and dry etching of SiN are carried out on the front-side of the wafer to pattern a microsieve with circular openings of 5 μm [9-10] on the suspended SiN/SiO_2 membranes. The SiN dry etching process is controlled to stop on the SiO_2 layer, thus creating a SiN microsieve on top of the SiO_2 membrane (Figure 3.2.c). From hereon, we define a group of circular sieves patterned in one suspended SiN/SiO_2 membrane as one microsieve segment of the whole microsieve wafer. At this stage, alloy films of Pd-Ag are deposited by simultaneous (dual) sputtering from pure targets of Pd and Ag (99.999%; Engelhard-Clal Co.) on the flat side of the SiO_2 membrane (the side without microsieves), using titanium (Ti) as an adhesion layer (Figure 3.2.d). The detailed dual-sputtering procedure and the properties of the-as deposited Pd-Ag films will be reported in chapter 5. In the current work, we deposit Pd-Ag films with thickness from 1000 down to 100 nm with a Ag content of 23 at wt%. Besides Pd-Ag, Pd and Pd-Cu films are also deposited on the supporting microsieves.

Next, the SiO_2 and then the Ti are removed in BHF solution through the opening of the sieves to reveal the back surface of the Pd-Ag film, therefore forming a Pd-Ag membrane (Figure 3.2.e). A detailed design of the parallelogram-shaped structure that can be etched by potassium hydroxide solution (KOH) into <110>-Si is depicted in Figure 3.3.a [5-8].

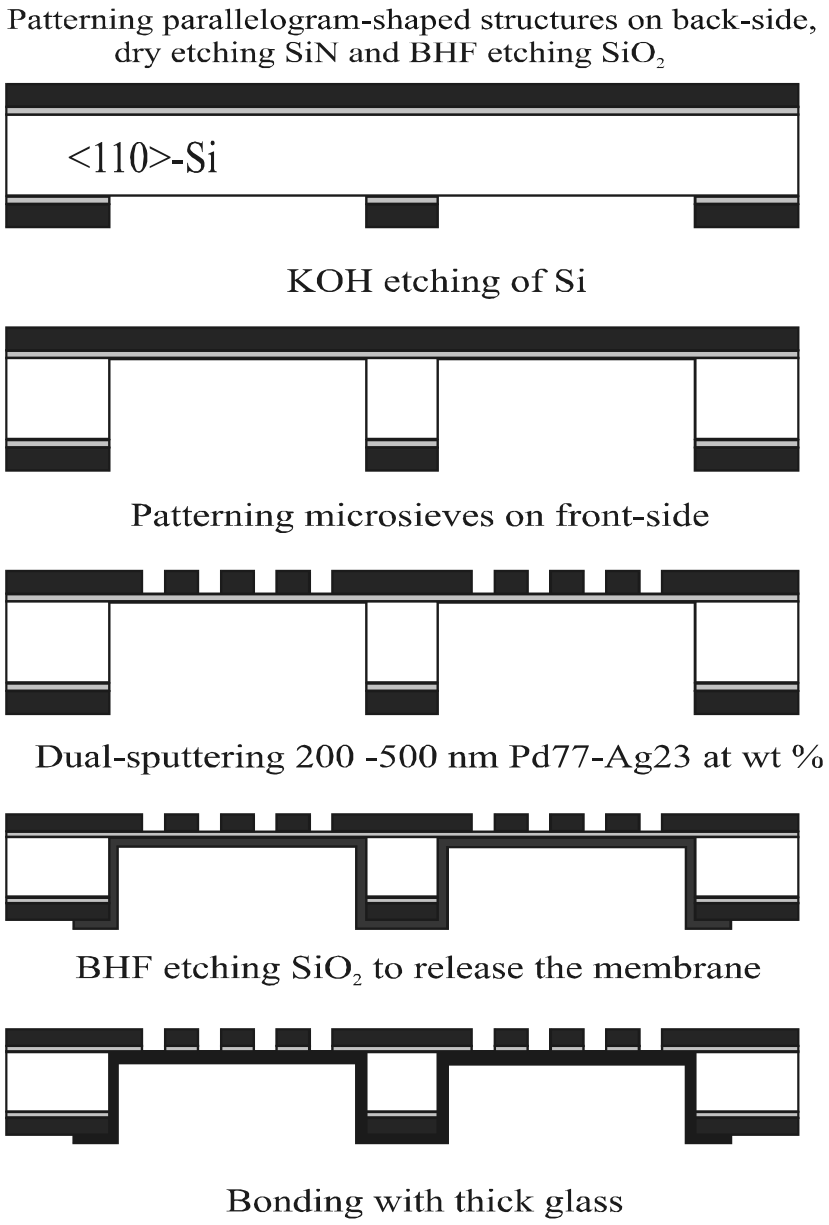

***Figure 3.2**: Fabrication process of the Pd-Ag membrane module.*

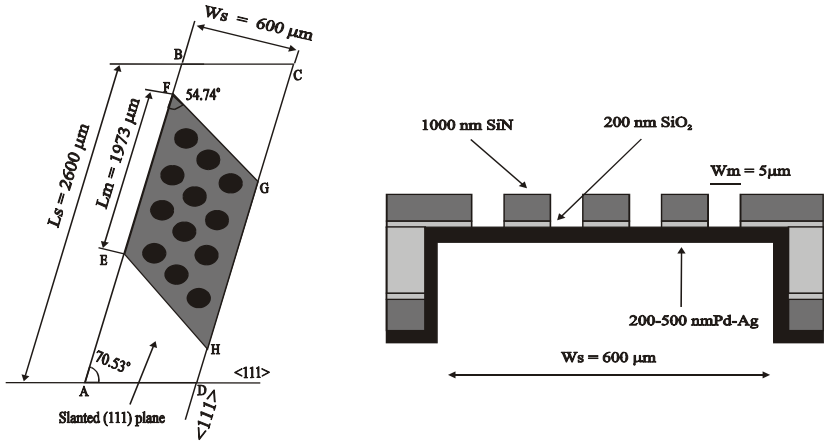

(a) **(b)**

Figure 3.3*: (a) A parallelogram-shaped structure (ABCD) is KOH etched through a <110>-Si, creating a suspended bilayer SiN/SiO_2 membrane (EFGH). (b) A cross-section of one membrane segment shows the Pd-Ag film/microsieve.*

(b)

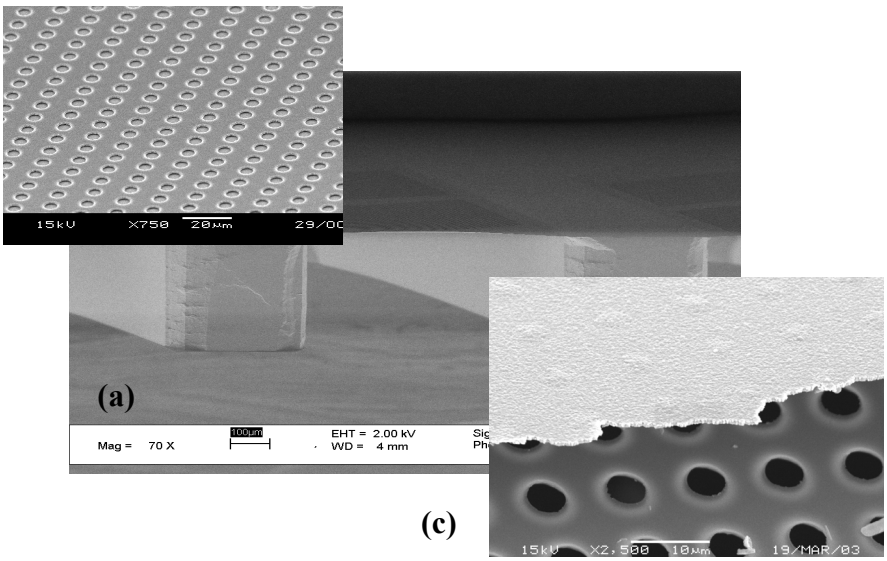

(c)

Figure 3.4: *SEM pictures of the microfabricated membrane. (a) An overview of membrane and support structure in <110>-Si. (b) Pd-Ag film on the SiN microsieve as seen from top of Figure (a); (c) Partial Pd-Ag film on the SiN microsieve as seen bottom of Figure (a).*

A cross-section of the Pd-Ag membrane on the microsieve segment is depicted in Figure 3.3.b, while Figure 3.4 is a Scanning Electron Microscopy image (SEM) of ca. 500 nm Pd-Ag membrane on the SiN supporting microsieve. As shown, the fabricated Pd-Ag membrane is uniform in thickness, and has a smooth surface, and seems to be defect-free.

As mentioned above, *depositing the film on the planar surface of the sacrificial layer (SiO_2 in our case) and release it later seems to be the key point to obtain such good submicron films*. Additional advantages like a low gas transfer resistance etc. of the present microfabricated structures used for hydrogen separation will be further discussed in the measurement chapter (chapter 6).

3.2.2. Membrane packaging and the construction of a large membrane module

Finally, the silicon wafer is bonded between two glass wafers as described in the previous chapter (section 2.2.3) [11-12].

The present packaging membrane technology would allow the construction of a larger module, in which the larger (and thicker) glass plates are used to house a number of membrane wafers (Figure 3.5), thus obtaining large Pd area for separation. Additionally, this larger module can be operated in a parallel mode, thus using the principle of "numbering-up"[13,14] instead of scaling-up to increase hydrogen throughput. This proposed unit may find the application in an on-site hydrogen production system, where small, natural gas-based reformers, being developed for distributed fuel cell power system, could potentially be used to generate hydrogen rich reformate streams. Purification is an essential step to remove impurities in the reformate that may poison the storage unit or fuel cell, and to remove non-hydrogen species that can dramatically increase the size of the on-site and on-board storage system [15].

The numbering-up principle has certain advantages over conventional scale-up. Conventional scale-up entails going from laboratory scale to a single large unit through a series of costly laboratory experiments, simulations, and pilot plan testing [16]. While, as each microfabricated-based membrane would behave exactly alike, individually and in replicated units, numbering-up would be considerably shorter and less expensive, allowing for faster transfer time to the market etc. We think that in the certain application, these advantages provided by the numbering-up of the microfabricated membrane may override the economies of conventional large plants.

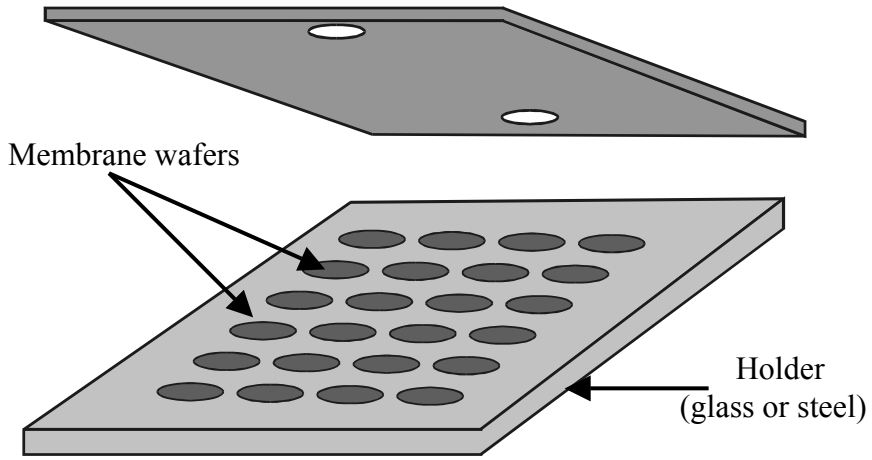

***Figure 3.5**. A numbering-up of membrane wafers.*

3.3. Microfabrication results and discussion

3.3.1. Membrane on the supporting microsieve

The width of the microsieve segment is equal to that of the-as designed parallelogram-shaped structure of 650μm (Figure 3.3), while its length *Lm* is given by [5]:

$$Lm \sim Ls - 2\sqrt{3}\,t + \frac{3\sqrt{2}}{4}W \qquad (1)$$

with *Ls* the length and *W* the width of the parallelogram-shaped structure, and t the thickness of silicon wafer. Applying equation (1) with *Ls* = 2600 μm, *t* = 380 μm and *W* = *Ws* = 600 μm, gives a length *Lm* of 1920 μm. As a result, etching one parallelogram-shaped structure of 2600 μm by 600 μm through a <110>-Si creates a suspended area of ca. 1920 μm by 600 μm for later sieves patterning. In the current design, the porosity of the supporting microsieve, and therefore the porosity of the Pd-Ag film in the microsieve, is about 20 % (see Figure 3.4.c). Thus one microsieve segment creates an effective area of ca. 0.23 mm^2 for hydrogen separation. And several hundreds of such microsieve

segments could be patterned in the 4 inch silicon wafer to create a large total membrane area for hydrogen separation.

3.3.2. Mechanical strength of the membrane

The mechanical strength of the membrane depends on that of the Pd-Ag film on the SiN microsieve and the SiN microsieve, which are discussed in a next paragraph.

According to van Rijn et al., the maximum trans-membrane pressure P_{max} for a thin, brittle membrane is calculated as [9]:

$$P_{\max} = 0.58 \frac{t\sigma_{yield}^{3/2}}{WE^{1/2}} \tag{2}$$

where t is the thickness of the membrane, σ_{yield} the yield strength of the membrane material, W the width of the shortest side of the membrane, and E the Young's modulus of the membrane material. For a perforated membrane - *the microsieve membrane*, this has to be multiplied by a strength reduction K (K<1) due to the perforation [9]:

$$P_{\max} = 0.58K \frac{t\sigma_{yield}^{3/2}}{WE^{1/2}} \tag{3}$$

Setting equation 3 for the SiN microsieve resting on the silicon support with $\sigma_{yield} = 4*10^9$ Pa, $E = 2.9*10^{11}$ Pa, $W = Ws = 600$ μm, $t = 1$ μm, and $K = 0.7$, we find a P_{max} of ca. 3.2 bars for the present supporting microsieve. In addition, equation 3 suggests that one may produce a stronger supporting microsieve by reducing its width.

Van Rijn et al., also derived an equation that may be used to predict the breaking pressure for the ductile material membranes [9]:

$$P_{\max} = 6.4 \frac{t\sigma_{yield}^{3/2}}{WE^{1/2}} \tag{4}$$

Supposing that the deposited Pd-Ag membrane behaves like the ductile materials, setting equation 4 with $\sigma_{yield} = 80*10^6$ Pa, $E = 112*10^9$ Pa, $W = Wm = 5$ μm, $t = 0.5$ μm, we find a P_{max} of ca. 13 bars for the 500 nm thick Pd-Ag film

resting on the current microsieve. Also, the thinnest fabricated membrane of 100 nm thick Pd-Ag on a microsieve with a smaller pore size of 3 μm may withstand a pressure difference of ca. 4 bars.

The rupture strength of the membranes at room temperature is measured in the set up that was described in [9]. Tests showed that the 500 nm thick Pd-Ag membrane on the current microsieve design broke at pressure differences of 4.5 ±0.5 bars between the two sides of the membrane. This measured membrane strength is about 50 % higher than the expected value of 3 bars.

Additionally, the mechanical strength of several other membranes is measured and data is given in Table 3.1. Note that an expected broken pressure

Table 3.1*: Mechanical strength of the Pd-Ag membranes on the microsieve.*

METAL FILM THICKNESS (NM)	SIEVE SIZE (μM)	EXPECTED BROKEN PRESSURE OF THE MICROSIEVE (BAR)	EXPECTED BROKEN PRESSURE OF THE METAL FILM (BAR)	EXPECTED BROKEN PRESSURE (BAR)	MEASURED BROKEN PRESSURE (BAR)
500	5	3.2	13	3.2	4.5±0.5
250	5	2	5	3.2	3.4±0.5
100	3	3.2	3.5	3.2	2 ±0.3*

** The microsieve was not broken, only the metal film was broken.*

of the two component membrane -Pd-Ag film/microsieve membrane in Table 3.1 was equally taken to that of a weaker component, normally the supporting microsieve. And the mechanical strength test is performed for 5 to 7 times for each membrane. We observe from the mechanical tests that the strength of the membranes with the thickness down to about 250 nm is reasonable to the predicted values. However, the strength of the 100 nm thick membrane is much lower than expected. The use of the mechanical properties of the bulk materials (E and σ_{yield}) in predicting the strength of this very thin membrane might be far

from appropriate. It is well known that the mechanical properties of the very thin films may significantly differ with that of the thick films [17-18]. Nevertheless, based on the result of the mechanical strength tests we conclude that the membranes are mechanically strong enough to operate under the desired pressure gradient.

3.4. Preliminary hydrogen permeation results

Because the separation results will be described in detail in chapter 6, the separation results are therefore briefly presented in a next paragraph.

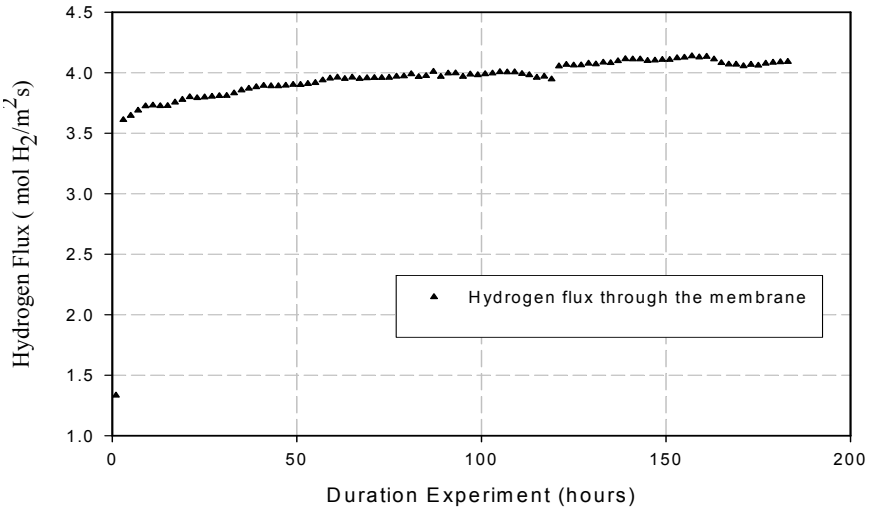

Figure 3.6*: Hydrogen flow rate through the membrane as a function of time at temperature of 723 K, hydrogen pressure of 0.83 bars in retentate. Note that after measuring for ca.125 hours, the feed flow rate was increased 50% from 600 to 900 ml.min^{-1}.*

3.4.1. Separation flux

The permeability of the membrane was determined for H_2 and helium (He). The hydrogen flow rate through the 500 nm Pd-Ag membrane versus the duration of

the experiment is given in Figure 3.6. The flux is defined as the molecular hydrogen flow through the membrane divided by the free Pd-Ag area (mol $H_2/m^2.s$). At a membrane temperature of 723 K and a hydrogen partial pressure of 0.83 bars at the retentate, a high hydrogen flux of ca. 4 mol $H_2/m^2.s$ is measured. This flux is one to two orders of magnitude higher than that of the conventional membranes [19-29], and is reasonable to that of the microfabricated membranes [30-31] (see Table 6.2). More measurement results will be presented in chapter 6.

3.4.2. Membrane selectivity

Possible membrane leaks during the permeation experiment can be detected by measuring the He concentration at the permeate side. However, no He was found during the experiments. Therefore, in order to calculate a minimum selectivity of H_2 over He, the detection limit of the gas chromatograph for He is used as the maximum He concentration. In this way, a minimal separation factor of 1500 for H_2 to He (or equivalent to about 4000 for H_2 to N_2) is calculated. This high selectivity indicates that the microfabricated membrane is most likely defect-free. We believe that depositing the Pd-Ag separation layer on a very smooth and clean silicon oxide layer, and preparing the membrane in a dust-poor clean room environment were the key parameters to get to this result [32].

3.5. Discussion and conclusions

Very thin and strong Pd-Ag alloy membranes were microfabricated and tested. The Pd-Ag films were sputtered onto a planar surface support (SiO_2/SiN microsieve) and released later, creating defect free, submicron thick Pd-Ag films. The fabrication method also allows the creation of large membrane modules that consist of a number of membrane wafers, thus obtaining a large Pd area for separation.

The microfabicated membranes achieved high permeation rate and high hydrogen selectivity although the flux through the thinnest membranes have not been determined yet; flow rates of ca. 4 mol $H_2/m^2.s$ were measured with a selectivity above 1500 for H_2/He.

Table 3.1 shows that by depositing metal films on the supporting microsieve allows us to obtain thinner and stronger membranes in comparison with the membranes fabricated by using the technology presented in chapter 2.

***Table 3.2**: Advantages and limitations of the two membrane processes.*

	WAFER SUPPORT	EXTRA LAYER ON THE SUPPORT	ETCHING OF THE EXTRA LAYER	FABRICATION OF MICRON THICK MEMBRANE	FABRICATION OF ULTRA THIN MEMBRANE
Process chapter 2	<110>	SiO_2	Wet	Yes	Difficult
Process chapter 3	<110>, <100>*	SiO_2 + SiN	Wet + dry	Yes	Yes

** Note that <100>-Si wafer can also be used as the support for the microsieve.*

For example, the mechanical strength of the 500 nm thick membrane on the supporting microsieve is ca. 30% higher than that of the 1000 nm thick membrane fabricated in chapter 2.

However, a flux of ca. 4 mol $H_2/m^2.s$ was measured through the 500 nm thick Pd-Ag membranes. This flux is only ca. 10% higher than that through the 700 nm thick membrane presented in the chapter 2 although the membrane thickness was reduced by 40%. As will be discussed in chapter 6 that the hydrogen transport through submicron Pd-Ag film seems to be governed by surface reactions, the separation flux is therefore not proportionally increased by a reduction of the membrane thickness [20-22,25].

Although the separation result has not yet proved advantages in comparison to that reported in chapter 2 (see detail data on Table 6.2), the technology developed in this chapter suggests that it is possible to produce several kinds of membranes. These membranes can be metal and non-metal, which may setup new applications [33-34]. For example, if an ultrathin 10-nm

SiN membrane (t = 0.01) is supported on a microsieve with 5 μm sieves (W = 5 μm), this membrane may withstand a pressure difference of ca. 4.7 bars (see equation 3). Actually, this SiN membrane will be fabricated in the next chapter for creating a nanosieve membrane [33]. Additionally, the technology present here may be used to fabricate Ag-based membranes for oxygen separation [35].

Although the current membrane process has above advantages from a fabrication as well as an application point of view in comparison with the technology presented in the chapter 2, its main draw back is that it requires the use of a defect free SiN layer. The SiN material is inert to most wet etching solutions, dry etching procedure is needed to pattern structures. Consequently, the use of the SiN layer will certainly result in a higher membrane fabrication cost. Advantages and limitations of the two membrane processes are summarized in Table 3.2.

3.6. References

[1] K.D. Wise and K. Najafi, "Microfabrication Techniques for Integrated Sensors and Microsystems", Science, 254, 1335 (1991).

[2] M.C. Elwenspoek and H.V. Jansen, "Silicon Micromachining", Cambridge, 1999.

[3] M.J. Madou**, "**Fundamentals of Microfabrication: The Science of Miniaturization", CRC Press, 2002.

[4] J.G.E. Gardeniers, H. Tilman, C.C.G. Visser, "LPCVD Silicon-Rich Silicon Nitride Films for Applications in Micromechanics, Studied with Statistical Experimental Design" J. Vac. Sci. Technol., A14, 2879 (1996).

[5] D.L. Kendall, "Vertical Etching of Silicon at very High Aspect Ratios", Rev. Instr. Sci., 9, 373 (1979).

[6] M. Vangbo and Y. Backlund, "Precise Mask Alignment to the Crystallographic Orientation of Silicon Wafers Using Wet Anisotropic Etching", J. Micromech. Microeng., 6, 279 (1996).

[7] P. Krasuse, E. Oermeier and W. Wehl,"Backshooter- a New Smart Micromachined Single –Chip Inkjet Printhead", Proc. IEEE. Transducer'95, 325 (1995).

[8] A. Holke and H.T. Henderson, "Ultra-deep Anisotropic Etching of (110) Silicon", J. Micromech. Microeng, 9, 51 (1999).

[9] C.J.M. van Rijn, M. Wekken, W. Nijdam and M.C. Elwenspoek, " Deflection and Maximum Load of Microfiltration Membrane Sieves Made with Silicon Micromachining," J. Microelectromech. Syst., 6, 48 (1997).

[10] S. Kuiper, "Development and Application of Microsieves", Ph.D thesis, University of Twente (2000).

[11] H.D. Tong, J.W. Ervin Berenschot, M.J. De Boer, J. G. E. Gardeniers, H. Wensink, H.V. Jansen, W. Nijdam, M.C. Elwenspoek, F.C. Gielens, and C.J.M. Rijn, "Microfabrication of Palladium–Silver Alloy Membranes for Hydrogen Separation", J. Microelectromech. Syst., 12, 622 (2003).

[12] H. Wensink, "Fabrication of Microstructures by Powder Blasting", Ph.D Thesis, University of Twente, 2002.

[13] M. Matlzosz, S. Rode, J.M. Commenge, "Microstructures for Smart Reactors: precision Performance in Industrial Production", Proc. International Conference on Microreaction Technology 5 (IMRET5), 13, Springer, 2001.

[14] C. Wille, V. Autze, H. Kim, U. Nickel, S. Oberbeck, T. Schwalbe, L. Unverdorben, "Progress in Transferring Microreactors from Lab into Production –an Example in the Field of Pigment technology", Proc. International Conference on Microreaction Technology 6 (IMRET6), 7 (2002).

[15] S. Lasher, M. Stratonova and J. Thijssen, " Hydrogen Technical Analysis," in Proc. of the 2001 DOE hydrogen program review.

[16] R.W. Baker, "Future Directions of Membrane Gas Separation Technology", Ind. Eng. Chem. Res., 41, 1393 (2002).

[17] M. Ohring, "The Material Science of Thin films", Academic Press (1991).

[18] J.L. Vossen and W. Kern, "Thin Film Processing II", Academic Press (1991).

[19] R. Hughes, "Composite palladium membranes for catalytic membrane reactors", Membr. Techno., 131, 9 (2001).

[20] R. Dittmeyer, V. Hollein and K. Daub, "Membrane Reactors for Hydrogenation and Dehydrogenation Processes Based on Supported Palladium", J. Mole. Catal. A., 173, 135 (2001).

[21] J. Shu, B.P.A. Grandjean, A. VanNeste, J. Kaliaguine, "Catalytic Palladium-Based Membrane Reactors: review", Can. J. Chem. Eng., 69, 233 (1991).

[22] F.A. Lewis, "The Palladium Hydrogen System", Academic Press (1967).

[23] A.C. Markrides, M.A. Wright, D.N. Jewett, US Patent 3,350,846 (1967).

[24] R. Goto, "Purification of Hydrogen by Selective Osmosis with Palladium Alloy Membranes", KagaKu KogaKu, 34, 381 (1970).

[25] T.L. Ward and T. Dao, "Model of Hydrogen Permeation Behavior in Palladium Membranes", J. Membr. Sci., 153, 211(1999).

[26] J.P. Collins and J.D. Way, "Preparation and Characterization of a Composite Palladium-Ceramic Membrane", Ind. Eng. Chem. Res., 32, 3006 (1993).

[27] J.P. Collins, R.W. Schwartz, R. Sehgal, T.L. Ward, C.J. Brinker, G.P. Hagen, C.A. Udovich, "Catalytic Dehydrogenation of Propane in Hydrogen Permselective Membrane Reactors", Ind. Eng. Chem. Res., 35, 4398 (1996).

[28] Xomeritakis, G., and Y.S. Lin, "CVD Synthesis and Gas Permeation Properties of Thin Palladium/Alumina membranes", AIChE. J., 44, 174 (1998).

[29] K.L. Yeung and A. Varma, "Novel Preparation Technique for Thin Metal–Ceramic Composite Membranes", AIChE J., 41 (9), 2131 (1995).

[30] A.J. Frank, K.F. Jensen, M.A. Schmidt, " Palladium Based Membranes for Hydrogen Separation and Hydrogenation/Dehydrogenation," Proc. IEEE. MEMS 99, 382 (1999).

[31] S.V. Karnik, M.K. Hatalis and M.V. Kothare, "Towards a Palladium Micro-Membrane for the Water Gas Shift Reaction: Microfabrication Approach and Hydrogen Purification Results", J. Microelectromech. Syst., 1, 93 (2003).

[32] R.M. Vos and H. Verweij, "High-Selectivity, High-Flux Silica Membranes for Gas Separation," Science, 279, 1710 (1998).

[33] H.D. Tong, H.V. Jensen, V.J. Gadgil, C.G. Bostan, E. Berenschot, C.J.M. van Rijn, M.C. Elwenspoek, "A Silicon Nitride Nanosieve Membrane", Nanoletter, 2004.

[34] C.J.M. van Rijn, "Nano and Micro Engineered Membrane Technology", Elsevier Science (2004).

[35] R.E. Coles, "The Permeability of Silver to Oxygen", Brit. J. Appl. Phys.,14,342(1963).

Chapter 4

A silicon nitride nanosieve membrane

Abstract

An array of very uniform cylindrical nanopores with a pore diameter as small as 25 nm has been fabricated in an ultrathin micromachined silicon nitride membrane using focused ion beam (FIB) etching. The pore size of this nanosieve membrane was further reduced to below 10 nm by coating it with another silicon nitride layer. This nanosieve membrane possesses an adequate mechanical strength up to several bars of trans-membrane pressure, and it can withstand high temperatures up to 900 ^{o}C. In addition, it is inert to many aggressive chemicals such as hot concentrated potassium hydroxide (KOH), piranha ($H_2SO_4 + H_2O_2$), and nitric acid (HNO_3).

4.1. Introduction

The development of fluid-separation membranes started almost one century ago with the research on liquid filtration, and in the past decades, their use in gas separation units has been studied as well. In the beginning, these membranes consisted almost exclusively of a relatively thick layer (several micrometers) of nanoporous organic or inorganic material with nonuniform perforations and random pore diameters. Despite the success of nanoporous membranes in liquid filtration and gas separation, the selectivity and strength of the membranes are limited by the fairly broad pore-diameter distribution. However, a nanomembrane with perforations essentially of one size and cylindrical pore shape will have many potential applications, such as absolute sterile filtration (bacteria as well as viruses), size-exclusion-based separations [1-4], templates for nanosensors [5], and masks for stencils [6]. Depending on the specific application, bio- or blood- compatible materials should be used for the construction of the uniformly perforated membrane. Moreover, in most applications there is a need for nanoporous layers having an adequate mechanical strength with respect to trans-membrane pressure, a low flow resistance to enable high fluxes, and with sufficient thermal and chemical stability in harsh environments. Nanoporous membranes with arrays of cylindrical pores and uniform pore sizes between several tens down to below 10 nm will be called nanosieves in the following discussion.

Two types of nanosieves can be distinguished. The first kind uses a layer that is relatively thick with respect to the pore diameter, so that an array of nanochannels is created through the layer [2,3]. The second kind uses a membrane having a thickness on the order of or even smaller than the diameter of the nanopore so that the pores closely resemble an array of nanoholes inside the membrane. An interesting application for such an array of nanoholes is that fluid can be filtered against larger particles with a relatively high flux in comparison with an array of nanochannels. Nevertheless, for identical pore diameter, the nanochannel type has the advantage over the nanohole type of being mechanically more robust but has the disadvantage of having a much higher flow resistance. In this chapter, a technique is presented that combines the advantages of both techniques (i.e., a strong nanosieve membrane with a high throughput).

The nanopores are often machined in a suspended low-stress silicon-nitride (SiN) membrane [1,5-10] for several reasons, such as the availability of SiN membranes after standard micro system processing such as KOH etching of

a silicon support and the thermal stability and chemical inertness of SiN material. So far, electron beam lithography followed by reactive ion etching (RIE) [5,6], or FIB etching [7-10] have been used to create pores in the SiN membrane. Because the suspended SiN membrane should survive handling during the fabrication process and application, its thickness should be made adequate. However, the relatively thick membrane renders the creation of small pores due to the difficulty of etching pores with high aspect ratios. In the case of direct pore drilling by FIB, the beam diameter and especially the relative thickness of the SiN membrane limit pore diameters to 50 nm or greater [7-10].

Recently, several techniques have been developed to reduce the size of the previously FIB-drilled nanopores, but their applications for many pores are difficult [10], or time consuming [11]. However, a simple strategy to drill small pores directly by FIB is to reduce the thickness of the SiN membrane. Of course, it needs to be done without noticeably sacrificing the strength and perforated area of the membrane. In this chapter we report the fabrication of strong SiN nanosieve membranes with small and uniform poresize. The essence of the method is *the micromachining of an ultrathin nanosieve within a thin supporting microsieve using FIB with the smallest possible beam current to drill the holes*. In this way, uniform pores as small as 25 nm were drilled.

4.2. Fabrication of nanosieve membrane

Figure 4.1 is an overview of the nanosieve membrane, and Figure 4.2 shows its simplified process flow. The process starts with a microsieve supported by a <110> silicon frame (Figures 4.1.a and 4.2.a), for which its detailed fabrication process has been reported in chapter 3 [12]. This microsieve is conformally coated with 10-nm SiN by means of low-pressure chemical vapor deposition (LPCVD) [13] as shown in Figure 4.2.b. However, this layer is removed from the top of the microsieve support by dry RIE using a CHF_3/O_2 mixture. Subsequently, a wet buffered hydrofluoric acid (BHF) etching of the sacrificial SiO_2 results in a structure that has a 10-nm thin SiN membrane supported by the microsieve (Figure 4.2.b).

Finally, a dual FIB system (FEI Inc. FIB 200) with a 30-KV gallium beam is used to drill the pores in the nanomembrane and the nanosieve is formed (Figure 4.2.c). Before the FIB procedure, the samples were coated with 2 nm of chromium (Cr) to reduce charging during exposure to electron and ion

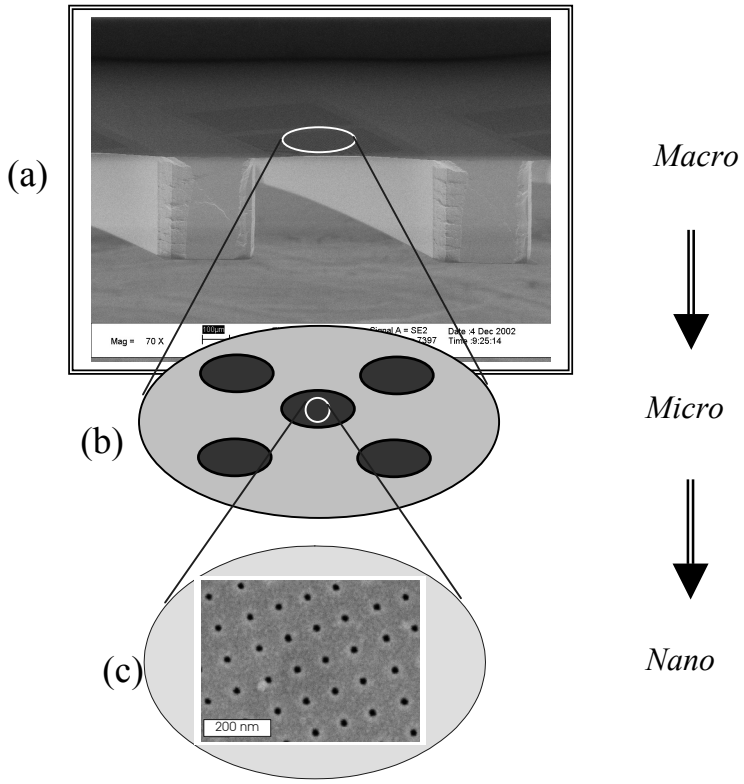

Figure 4.1*: SEM overview with close-ups of the nanosieve membrane. (a) A strong, thick silicon frame supports a thin SiN microsieve. (b) This microsieve supports a nanosieve. (c) The nanosieve.*

beams. The smallest possible FIB current of 1 pA is used, because such a current has a small beam diameter (ca. 10-nm full-width half-maximum (FWHM) corresponding to a current density of ca. 1.2 A/cm^2) and a narrow beam diameter distribution (uniform pores) [14,15]. The FIB process is controlled by a Matlab program, which digitally and repetitively scans the ion beam to make an array of pores with a dwell time of 10μs.

Figure 4.3.a is a high-resolution scanning electron microscopy image (HRSEM: LEO Gemini 1550, 2-nm lateral resolution) of the nanopores. As shown, the pores are circular with diameters of around 25 nm, and a pore pitch of around 115 nm. The drilled pores are uniform in size (<10% variation) over the whole 50×50 μm^2 patterned area. As discussed above, using a small ion beam current did enable the creation of such small pores with high uniformity.

Moreover, although the smallest current was used, the drilling time is still short due to drilling through an ultrathin layer. HRSEM images were taken from both sides of the membrane revealing that there is almost no difference between the top and bottom pore diameters. This indicates that the pore wall has a slope angle of nearly 90^{o} with respect to the lateral direction, which is consistent with the reported works that used small FIB currents [15].

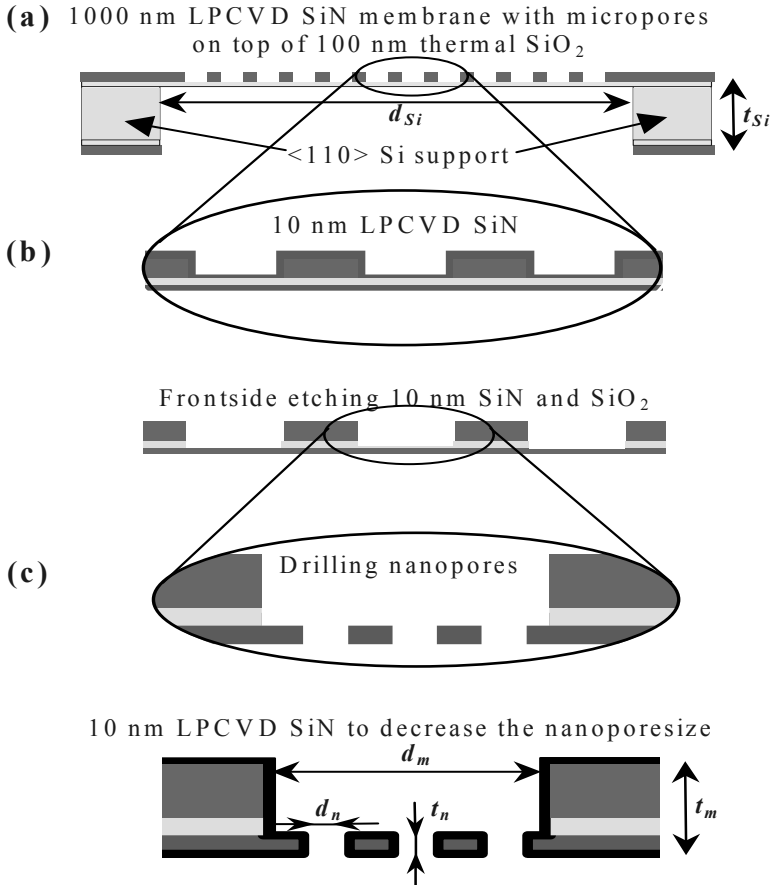

Figure 4.2*: Simplified process flow of the nanosieve membrane. (a) A<110>silicon frame is etched with KOH to support a 1000-nm thin SiN microsieve on top of a 100-nm thin SiO_2 membrane. (b) This microsieve consists of an array of 5μm circular perforations etched with RIE to support a 10-nm thin SiN nanomembrane. (c) This nanomembrane is etched with FIB with an array of nanopores forming the nanosieve.*

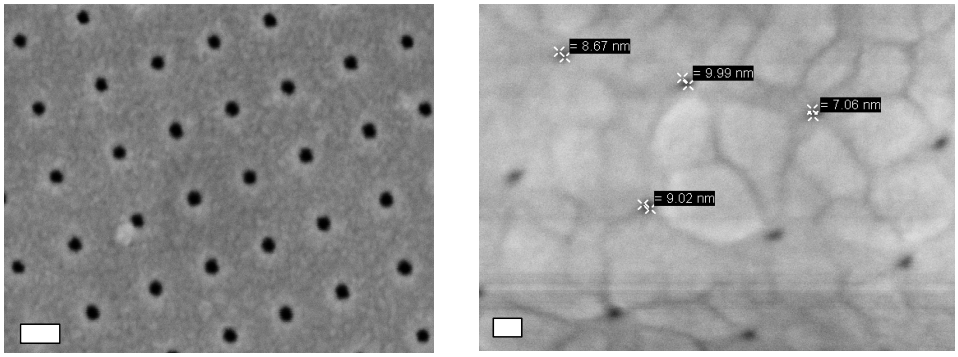

(a) (b)

Figure 4.3*: (a) Nanopores, 25 nm in diameter, were directly drilled by FIB in a 10-nm SiN membrane (110 Kx, scale bar: 50 nm). (b) Pores with sizes below 10 nm were obtained by coating the 25-nm pores with 10-nm LPCVD SiN (150 Kx, scale bar: 20 nm).*

To obtain even smaller pores, the FIB-drilled pores are coated with another ultrathin layer of LPCVD SiN. Prior to the coating, the samples were treated in oxygen plasma to remove hydrocarbon contaminants from FIB and SEM procedures, followed by the removal of Cr in a Cr etching solution; the samples were finally cleaned in deionized water. Using again LPCVD SiN has the advantage of minimizing stress due to thermal mismatch. Moreover, it exhibits conformal step coverage and high uniformity and completely covers the membrane unit [13]. The initial pores of around 25 nm (shown in Figure 4.3.a) were coated with 10-nm SiN at a deposition rate of 0.13 nm/s, and the HRSEM image of the coated pores is shown in Figure 4.3.b; all of the pores are now below 10 nm in size.

4.3. Characterization of nanosieve membrane

Important characteristics to categorize fluidic sieves are the permeability, strength, and selectivity. The permeability describes the ability of the sieve to achieve a high throughput, and the strength describes the ability of the sieve to withstand a certain flux without breaking. Finally, the selectivity describes the ability of the sieve to separate the desired component from the feed mixture.

Next, the viscous fluidic transport through the nanosieve will be discussed, and after that, we will discuss the molecular transport of gas molecules.

4.3.1. Flux calculations for liquid and gas separation

For viscous laminar flow at sufficiently small Reynolds number (Stokes or creeping flow) for a fluid medium with viscosity μ [Pa·s] through a circular opening with radius r [m] in an infinitely thin wall, the pressure difference Δp is proportional to the volume flow rate Φ_V [m^3/s] as [17]:

$$\Delta p = \Phi_V \cdot (3\mu / r^3)$$

However, for a wall with a finite thickness t, the equation is altered because of frictional losses with the walls with a correction factor of $C(t, r) = (1+8t/3\pi r)) \approx (1+0.85t/r)$ [16]. Moreover, in the case of an array of pores, the fluid flow in one pore will influence the flow in its neighboring pores. For a nanosieve with a square array of apertures and a fraction χ of perforated area, the correction is given by [21]:

$$C(\chi) = 1 - 0.344\chi^{1½} - 0.111\chi^{2½} - 0.066\chi^{3½} \approx 1 - 0.34\chi^{1½} \text{ for } \chi<20\%$$

Finally, for higher laminar flow rates an additional pressure drop will arise just before the entrance of the pores, resulting in a quadratic component to account for this nonviscous kinetic loss [22]. All the above mentioned effects were combined by van Rijn and Elwenspoek [1].

$$\Delta p = \Phi_V \cdot \left(\frac{3\mu}{r^3}\right) \cdot \left(1+\frac{0.85t}{r}\right) \cdot (1-0.34\chi^{3/2}) + \Phi_V{}^2 \cdot \left(\frac{\rho}{4\pi^2 r^4}\right) \quad \text{[Pa]} \quad (1)$$

where ρ [kg/m^3] is the mass density of the fluid medium. For water, $\rho = 998.2$ kg/m^3 and $\mu = 1.00\times10^{-3}$ Pa·s at 293 K. ($\rho = 997.0$ kg/m^3 and $\mu = 0.89\times10^{-3}$ Pa·s at 298 K.) Assuming an array of pores with 10-nm radius and 10-nm membrane thickness (i.e., $C(t, r) = 1.85$), a pore pitch of 100 nm (i.e., a density of 10^{14} pores/m^2 and a perforated fraction of 3% giving $C(\chi) = 0.995$), and neglecting kinetic losses, a trans-membrane pressure of ca. 1 bar (= 10^5 Pa) is calculated for a water flux of 2 L/m^2 s. Unfortunately, the number of nanopores is limited by the FIB system used in this study to less than 1 million, thus limiting the water flux for a nanosieve to 2×10^{-8} L/s. The kinetic losses become prominent

when $\Phi_V \geq 10^{-4} \cdot r = 10^{-12}$ m^3/s, which is 10^5 times the flux in the single nanopore; therefore, the kinetic losses are indeed negligible.

To calculate the trans-membrane pressure across the nanosieve for a certain flux of gas molecules, the mean free path λ of the molecule with respect to the pore diameter of the nanomembrane d_n is important. Following Knudsen's theory, when $d_n > \lambda/100$ many gas - gas collisions take place during transport through the orifice and the calculations closely resemble Stokes viscous flow as discussed before. However, when $d_n < \lambda$ the flow is molecular, meaning that only a few intermolecular collisions occur during transport through the membrane and the flow is limited by collisions with the walls. Therefore, for molecular gas transport the analysis of the flow is primarily a geometrical problem of determining the total open area and restrictive effect of the walls on the free flight of a molecule. Now, when two compartments are separated using a membrane with very small pores, the rate of escape through the membrane is equal to the rate at which the gas molecules strike the area of the pore. Therefore, if the area of the pore is $A = \pi r^2$ and the molar number of molecules that escape per unit time is Φ_M [mol/s], then the trans-membrane pressure can be calculated as [16]:

$$\Delta p = \Phi_M \cdot (\sqrt{2\pi MRT} / \pi r^2)$$

with M is the molar mass [kg/mol] of the gas, R is the universal gas constant [J/mol K] and T is the absolute temperature [K]. The fact that this number is proportional to $1/\sqrt{M}$ is the origin of Graham's law of effusion-the rate of effusion is inversely proportional to the square root of the molar mass M. Furthermore, the molecular flow resistance of a pore is caused by the random reflection of a low-energy molecule against the sidewall. Therefore, there is only a limited change for a molecule to enter the pore with radius r and height t (Figure 4.2.c). This correction depends on the aspect ratio $AR = t/r$ and is known as the Clausing factor $C \approx (1 + (0.46t)/(r))^{-1}$ [16]:

$$\Delta p = \Phi_M \cdot \left(\frac{\sqrt{2\pi MRT}}{\pi r^2}\right) \cdot \left(1 + \frac{0.46t}{r}\right) \qquad \text{[Pa]} \qquad (2)$$

A similar equation holds for molecular flow in the nanopore with $AR_n = t_n/r_n$ as well as in the micropore with $AR_m = t_m/r_m$. For gases, the mean free path is inversely proportional to pressure and is typically around 70 nm at a pressure

of 1 bar. This is much larger than the pore diameter of the membrane in this study; therefore, the flow is treated molecularly. Using the same sieve as in the example for viscous fluid flow with M = 0.032 kg/mol for oxygen, R = 8.3 J/mol K, and T = 293 K, a pressure drop of ca. 1 bar occurs for a gas flux of 90 mol/m^2 s, which resembles 2000 L/m^2 s; when the number of pores is limited to 1 million, this means a flux of 90×10^{-8} mol/s.

It should be noted that the hydrostatic calculation above (Equation 1) does not include the effect of electroviscous forces due to the electric double layer positioned at the interface of a fluid with the membrane surface. Electroviscous forces can be comparable to, and in some cases larger than the hydrostatic forces [23,24]. Moreover, the stick-slip flow transition, depending on the geometry and surface properties of the membrane material, may play a dominant role [25]. However, until now these effects have been studied only for relatively long channels, and more experimental data is needed to test the non-hydrostatic behavior of the nanosieve membrane. Also, the calculation concerning molecular flow (eq 2) is not aimed at applications where the gas mixture is separated with respect to molecular sizes. However, the separation of gases by nanosieve membranes with a pore diameter below 1 nm may be similar to that of silica and zeolite membranes, which was thoroughly described by Burggraaf and Cot [26]. Moreover, for low-flow conditions, the effects of leakage and outgassing may become very prominent and needs appropriate attention. Nevertheless, the hydrostatic calculations are very useful in applications concerning ultrafiltration. In filtration, generally a number of larger molecules, viruses, or gas bubbles should be separated from a fluidic medium. In such cases the exact absolute value of the flux is less important as long as all of the "unwanted" particles are filtered out completely. This is especially important in applications concerning sterile filtration.

4.3.2. Mechanical strength of nanosieve membrane

The mechanical strength of the nanosieve membrane is an important characteristic because of the fact that a high trans-membrane flux will cause a high trans-membrane pressure drop. The maximum trans-membrane pressure ΔP_{max} before a membrane with radius r_m and thickness t_n (see Figure 4.2.c) breaks may be predicted as [17]:

$$\Delta P_{\max} = 0.29.K \cdot \left(\frac{t_n}{r_m}\right) \cdot \sigma_{yield} \cdot \sqrt{\frac{\sigma_{yield}}{E}} \qquad \text{[Pa]} \quad (3)$$

with σ_{yield} the yield stress and E the Young's modulus of the membrane material, and K the non-perforated fraction of the membrane. Setting equation 3 with $\sigma_{yield} = 4\times10^9$ Pa and $E = 385\times10^9$ Pa for SiN, $r_m = 2.5\mu$m, $t_n = 0.01\mu$m, and $K = 0.8$; $\Delta P_{\max} = 3.8$ bar is calculated for the fabricated nanosieve membrane. This is close to the rupture strength of $P_{\max} = 2 \pm 0.2$ bar as found experimentally [17]. Equation 3 can be used in optimizing the dimensions of both the microsieve with respect to the silicon frame (d_{Si}, t_m), and the nanosieve with respect to the microsieve support (d_m, t_n). With respect to the ultrathin nanomembrane, it is important to notice that the layer is deposited in such a way that an atomically smooth and planar surface is guaranteed. Such extremely smooth and planar surfaces increase the strength of the membrane and exhibits a further downscaling of the membrane's thickness.

4.3.3. Chemical and temperature resistance

Experimentally, it is found that the chemical stability of the fabricated sieves is excellent; no change in the pore size is observed after dipping the membranes into aggressive solutions such as hot concentrated KOH (25% at 75 ^oC), piranha (H_2SO_4/H_2O_2 = 3/1 mixture at 100 ^oC), or $HN0_3$ (69% at 95 ^oC). Each test was conducted for 30 minutes. This property allows the nanosieves to be used in most separation environments and makes cleaning easy. In addition, the nanosieves survived at temperatures of up to 900 ^oC, allowing them to be used in harsh environments where any known polymeric membrane would fail [4].

4.4. Utilization of nanosieve membrane

The fabricated nanosieve membranes may be used for various size-exclusion-based separations in bioseparation and nanomedicine [1-4] with the advantage of gaining high separation fluxes, or improving dynamic responses of the process because of the drastic reduction in membrane thickness-10 to 30 nm for the present membranes compared to 9 μm for the microfabricated channel pores [2,3], and 100-200 μm for the polymeric membranes [4].

Additionally, the present membrane may be used as a shadow mask for stencils [5], or it may be integrated with other silicon-based components such as nanochannels [18], or nanopumps to set up innovative applications.

4.5. Conclusions

Ultrathin SiN nanosieve membranes with uniform cylindrical pores and a pore size down to below 10 nm have been demonstrated in this chapter. In addition, these nanosieve membranes possess adequate mechanical strength, possible high separation flux, and high chemical and thermal stability. These properties allow them to be used in numerous of applications in different sectors.

4.6. References

[1] C.J.M. Rijn and M.C. Elwenspoek, "Micro Filtration Membrane Sieve with Silicon Micromachining for Industrial and Biomedical Applications", IEEE Conf MEMS'95, 83 (1995).

[2] R.A. Freitas, "Nanomedicine", Stud. Health. Techno. Information., 80, 45 (2002).

[3] A.T. Desai, D.J. Hansford, L. Kulinsky, A.H. Nashat, G. Rasi, J. Tu, Y. Wang, M. Zhang, M. Ferrari, "Nanopore Technology for Biomedical Applications", Biomed. Microdevices, 2(1), 11 (1999).

[4] M. Mulder, "Basic Principles of Membrane Technology", Kluwer Academic Publishers: Norwell, MA (1998).

[5] J. Chen, M.A. Reed, A.M. Rawlett, J.M. Tour, "Large On-Off Ratios and Negative Differential Resistance in a Molecular Electronic Device", Science, 286, 1550 (1999).

[6] M.M. Deshmukh, D.C. Ralph, M. Thomas, J. Silcox, "Nanofabrication Using a Stencil Mask", Appl. Phys. Lett., 75, 1631(1999).

[7] C. Schmidt, M. Mayer, H. Vogel, "A Chip-Based Biosensor for the Functional Analysis of Single Ion Channels", Angew. Chem. Int. Ed., 39, 3137 (2000).

[8] J.E.M. Geoch, M.W. McGeoch, D.J.D. Carter, R.F. Schuman, G. Guidotti, "Biological-to-Electronic Interface with Pores of ATP

Synthase Subunit C in Silicon Nitride Barrier**",** Medical. Bio. Eng. Comput., 38, 113(2000).

[9] T. Schenkel, V. Radmilovic, E.A. Stach, S.J. Park, A. Persaud, "Formation of a Few Nanometer Wide Holes in Membranes with a Dual Beam FIB", Inter. Conf. on Electron, Ion and Photon Beam Technology and Nanofabrication (2003).

[10] J. Li, D. Stein, C. McMullan, D. Branton, M.J. Azis, J.A. Golovchenko, "Ion-Beam Sculpting at Nanometre Length Scales", Nature, 412, 166 (2001).

[11] A.J. Storm, J.H. Chen, X.S. Ling, H.W. Zandbergen, C. Dekker, " Fabrication of Solid-State Nanopores with Single Nanometre-Precision", Natural Material, 2, 537 (2003).

[12] H.D. Tong, J.W. Ervin Berenschot, M.J. De Boer, J. G. E. Gardeniers, H. Wensink, H.V. Jansen, W. Nijdam, M.C. Elwenspoek, F.C. Gielens, and C.J.M. Rijn, "Microfabrication of Palladium–Silver Alloy Membranes for Hydrogen Separation", J. Microelectromech. Syst., 12, 622 (2003).

[13] J.G.E. Gardeniers, C.C.G. Visser, H.A.C. Tilmans, "LPCVD Silicon-Rich Silicon Nitride Films for Applications in Micromechanics, Studied with Statistical Experimental Design", J. Vac. Sci. Technol. A, 14, 2879 (1996).

[14] L.R. Harriott, " Digital Scan Model for Focused Ion Beam Induced Gas Etching", J. Vac. Sci. Technol. B11, 2012 (1993).

[15] S. Lipp, L. Frey, G. Franz, E. Demm, S. Petersen, H. Ryssel, "Local material removal by focused ion beam milling and etching ", Nucl. Instrum. Methods Phys. Res., Sect.B., 106, 630 (1995).

[16] M.C. Elwenspoek and H.V. Jansen, "Silicon Micromachining", Cambridge Press, pp.216-355 (1998).

[17] C.J.M. Rijn, M. Wekken, W. Nijdam, M.C. Elwenspoek, "Deflection and Maximum Load of Microfiltration Membrane Sieves Made with Silicon Micromachning", J. Microelectromech. Syst., 6, 48 (1997).

[18] H.G. Craighead, "Nanoelectromechanical Systems", Science, 290, 1532 (2000).

[19] R.A. Sampson, "On Stoke's Current Function", Phil. Trans. Roy. Soc. London, A182, pp.449-518 (1891).

[20] Z. Dagan, S. Weinbaum, R. Pfeffer, "Theory and Experiment on the Three-Dimensional Motion of a Freely Suspended Spherical Particle at

the Entrance to a Pore at Low Reynolds Number", Chem. Eng. Sci., 38, 583 (1983).

[21] K. Tio and S. Sadhal, "Boundary Conditions for Stoke Flow Near a Porous Membranes", Appl. Sc. Res., 52, 1 (1994).

[22] S.J. Michel, "Fluid and Particle Mechanics", Pergamon Press: Oxford England, pp.101-102 (1970).

[23] P.Vainshtein and C. Gutfinger, "On Electroviscous Effects in Microchannels", J. Micromech. Microeng, 12, 252 (2002).

[24] I.H. Huisman, G. Trägårdh, C. Trägårdh, A. Pihlajamäki, "Determining the Zeta Potential of Ceramic Microfiltration Membranes using the Electroviscous Effect", J. Membr. Sci., 147 (2), 187 (1998).

[25] C. Cheikh and G. Koper, "Stick-Slip Transition at the Nanometer Scale", Phys. Rev. Lett., 91(15), 156102-1/4 (2003).

[26] A.C. Burggraaf and L. Cot, "Fundamentals of Inorganic Membrane Science and Technology", Elsevier: Amsterdam, pp.373-386 (1996).

Chapter 5

Preparation of palladium-silver alloy films by a dual sputtering technique

Abstract

Submicron thick palladium-silver alloy films with 23wt% of silver content (Pd-Ag23) have been synthesized by simultaneously sputtered from pure targets of Pd and Ag. Full characterizations of the deposited films were performed using X-ray photoelectron spectroscopy (XPS), high-resolution scanning electron microscope (SEM), high-resolution transmission electron microscope (TEM) and X-ray diffraction (XRD). The results revealed that the dual sputtering technique is a powerful method to deposit Pd-Ag alloy films with a high composition control and fine microstructures. The characterized Pd-Ag alloy films were then deposited on microfabricated support structures (chapters 2 and 3) to form Pd-Ag membranes for hydrogen separation.

5.1. Introduction

Up to now many methods have been developed to deposit Pd or Pd alloy films on porous supports to form membranes, including physical vapour deposition, electroless plating, electrodeposition, chemical vapor deposition (CVD), micro-emulsion, pyrolysis, pore-plugging by liquid impregnation and sputtering etc. [1-7]. Among the mentioned techniques, the most often used methods are electroless plating, CVD and sputtering. Under properly controlled conditions all three methods produce good quality thin Pd/Ag membranes, with hydrogen to nitrogen selectivity over 3000 at temperatures above 300 ^{o}C [9]. The two chemical methods (electroless plating and CVD) have the advantages of ease to scale up and flexibility to coat metal film on supports of different geometry, but the main disadvantage is the difficulty to control the compositions of the metal alloy deposited [5,9]. Sputtering has several advantages like: (a) synthesis of ultrathin films with minimal impurity; (b) easily controllable process parameters; (c) flexibility for synthesizing alloys; and (d) the ability to generate nanostructured films [10-13]. The last two points are very important in membrane preparation for hydrogen separation because alloy membranes help to overcome the problem of hydrogen embrittlement, while the nanostructured films may have unique size-dependent properties e.g., a high hydrogen permeation [10,11].

Due to the mentioned advantages, sputtering has frequently been used to fabricate (sub) micron thick Pd-Ag alloy layers. Mostly, such layers are obtained by sputtering from a single alloy target of Pd-Ag. However, it was found that the sputtered layers have a significantly lower Ag content than the original target, due to a short target equilibration times [14-15]. For instance, Xomeritakis and Lin found a silver concentration of 15wt% for a film sputtered from a Pd-Ag25 at wt% target [15]. To avoid this compositional control problem, this chapter focuses on the preparation of submicron thick Pd-Ag23 wt% alloy films with high composition control using a dual sputtering technique. Different techniques are used to characterize the microstructures of the deposited Pd-Ag film. This well-characterized dual sputtered Pd-Ag alloy film is deposited on the support structures (chapter 2 and chapter 3) to realize Pd-Ag membranes for hydrogen separation.

5.2. Dual sputtering experiment

5.2.1. Experiment setup and sputtering conditions

Experiments have been carried out in a DC magnetron sputtering system (Balzers Cryo, 2 inch diameter targets) that accommodates three targets, of pure Pd, Ag and Ti (99.99%; Engelhard-Clal Co.), each target having its own controllable power source. The sputter guns are arranged in a convergent manner, with the substrate rotating about its center with a speed of ca. 15-20 rpm. The metal films (Pd, Ag, or alloys) were sputtered onto 4 inch, (100) silicon substrates with 500 nm of a wet-thermal grown SiO_2 as an anti diffusion layer, mounted a distance of 13 cm from the metallic targets. Before sputtering, the system was pumped down to a base pressure of 10^{-7} mbar.

The main objective of this chapter is the fabrication of a Pd-Ag alloy membrane, which is used for high temperature hydrogen separation. The deposited film therefore should be a film with accurate composition, high-density (non-porous), crack-free, and fine grain size etc. To realize the above desired films, the well-known principle of the 'Thornton model for sputtered films' [16,17] in combination with the works of Ying and co-workers for sputtered Pd-based films [10,11] were consulted in choosing sputter pressure and sputter temperature. For instance, Ying and co-workers reported that they obtained thin, crack-free Pd films with a high-density and fine grain size at an Ar sputter pressure between 0.1 and 7 Pa [10,11]. Their claim is reasonable with a sputtering pressure that deduced from the Thornton model for sputtered films. The same authors [10,11] explained that at high sputter pressures (10-100 Pa) the metal atoms collide with argon atoms and lose energy. This cooling leads to a high supersaturation of metal atoms, which can cause homogeneous nucleation to form nanocrystalline particles in the gas phase. As the gas pressure is lowered, homogeneous nucleation decreases, and the thermal atoms are likely to deposit directly onto the substrate, forming granular thin films with grain sizes in the nanometer range. Therefore, most of our experiments have been carried out at the Ar pressure from 0.1 to 1 Pa.

Also, the work of Thornton [16,17] and others [12,13] were consulted to choose substrate temperatures during sputtering. As the melting points (Tm) of Pd and Ag are 1828 and 1234 K, respectively, sputtering the films at substrate temperatures (Ts) between 700 and 800 K (Ts/Tm ~ 0.4) would yield

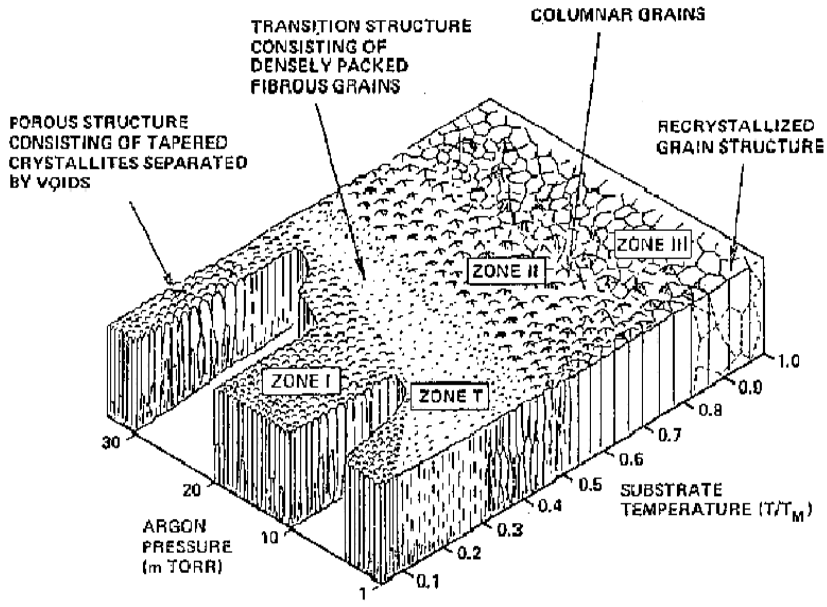

***Figure 5.1**: Structural model for sputtered films [16-17].*

high-density films with fine grain sizes. However, as Xomeritakis et al. reported that beyond a certain substrate temperature of about 700 K, tensile stresses develop in the sputtered films and may generate defects during cooling to the ambient [15], we mostly sputtered the films at the substrate temperature from 673 to 700 K. In addition, these temperatures are close to the temperature that membranes will be operated in a separation experiment (673-723 K), thus may minimize the thermal stress in the deposited film [12]. The pressure and the temperature during sputtering are given in Table 5.1. By using this set of process parameters, the realized Pd-Ag films may have microstructures that fall in a zone T in the Thornton model for sputtered films (Figure 5.1).

5.2.2. Individual sputter rate of Pd and Ag

Before doing a dual sputtering, it is important to determine an individual sputter rate of Pd and Ag. Therefore, several single sputter runs of Pd and Ag were done on silicon wafers with photoresist patterns. After sputtering, the

resist was removed by acetone in an ultrasonic bath, leaving a patterned metal layer of which the thickness was measured with a Dektak Surface Profiler (Veeco Dektak 8; 0.1 nm resolution). From these data, the sputter rate of each metal is calculated and given in the Table 5.1.

***Table 5.1**: Dual sputtering parameters for the Pd-Ag 23wt% and Pd-Cu 23wt% alloy films.*

ALLOYS	MET	PRESS. (PA)	TEMP. (K)	SINGLE SPUT. POWER (W)	SINGLE SPUT. RATE (NM/MIN)	DEN. (KG/M^3)	DUAL SPUT. POWER (W)	EXP. COMPS. (WT%)
Pd-Ag	Pd	0.1-1	673 to 700	135	25	12000	135	Pd77-Ag23
	Ag			26	8.5	10500	26	
Pd-Cu	Pd	0.1-1	300 to 700	135	25	12000	135	Pd77-Ag23
	Cu			105	10	8900	105	

5.2.3. Dual sputtering

After determining the individual sputter rate of Pd and Ag, the Pd-Ag films were synthesized by simultaneously sputtering from pure targets of Pd and Ag on the silicon substrate described in the previous section, which contained a 20 nm thick adhesion layer of Ti sputtered just before. During sputtering, the power supplies for Pd and Ag targets were 135 W and 26 W, respectively, corresponding to sputter rates of 25 nm/min for Pd and 8.5 nm/min for Ag. If these numbers are converted to weight concentrations, using (bulk) densities of

the metals, an alloy composition of Pd-Ag23 at wt % is expected. We did sputter materials at rather low sputter rates, e.g., ca. 4.1 nm/s for Pd and 1.4 nm/s for Ag, as it may help to yield films with fine- (nano-) structures [10,11]. A sputter time was used to get the desired film thickness, e.g., 15 minutes are needed to achieve a 500 nm thick Pd-Ag film. Also, the thickness of several sputtered films was checked by a Dektak Surface Profiler and by a high-resolution scanning electron microscopy (SEM). The results of these three methods were in agreement with each other.

5.3. Characterization of the dual sputtered Pd-Ag film

5.3.1. Compositions

The composition of the deposited Pd-Ag films was checked by X-ray Photoelectron Spectroscopy (XPS) (PHI Quantera Scanning ESCA Microprobe), and a representative XPS result is shown in Figure 5.2. It can be seen that the composition is constant throughout the alloy film, and that the Ag content is just a little lower than expected, which might be due to the fact that the deposition rates of the metals in the dual-sputtering state are slightly different from those in the calibration runs in which only one target was used (perhaps due to a slight interference of the plasma fields on the two targets during dual-sputtering).

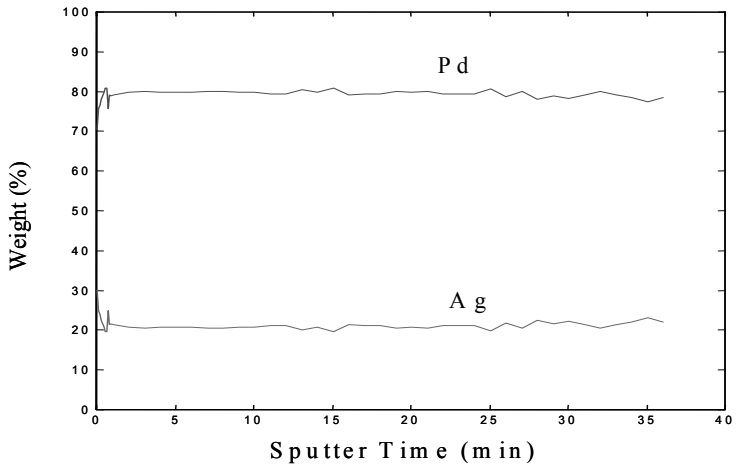

Figure 5.2*: XPS depth profile of the 300 nm dual-sputtering Pd-Ag film.*

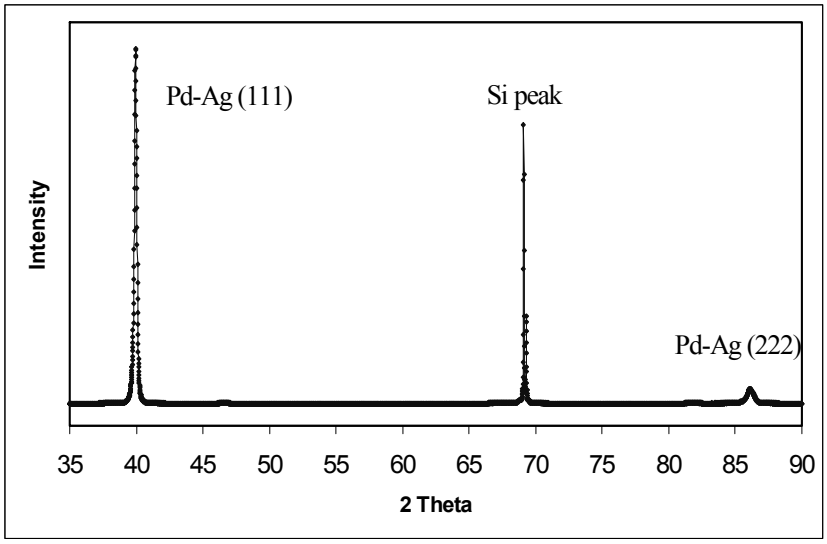

***Figure 5.3**: XRD pattern of the deposited Pd-Ag layer on a thin layer of SiO_2 on a silicon wafer.*

Furthermore, using bulk metal densities (12 $gr.cm^{-3}$ for Pd and 10.5 $gr.cm^{-3}$ for Ag) to calculate the composition of the thin film could also be a reason for the lower Ag concentration. It has often been reported that, depending on the deposition conditions, the density of sputtered films is lower than that of bulk material [13].

5.3.2. Phase and microstructures

The crystalline properties of the deposited Pd-Ag layer were investigated by X-Ray Diffraction (XRD) (Philips, CuKα radiation). The results are shown in Figure 5.3. The XRD pattern consists of (111) and (222) diffraction peaks, where the (111) peak corresponds to a lattice spacing of 2.268 Å, to be compared with the corresponding {111} lattice spacing of pure Pd and pure Ag of 2.246 Å and 2.359 Å [15], respectively. The results indicate that the deposited Pd-Ag layer was an alloy of pure Pd and pure Ag, and exhibits a preferential orientation in the [111] direction.

The average crystallite size was calculated by applying Scherrer's equation to the (111) peak and found to be about 35 nm, which is quite

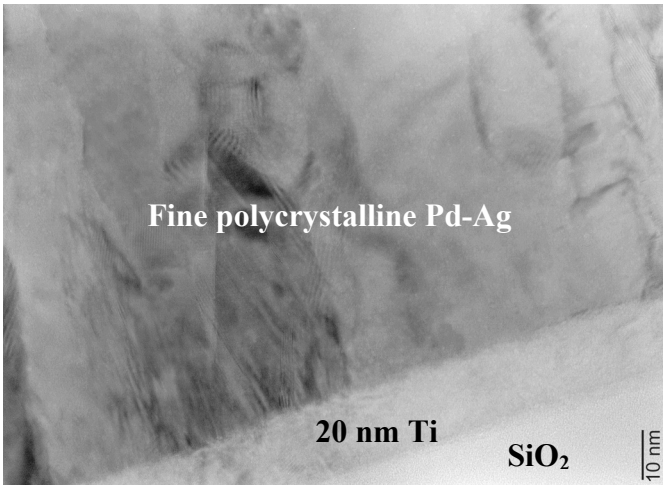

***Figure 5.4**: TEM image of the Pd-Ag film shows a non-porous film with fine polycrystalline structures.*

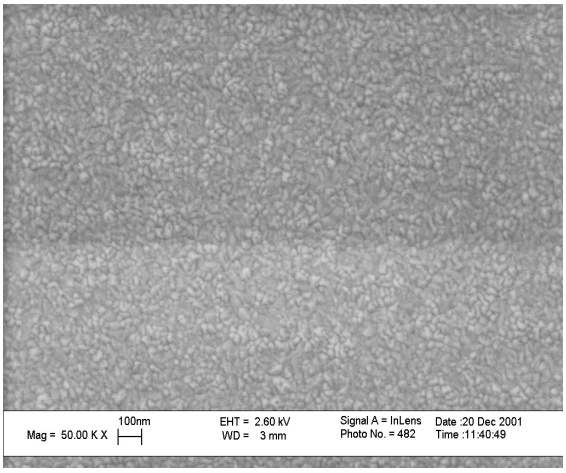

***Figure 5.5**: SEM image of the dual Pd-Ag film, deposited at the substrate temperature of 673 K.*

consistent with the grain size of sputtered Pd-Ag layer reported by Xomeritakis et al [15]. However, this grain size was about 2 times higher than that reported for the nanostructured Pd films [10,11], probably due to the fact

that our films were synthesized at higher substrate temperature than in [10,11]. Although the substrate heater was turned-off after the sputtering, the substrate (in vacuum) was still at high temperatures for several hours, makes the film grain growths.

Additionally, the microstructures of the deposited Pd-Ag film were studied by a transmission electron microscope (TEM) (Philips CM30 Twin STEM) and presented in Figure 5.4. As can bee seen that the layer is a non-porous film with fine polycrystalline structures.

Furthermore, the surface morphology of the layer was investigated by a high-resolution scanning electron microscope (SEM) (LEO Gemini 1550 FEG-SEM) and shown in Figure 5.5. As shown, the Pd-Ag film has smooth and uniform surface. The grain size of the film is about 40 to 50 nm (as looked on the surface), which is a little larger than that by the X-ray calculation.

5.4. Fabrication of Pd-Cu alloy

We also used the dual sputtering to fabricate other metal alloy membranes like Pd-Cu for hydrogen separation [18]. A reason for fabricating the Pd-Cu membrane is that the Pd-Cu membrane has been reported to have high resistance to poisoning by hydrogen sulfide and sulfurous constituents in gas mixtures while maintaining a desirable set of properties [19,20]. Sputter parameters for realizing the Pd-Cu alloy films is given in Table 5.1. About 20 Pd-Cu alloy membranes with thickness from 200 to 750 nm were successfully fabricated, then tested with respect to the hydrogen separation (see chapter 6 for separation results).

The results of the thin film fabrication suggest that the dual sputtering method may be used to fabricate many other types of alloy films with highly accurate compositional control for other applications [21,22].

5.5. Application in membrane fabrication

Finally, the characterized Pd-Ag films with the thickness from 100 to 1000 nm are deposited on the microfabricated supporting structures (chapter 2 and chapter 3) to form the Pd-Ag membranes for hydrogen separation. Figure 5.6

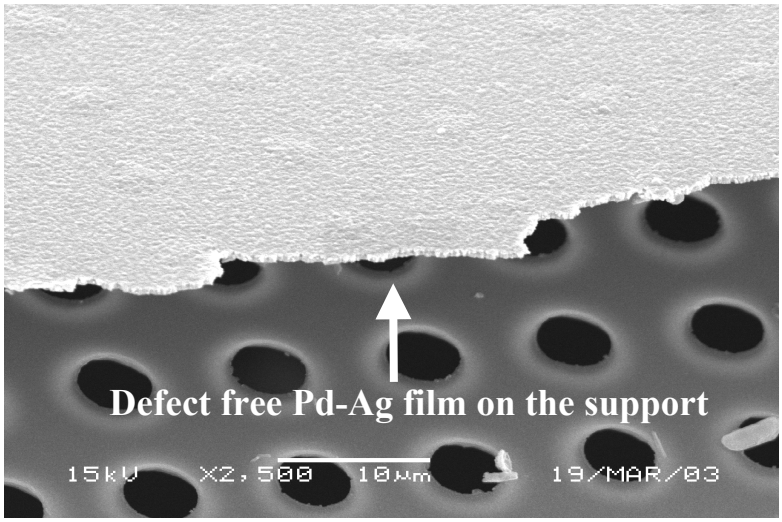

***Figure 5.6**: Pd-Ag membrane on the supporting microsieve.*

shows a part of Pd-Ag membrane on the supporting microsieve. As shown, the deposited Pd-Ag film has a smooth surface, and is free from defects. Also, in chapters 2 and 3 we briefly reported that the fabricated Pd-Ag membranes achieved the high hydrogen separation flux and high selectivity. More measurement data of the Pd-Ag film with respect to the hydrogen separation flux, selectivity, and film stability will be presented and discussed in chapter 6.

5.6. Conclusions

The dual sputtering procedure has been developed to synthesize submicron thick Pd-Ag alloy films with high composition control. Crack-free Pd-Ag alloy films with high density (non-porous), smooth surface, and fine polycrystalline structures were obtained. The information from the fabrication and characterization of the dual sputter procedure helps to realize submicron thick Pd-Ag membranes, which achieved high fluxes and selectivity. In addition, other alloy membranes with accurate composition like Pd-Cu membranes were successfully fabricated.

The results of the thin film fabrication suggest that the dual sputtering method may be a powerful technique to synthesize alloys with accurate composition for different applications.

5.7. References

[1] A.C. Markrides, M.A. Wright, D.N. Jewett, US Patent 3,350,846 (1967).

[2] A.G. Knapton, "Palladium Alloys for Hydrogen Diffusion Membranes", Platinum Metal. Rev., 21, 44 (1977).

[3] J. Shu, B.P.A. Grandjean, A. VanNeste, J. Kaliaguine, "Catalytic Palladium-Based Membrane Reactors: review", Can. J. Chem. Eng., 69, 233 (1991).

[4] J.P. Collins and J.D. Way, "Preparation and Characterization of a Composite Palladium-Ceramic Membrane", Ind. Eng. Chem. Res., 32, 3006 (1993).

[5] R. Hughes, "Composite Palladium Membranes for Catalytic Membrane Reactors", Membr. Techno., 131, 9 (2001).

[6] R. Dittmeyer, V. Hollein and K. Daub, "Membrane Reactors for Hydrogenation and Dehydrogenation Processes Based on Supported Palladium", J. Mole. Catal. A., 173, 135 (2001).

[7] Xomeritakis, G., and Y.S. Lin, "CVD Synthesis and Gas Permeation Properties of Thin Palladium/Alumina membranes", AIChE. J., 44, 174 (1998).

[8] J. Xu, "Hydrogen Permeation and Diffusion in Iron-Base Super Alloys", Acta Metal Mater., 41(5), 1455 (1993).

[9] Y.S. Lin, "Microporous and Dense Inorganic Membrane: Current Status and Prospective", Sep. Pur. Techno., 25, 39 (2001).

[10] K.J. Bryden and J.Y. Ying, "Nanostructured Palladium Membrane Synthesis by Magnetron Sputtering", Mater. Scie. Eng A., 204, 140 (1995).

[11] J.Y. Ying, "Structure and Morphology of Nanostructured Oxides Synthesized by Thermal Vaporization/Magnetron Sputtering and Gas Condensation", J. Arerosol Sci., 24, 315 (1993).

[12] M. Ohring, "The Material Science of Thin films", Academic Press (1992).

[13] J.L. Vossen and W. Kern, "Thin Film Processing II", Academic Press (1991).

[14] B. McCool, G. Xomeritakis and Y.S. Lin, "Composition Control and Hydrogen Permeation Characteristics of Sputter Dposited Palladium-Silver Membranes", J. Membr. Sci., 161, 67 (1999).

[15] G. Xomeitakis and Y.S. Lin, "Fabrication of Thin Metallic Membranes by MOCVD and Sputtering", J. Mem. Sci., 133, 217 (1996).

[16] J.A. Thornton, "High Rate Thick Film Growth", Ann. Rev. Mater. Sci., 7, 239 (1977).

[17] J.A. Thornton, "Structure -Zone Models of Thin Films", SPIE, 82, 95 (1987).

[18] H.T. Hoang, H.D. Tong, F.C. Gielens, H.V. Jansen, M.C. Elwenspoek, "Fabrication and Characterization of Dual Sputtered Pd–Cu Alloy Films for Hydrogen Separation Membranes", Materials Letters, 58, 525 (2004).

[19] F. Roa, M.J. Block, J.D. Way, "The Influence of Alloy Composition on the H_2 Flux of Composite Pd-Cu Membranes", Desalination, 147, 411 (2002).

[20] S.E. Nam, K.H. Lee, "Hydrogen Separation by Pd Alloy Composite Membranes: Introduction of Diffusion Barrier", J. Membr. Sci., 192, 177 (2001).

[21] R.C. Hughes, W.K. Schubert, T.E. Zipperian, J.L. Rodriguez and T.A. Plut, "Thin Films of Pd/Ni Alloys for Detection of High Hydrogen Concentrations," J. Appl. Phys., 62, 1074 (1987).

[22] C.L. Shih, B.K. Lai, H. Kahn, S.M. Phillips, A.H. Heuer, "A Robust Co-Sputtering Fabrication Procedure for TiNi Shape Memory Alloys for MEMS", J. Microelectromech. Syst., 10, 69 (2001).

Chapter 6

Hydrogen separation of the Microfabricated Pd-based membranes

Abstract

In this chapter, a short background on hydrogen permeation through Pd-based membranes is given. Then, hydrogen separation results with respect to the separation flux and selectivity of the membranes fabricated in the chapter 2 and chapter 3 are presented. Subsequently, several advantages of the microfabricated membranes used for hydrogen separation are discussed. Afterwards, influences of steam and CO_2 to the separation results are presented. Finally, surface morphologies of the membranes, which already performed separation or annealed at high temperatures are investigated using a high-resolution scanning electron microscopy (SEM).

6.1. Introduction

After fabrication at the University of Twente the membranes were sent to the Process Development Group, University of Eindhoven, for characterization with mainly respect to the hydrogen permeation flux and the membrane selectivity. Because separation results of the microfabricated membranes have been thoroughly described in a PhD thesis of F.C. Gielens, a second researcher working on this project [1], only main separation results are presented in this chapter.

As briefly reported in chapter 2 and chapter 3 with the microfabricated membranes we obtained high separation fluxes and high selectivity; fluxes of up to 4 mol $H_2/m^2.s$ were measured with a minimal selectivity of 1500 for H_2/He (or 4000 for H_2/N_2) (Figure 2.10 and Figure 3.5). More measurement data of the microfabricated membranes will be provided in this chapter. Generally, the obtained fluxes are approximately one order of magnitude higher than the fluxes reported in the literature for Pd or Pd-based alloy membranes deposited on porous supports. To figure out reasons why with microfabricated membranes we achieved the high fluxes, several advantages of the microfabricated membranes using in a hydrogen separation are discussed. Subsequently, influences of steam and CO_2 to the permeation flux are presented. Finally, because a large drop in membrane selectivity could be observed sometime, surface morphologies of the membranes after having been used for separation or have been annealed at high temperatures are investigated by SEM.

6.2. Hydrogen transport in Pd-based membranes

The permeation mechanism of hydrogen through Pd-based membranes was already presented in Figure 1.1. As presented, this permeation mechanism involves several steps in series [2-7]. These are, in order from the high hydrogen partial pressure side to the low hydrogen partial pressure side;

1) transport from the bulk gas to the gas layer adjacent to the surface,
2) dissociative adsorption onto the surface,
3) transition of atomic H from the surface into the bulk metal,
4) atomic diffusion through the bulk metal,
5) transition from the bulk metal to the surface on the low partial pressure side,

6) recombinative desorption from the surface, and
7) gas transport away from the surface to the bulk gas.

The overall observed rate of permeation might be limited by one step if it is much slower than the others, or it may be governed by a combination of steps. Generally, to obtain high hydrogen separation flux, the Pd membranes are desired to be as thin as possible to speed up the diffusion step (step 4), while clean membrane surfaces help to speed up surface reactions (steps 2 and 6).

Since hydrogen molecules dissociate into atoms to diffuse through metals, transport is calculated from the atomic flux. Fick's law $J = D\ \Delta C$ describes the flux of hydrogen atoms, J, through a homogeneous phase as:

$$J_H = D\,(C_{entry} - C_{exit})/2t \tag{1}$$

where D is diffusivity, C_{entry} and C_{exit} are the concentration of hydrogen atoms dissolved in the membrane at the interfaces of entry and exit, respectively, and t is the membrane thickness.

However, the relationship between flux and diffusivity often has been written in terms of gas pressures or powers of the gas pressure rather than in terms of concentrations [2-3,6-8]. This is a more convenient form to obtain the flux by experimentally determined values of pressure.

When hydrogen atoms form an ideal solution in the metal (Sievert's law hydrogen solubility dependence) and diffusion through the bulk metal is the rate-limiting step (diffusion through relatively thick films), C_H (C_{entry} and C_{exit}) is related to the partial pressure of hydrogen in equilibrium with the metal as:

$$C_H = K_S\,(p^{1/2}) \tag{2}$$

where K_S is the Sieverts constant and P is the partial pressure of hydrogen in equilibrium with the metal. Equation 2 is commonly known as the Sievert's law of hydrogen solubility dependence. [6-8]. The power of 1/2 comes from the dissociation of hydrogen molecules into twice as many atoms at low concentration. The flux of hydrogen molecules, J, in terms of pressure using equations 1 and 2 becomes:

$$J = DK_S\,(p_1^{1/2} - p_2^{1/2})/2t \tag{3}$$

where P_1 and P_2 are the partial pressures of hydrogen in equilibrium with the metal in the retentate and permeate, respectively. The hydrogen flux is inversely proportional to the membrane thickness, suggesting that thinner membranes give higher fluxes.

As the membrane becomes thinner, at some "critical thickness" the solid-state diffusion will become rapid enough that other rate processes will begin to impact, and eventually limit the permeation rate. Deviations from Sievert's law behavior have been reported and attributed to various factors including the surface processes [6-10], surface poisoning [11-12], and grain boundaries [13]. Lewis [2] and others [5-8] suggested better approximations of the hydrogen concentration by a general power law to relate the concentration to the pressure

$$C_H = K_S (p^n) \tag{4}$$

leading to

$$J = DK_S (P_1^n - P_2^n)/2t = Q (P_1^n - P_2^n)/t \tag{5}$$

In this empirical equation, the hydrogen pressure exponent n is often used as an indicator for the rate-controlling step of the overall permeation through a metal composite membrane. When diffusion through the bulk metal is the rate-limiting step and hydrogen atoms form an ideal solution in the metal (Sievert's law), n is equal to 0.5. A value of n greater than 0.5 may result when other processes like surface reactions, gas-phase resistance etc. influence the permeation rate or when the Sievert's law is not valid.

However, given the complexity of the overall transport mechanism, plus the difficulty in controlling and quantifying factors such as poisoning, surface or grain boundary contamination, and influence of grain size, it is not surprising that there is no agreement among experimental observations for very thin films by different research groups. For instance, Uemiya et al. have concluded that diffusion-limited permeation extends to thicknesses less than 10 μm [14]. However, Ward and Dao predicted that the diffusion would still dominate on whole separation process in membranes with the thickness below 1 μm [7]. Also, there is still uncertainty about the conditions under which "surface processes" become dominant, and the about impact of those processes.

The term Q in equation 5 is called the metal permeability, $Q = DK_S/2$, a pressure-independent constant. A derived quantity, the "permeance" is the flux divided by the pressure driving force, (p_1^n - p_2^n),

$$\text{permeance} \equiv J/(P_1^n - P_2^n)/t = Q/t \quad (6)$$

It should be noted that several metals in groups 3-5 of the periodic table have a higher hydrogen permeability (Q) than Pd [5,15], but they are not compatible with many feed streams due to their high chemical reactivity (John P Collins etc), therefore they are not often used for hydrogen separation. For instance, the hydrogen permeability of tantalum, zirconium, and niobium etc. is few times higher than that of Pd [15]. However, they are easily to be oxidized, which prohibits the dissociative adsorption of hydrogen molecules to hydrogen atoms on the membrane surfaces ($K_S \approx 0$), leading to almost no separation flux.

The diffusivity D of hydrogen in Pd-based membranes can be written as:

$$D = D_o \exp(-E_d/RT) \quad (7)$$

with E_d being the activation energy for diffusion, D_o a temperature independent constant, and R the universal gas constant and T the absolute temperature. Therefore, doing separation at high temperature will increase the hydrogen diffusivity, thus increasing the hydrogen separation flux (see equation 5). However, high temperature decreases hydrogen solubility, leading to lower Sieverts constant [16-17]. This effect tends to flatten the temperature dependence of the hydrogen flux. Therefore, hydrogen separation experiments through the Pd-based membranes are often performed at temperatures from 573 to 773 K in literature (see data for temperature in Table 6.2).

6.3. Measurement setup and measurement procedures

The permeability of the membrane was determined for H_2 and helium (He) with a separation setup shown in Figure 6.1. Nitrogen (N_2) was used as a sweep gas at the permeate side. All feed flow rates were measured and controlled with mass flow controllers (Bronkhorst High-Tec, EL-FLOW). The permeate

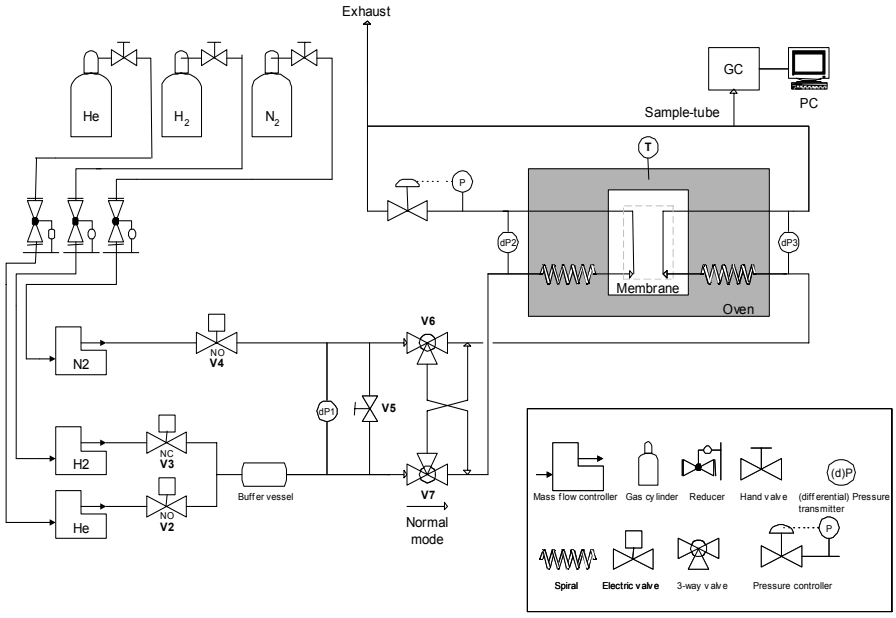

***Figure 6.1**: A schematic drawing of a separation setup.*

pressure was measured and controlled with an absolute pressure controller (Bronkhorst High-Tec, EL-PRESS). The trans-membrane pressure, the pressure drop over the permeate side, and the pressure drop over the retentate side were also measured (Hottinger Baldwin Messtechnik, PD1). A temperature-controlled oven was used to ensure isothermal operation. The H_2 and He concentrations in the permeate were measured by a Gas Chromatograph (GC) equipped with a Thermal Conductivity Detector (TCD) and a 5Å molecular sieve column. Argon (Ar) was used as the carrier gas, which gives the TCD a high sensitivity to H_2 and He, and a poor sensitivity to N_2. The purity of all gases used was 5N.

The membrane module was placed in the stainless steel holder (see Figure 2.9)[2], which was installed in an oven for isothermal operation. The H_2/He feed and the sweep gases were preheated in spiral channels placed in the same oven. The retentate flow was varied between 300 and 1000 ml/min and the H_2 molar fraction was varied from 0.1 to 0.9 mol/mol. The permeate gas flow was kept constant at 300 ml/min. The experimental set-up was controlled by a PLC. A PC with Labview handled the data-acquisition at 100 Hz.

The set-up was running fully automatically 24 hours a day, and could handle 100 recipes without user intervention. For each recipe, 4 samples per hour were taken of the permeate and analyzed by GC [1,18].

If an average molar fraction of H_2 in permeate is C (mol/mol) as measured by GC, a permeate flow rate is F (mol/s), and a membrane area is A (m^2), then an average hydrogen flux J through the membrane is calculated as:

$$J = FC/A \text{ (mol } H_2/m^2.s) \quad (8)$$

6.4. Hydrogen separation properties of the membranes

6.4.1. Separation flux

By using the separation setup present in Figure 6.1, hydrogen fluxes versus the duration of the experiment of many membranes fabricated as described in chapter 2 and chapter 3 were measured. Information of membranes and their measured average fluxes are given in Table 6.1. An example of the measured hydrogen flux versus the measuring duration of membrane M4 (500 nm Pd-Ag on the supporting microsieve) is presented in Figure 6.2.

Data of Table 6.1 show that, depending on the experimental conditions (temperature and retentate hydrogen pressure) and membrane characteristics (membrane thickness and membrane material), hydrogen separation fluxes from 0.6 up to 4.2 mol $H_2/m^2.s$ have been measured. The highest fluxes of ca. 4 mol $H_2/m^2.s$ were measured through the 500 nm Pd-Ag membrane on the supporting microsieve at 723 K and 0.83 bar H_2 retentate pressure (Figure 6.2).

Figure 6.2 shows that the flux is rather stable; it was first increased from ca. 3.6 to 4 mol $H_2/m^2.s$ over a period of about 50 hours, then became stable. The increase of the flux in the first measuring period may be explained due to an increase in Pd grain size, as was supposed by Lin [19]. However, the increasing of the flux in our membranes is much less than that observed by Lin, although the increase in Pd grain size was also observed.

Furthermore, after measuring for a period of ca. 120 hours, the retentate flow rate increased by about 50% from 600 to 900 $ml.min^{-1}$ to investigate the flux changing. However, there was only a very small increase of the separation

***Table 6.1**: Membranes properties and the measured hydrogen fluxes.*

MEMBR. NAME	MAT.	SUPPORT TYPE	THICKNESS (μM)	MEMBR. AREA (MM^2)	TEMP (K)	$P_{RETENTATE}$ (H_2) (BAR)	FLUX (MOL $H_2/M^2.S$)
M1	Pd	<110>-Si	1	8.8	723	0.3	0.6 - 0.7
M2	Pd	Microsieve	1	3.3	723	0.8	1.7 - 1.8
M3	Pd-Ag	<110>-Si	0.7	8.8	723	0.83	3.3 - 3.6
M4	Pd-Ag	Microsieve	0.5	3.3	723	0.83	3.6 - 4
M5	Pd-Cu	Microsieve	0.5	3.3	723	0.8	1.5 - 1.7

flux, suggesting that the previous separation flux of about 4 mol $H_2/m^2.s$ is a rather stable value in this measurement condition.

Additionally, to investigate the membrane stability, one membrane was measured for a period of ca. 1000 hours, during which the membrane experienced a change of gas type and concentration, as well as temperature cycles between 300-723K. The measured results showed no significant reduction in the membrane flux or the membrane selectivity, suggesting excellent membrane stability at this range of temperature. In the case of direct depositing the metal films on the porous supports to form a membrane, probably strong interactions between the metal and the supports took place, especially when a top layer on the supports has very small pores, leading to instability of their membrane in terms of both the separation flux and the selectivity [8,20].
However, in the microfabricated membrane constructions (Figure 6.3.b and Figure 6.3.c), the Pd-based films are free-standing with a period of the slit width (28 μm) or the sieve diameter (5 μm) on SiO_2 and SiN, which materials are both well known as good anti-diffusion barriers in IC technology. Therefore, in the typical range of temperatures in which hydrogen separation is performed (up to 773 K), there is almost no diffusion of the metals (Pd, Ag, or Pd-Ag) into the support, contributing to the good stability of the membrane.

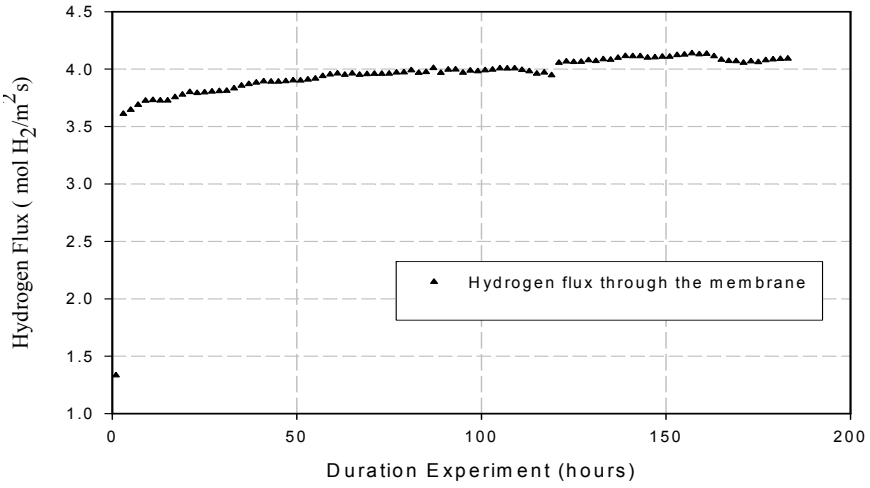

***Figure 6.2**: Hydrogen flow rate through the 500 nm Pd-Ag on the microsieve membrane as a function of time at temperature of 723 K, hydrogen pressure of 0.83 bars in retentate. Note that after measuring for ca.125 hours, the feed flow rate was increased by 50% from 600 to 900 ml.min^{-1}.*

It should be mentioned here that Table 6.1 provides flux data through the membranes with thickness of 500 nm or greater. The separation experiments for the thinner membranes have not been finished yet, although the very thin membranes e.g., membranes with thickness down to 100 nm, were successfully fabricated (chapter 3). The main reason was that during doing separation for membranes with thicknesses from 1000 nm down to 500 nm, we found that hydrogen transport through these membranes was limited by the surface reactions or other factors, not by the diffusion as we expected (discussed in a section 6.4.3). This implied that we would not gain much in flux by using the thinner membranes for separation. For instance, the flux of membrane M4 was increased only ca. 10% in comparing to that of membrane M3, while its thickness was about 40% thinner than that of M3 (Table 6.1). Additionally, the measured fluxes of ca. 4 mol $H_2/m^2.s$ were rather high and somehow met our expectation with respecting to flux at that time. We therefore decided temporarily not to measure the very thin membranes. Rather, separations using membranes with thickness from 500 to 1000 nm must be continued to have a better understanding of membrane properties. Also, other important membrane

issues e.g., membrane resistances against several poisoning gases, an improvement of a membrane packaging should be studied as well. Of course, the separation for the very thin membranes would be interesting, therefore it will be performed if time allows.

Although the fluxes through the very thin membranes have not been measured yet, the fluxes achieved in our work are already approximately one order of magnitude higher than the fluxes reported in the literature for thin Pd or Pd alloy membranes deposited on porous supports (see Table 6.2). In Table 6.2, all permeances were calculated based on n = 1. Also, permeate hydrogen pressures were taken to be zero for all permeance calculations in Table 6.2 because it was difficult to pick up exact values of $P_{permeate}$ from literature reports.

6.4.2. Advantages of the microfabricated membranes used for hydrogen separation

Because the fluxes of the microfabricated membranes are about one decade larger than that of the conventional membranes, several advantages of the microfabricated membranes used for hydrogen separation are discussed.
It has been reported that there are significant discrepancies in the literature on hydrogen permeation data through various thin Pd-based membranes prepared by different methods [7]. Also, these discrepancies could not be explained by the differences in membrane thickness, compositions, and preparation methods [7,19]. We suggest that the reasons for obtaining such high fluxes for the microfabricated membrane are:

1) thin membranes with the high composition control were used [21].
2) microfabricated membranes have a very low resistance to the mass transfer, as virtually no support layer is present.

Of these two advantages, the former has been often discussed in the literature [7,19,22], the latter is however a unique advantage of the microfabricated supports and has not been discussed in detail yet. Therefore it will be discussed here. For later discussions, three membrane supports; the conventional porous support of γ-α Al_20_3 [23], <110>-Si support (chapter 2 this thesis), and supporting microsieve (chapter 3 this thesis) are depicted in Figure 6.3.

***Table 6.2**: Comparison of the permeation result to the literature data of thin Pd and Pd-alloy membranes on porous supports.*

MEMBR.	THICK. (μM)	TEMP. (K)	PRESSURE $P_{RETENTATE}$ (H_2) (BAR)	FLUX (MOL $H_2/M^2.S$)	PERMEANCE (MOL $H_2/M^2.BAR^1$)	SELEC. (H_2/HE)	REFS.
Pd/SS	5	623	1	0.15	0.15	100-200	[6]
Pd/γ-α Al_20_3	7-15	623	1	0.1-0.125	0.1-0.125	100-1000	[6]
Pd/SS	11.4	823	1.5-10	0.71	0.47	380	[8]
Pd-Cu/SS	11	723	3.45	0.81	0.27	1150*	[24]
Pd-Ag/γ-α Al_20_3	0.16-0.52	573	Not given	0.01		Up to 116**	[27]
Pd and Pd-Ag/ γ-α Al_20_3	0.1-1.5	573	1	0.01-0.02	0.01-0.02	30-200	[28]
Pd-Cu/ SS	2	723	1	0.84	0.84	3000*	[43]
Micro.Pd	0.2	373	0.5	4.5	9	UnKnown	[44]
Micro.Pd	0.2	723	0.2	0.6-0.7	3-3.5	> 1500	Chap.2
Micro. Pd-Ag	0.5	723	0.83	.6-4.2	4.3-5	>1500	Chap.3
Micro. Pd-Cu	0.5	723	0.8	1.7	2.125	> 1500	Chap.5

** Selectivity for H_2/N_2 ; SS: porous stainless steel;*

It is known that the mass transfer resistance associated with viscous flow (Hagen-Poiseuille type) or diffusion through the porous support could be significant in the composite membrane [7,22]. The viscous flow with flux J through the porous support may be calculated as [22]:

$$J = \frac{\varepsilon}{8\eta\tau}\frac{r^2}{RTt} Pm * \Delta P \qquad (9)$$

where the driving force $\Delta p = P_1 - P_2$, ε the porosity, τ the tortuosity, r the average pore diameter, t the thickness of the porous medium, η the viscosity of the gases, the mean pressure Pm = 0.5 (P_1+P_2) with P_1 and P_2 the pressure at the inlet and outlet of the porous support respectively. Applying equation 1 Ward and Dao estimated that to have a viscous H_2 flow of 10 mol/m^2.s at 673 K through a 1mm thick porous support with porosity of 50%, tortuosity of 3, and average pore diameter of 5μm would require a H_2 pressure drop of approximately 0.4 bar within the support, assuming P_2=0 and no other mass transfer resistance [7]. Moreover, Ward and Dao only estimated the pressure drop within the micro-porous support layer e.g., an α-alumina layer with micro-pore sizes shown in Figure 6.3.a, the pressure drop within a nano-porous transition layer - a layer between the micro-porous layer and a deposited film e.g, a γ-alumina layer with nano-pore sizes in Figure 6.3, was not taken into account in their calculation. It is however well-known that the presence of this transition layer (with very small pores) is vital in the fabrication of gastight thin-film membranes on porous supports [22]. Although the transition layer is often about one micrometer thin, t in equation 9, it however consists of very small pores of a few tens of nm, i.e. very small r in equation 9, leads to a relatively large amount of the pressure drop. For instance, a calculation based on equation 9 shows that to have the above H_2 flow (a viscous H_2 flow of 10 mol/m^2.s at 673 K) through a transition layer of 1 μm thick with pore sizes from 50 to 100 nm would require a pressure drop between 1 to 4 bar within the transition layer.

Generally speaking, the loss of the pressure within the porous supports is considerably large. It is even a considerable loss in hydrogen separation using micron-thick membranes because micron-thick metal membranes often perform separation at relatively low hydrogen pressures, e.g., around 1 to 2 bars (see data from Table 6.2). A reason of using low hydrogen pressure has not been

explained clearly, but probably due to a limitation of mechanical property of the thin membranes, or/and an economic factor. Note, although Collin et al. [8] and Roa et al. [24] performed their separations with the retentate hydrogen pressures higher than 3 bars, but their membranes were ca. 11 μm in thickness. Obviously, the presence of the porous support in the conventional membrane construction significantly reduces the driving force across the Pd layer, thus strongly restricting the separation flux.

In the microfabricated membrane construction (Figures 6.3.b, 6.3.c), at the same hydrogen flow would have only to travel through supports with much larger dimensions, e.g., r = 28 and r = 600 μm in Figure 6.3 b and 6.3.c, respectively, to access the Pd membrane surface, thus requiring a much smaller pressure drop. For instance, computer simulations (using flow solver CFX4.2) gave a pressure drop of only few tens of mbar from the inlet to the membrane surface in the membrane configuration shown in Figure 6.3.b [25]. The value of the pressure drop is even lower in the membrane construction in Figure 6.3.c. Due to the considerably smaller the pressure drop, the microfabricated membranes lead to much higher separation driving force across the separation layer, thus obtaining higher separation flux.

6.4.3. Limitation in hydrogen transport though the Pd-based membranes

As presented in the section 6.2 the permeation of hydrogen through the metal membranes involves several steps in series. The overall observed rate of permeation might be limited by one step if it is much slower than the others, or it may be governed by a combination of steps. And in practice it is important to determine which step is the rate-limiting step on the whole separation transport. For instance, if the diffusion through the membrane is the rate-limiting step, then reducing the membrane thickness leads to an increase of the separation flux.

Also, it was discussed that hydrogen transport through the metal films is frequently described by the empirical equation,

$$J = Q\,(P_1^n - P_2^n)/t \qquad (5)$$

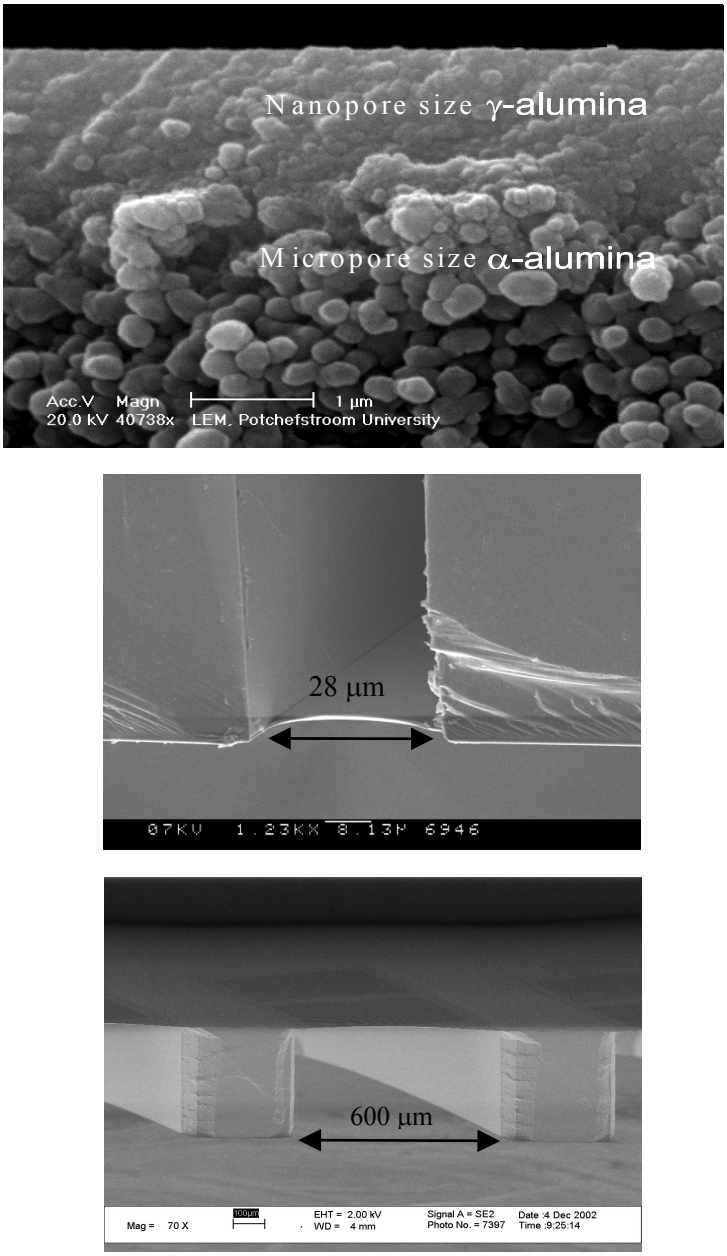

***Figure 6.3**: SEM images of conventional porous support and microfabricated supports show a big advantage of the latter over the former with respect to low mass transfer resistance. (a) γ-α alumina (after [23]). (b) Supporting in <110>-Si (chapter 2 this thesis). (c) Supporting microsieve (chapter 3 this thesis).*

In the above equation, the hydrogen pressure exponent *n* may be used as the indicator for the rate-controlling step of the overall permeation through a metal composite membrane.

***Table 6.3**: Data of membranes used in a limitation transport study.*

MEMBRANE NAME	MATERIAL	SUPPORT TYPE	THICKNESS (μM)
M6	Pd	Microsieve	1
M7	Pd-Ag	<110>-Si	0.7
M8	Pd-Ag	<110>-Si	1.2
M9	Pd-Ag	Microsieve	0.7

The results of the experiments with varying H_2 concentration in the feed at 673 and 723K for several membranes are given in Figure 6.4.a and 6.4.b, respectively. The type of the membranes used in these experiment series is given in Table 6.3. To determine which step limits the H_2 transport rate, the measured fluxes are plotted against the difference in H_2 partial pressure of the feed inlet and the permeate outlet. Then they have been fitted to equation 1 to obtain the corresponding value of *n*. More detail has been reported elsewhere [1]. As can be seen that the *n*-value close to 1 is obtained for all the measured membranes. This *n*-value indicates that the whole separation process is controlled by the surface reactions or other factors, but not by diffusion step. This result is consistent with the common observation for sub-micron thick Pd-based membranes in literature [5-7,9, 26-28], but it was indeed not our expectation. According to the prediction of Ward and Dao that diffusion of hydrogen atoms is rate-limiting may be extended for a membrane with a thickness below 1μm [7]. Therefore, we did expect that by using techniques of microfabrication to produce sub-micron thick Pd-based membranes - with very clean surfaces (no poisoning), well controlled microstructures, and the low mass transfer resistance - diffusion through these membranes would limit the transfer.

The fact that hydrogen transport though our membranes were governed by surface reactions may be caused by several reasons;

1) the diffusion of hydrogen atoms through the sub-micron thick Pd-based film may be extremely fast, therefore its influence on the overall hydrogen transport is very small.
2) in the case of Pd-Ag alloy film, Pd and Ag from the film segregate to the two sides of the membrane, adding an extra resistance to the surface processes [29]. However, as we also observed the *n* values close to 1 for pure Pd membranes, therefore the segregation of elements in the alloys should not be the main reason for the dominance of the surface reactions.
3) the membrane surface was possibly polluted or poisoned during the fabrication process or during measurement [19].

To investigate the hypothesis that the membrane was contaminated during processing, several membranes were checked by X-ray photoelectron spectroscopy (XPS) and Energy dispersive X-ray (EDX) before bonding them between the glass substrates, but there was no indication of contamination on the Pd-based film surfaces. However, we could not check the membrane states after the bonding step due to the coverage by the glass substrates, so it remains unknown whether contaminations may arise from the anodic bonding process. Since this process was carried out in vacuum, such contamination is not expected. It is possible that the membrane became polluted with carbon, introduced from the graphite sealing, a possibility reported by Lin [19].

We suppose that although thick Pd-based membranes are reported to be fairly immune to surface poisoning [30-31], but since our membranes are thin and so permeable, they may foul with impurity concentrations that would go unnoticed with thick Pd membranes or alloys. This issue however will be further discussed in a section 6.5.1 (a steam influence section).

6.4.4. Membrane selectivity

Separation membrane should not only allow a high flux, but also a high selectivity. The selectivity of the microfabricated membranes for hydrogen over other gases like He and N_2 is therefore measured and presented here.

Possible membrane leaks during the permeation experiment can be detected by measuring the He concentration at the permeate side. However, no He was found during the experiments. Therefore, in order to calculate a

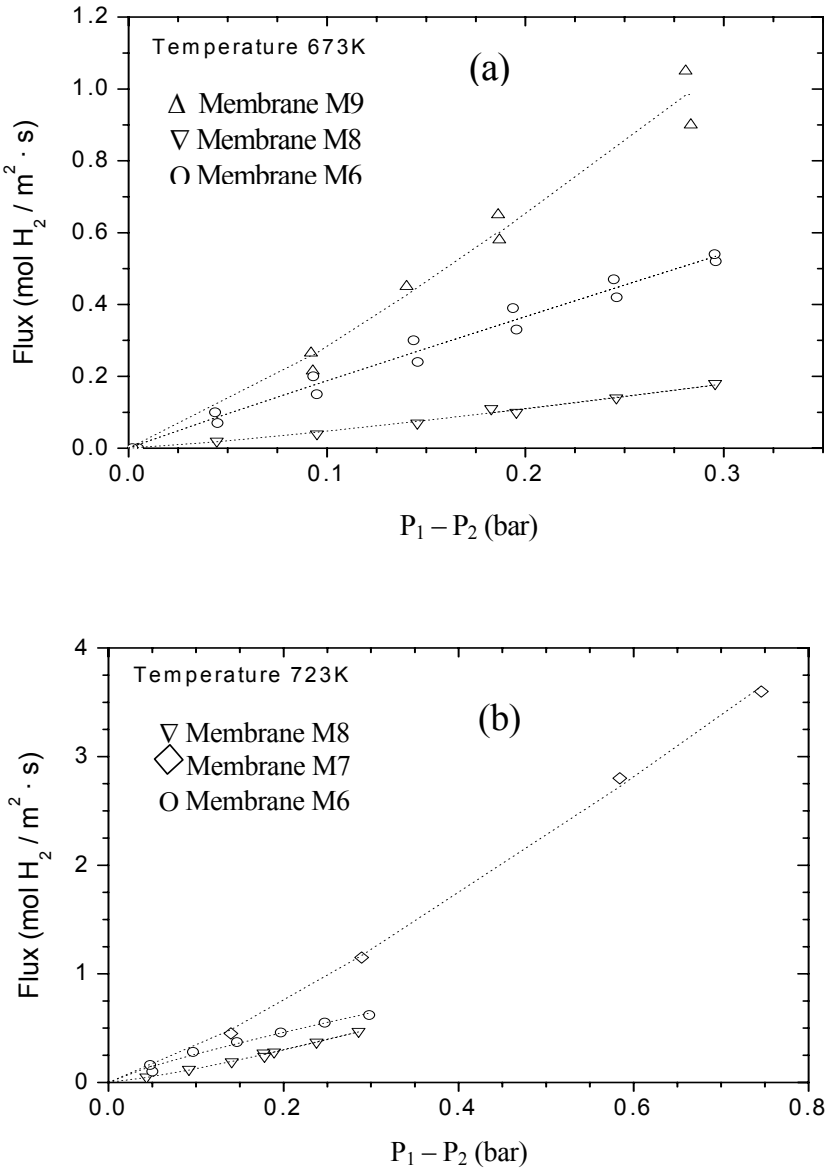

***Figure 6.4**: Hydrogen flux as function of the hydrogen partial pressure in the retentate shows n close to 1: (a) Measurements at 673 K. (b) Measurements at 723 K (the lines to guide the eye).*

minimum selectivity of H_2 over He, the detection limit of the gas chromatograph (GC) for He is used as the maximum He concentration. In this way, a minimal separation factor of 1500 for H_2 to He (or equivalent to about 4000 for H_2 to N_2) was calculated. Recently, by using new GC with the better detection limit for He, a minimal separation factor of 2850 for H_2 to He has been obtained. This high selectivity indicates that the microfabricated membranes are most likely defect-free.

We discussed in the section 1.4 of chapter 1 that in the conventional technology the separation layers (Pd-based films) are directly deposited on porous supports, which leads to several problems. One of them is that the micron-thick metal films could not cover up the supports completely, consequently leading to the membrane defects, i.e. raising the membrane leakage. A principle difference of microfabrication approaches is that the separation layers are first deposited onto dense, atomically smooth, and clean surfaces of previously microfabricated supports, then etched free later (see Figures 2.2.d and 3.2.d). As deposited on the dense and smooth surface, the deposited films, even the sub-micron thick films, can cover the support completely, leading to defect-free membranes.

Preparing the membranes in a dust-poor clean room environment was the key point to get defect-free membranes. Vos and Verweij claimed that the use of a clean room reduced the average concentration of particles of 0.5 μm from 18 million m^{-3} in normal laboratory air to less than 100 m^{-3} in a class 100 clean room, where our membranes are prepared [32]. Without clean-room conditions, the number of defects caused by particles from the air was estimated to be at least five defects of $Ø > 0.5$ μm.cm^{-2} of membrane surface. This number dropped to <<1 when our clean room conditions were applied.

6.5. Influence of steam and CO_2 on the H_2 flux

In practice, hydrogen is commonly to be separated from hydrogen gas mixtures containing other gases like CO_2, steam, and CO etc. Therefore, influences of CO_2 and steam on the H_2 permeation behavior of membranes M1 (1000 nm Pd on <110>-Si) and M4 (500 nm Pd-Ag on microsieve) are briefly presented and discussed here.

To study the influences of CO_2 and steam on the H_2 permeation, the measurement setup presented in Figure 6.1 had to be modified, and the detail of

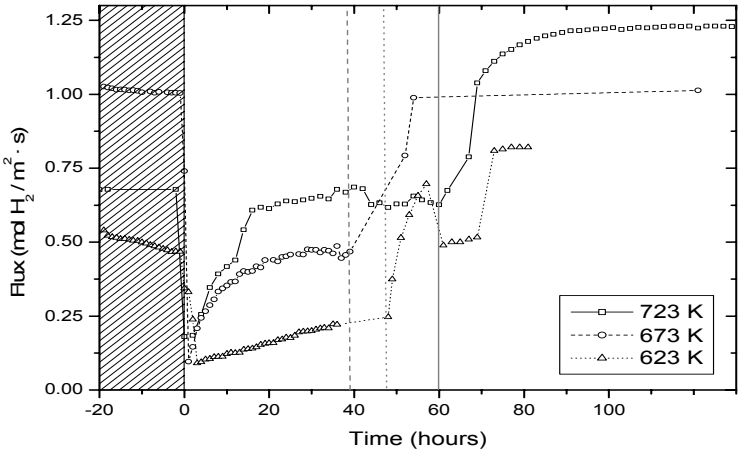

***Figure 6.5**: Influence of steam on the flux at 623 673, and 723 K of the membrane M1. The steam and H_2 concentration was 20 vol.%. Except for the measurement at 723 K the steam concentration was 30 vol.% from 0 to 14 hours and for the measurement at 623 K the H_2 concentration was 10 vol.% from 59 to 63 hours.*

the modifications were reported in [1]. Then influences were studied at feed concentrations of 20 vol.% CO_2 or H_2O, 20 vol.% H_2 and 60 vol.% He at temperatures of 623, 673 and 723 K.

6.5.1. Influence of steam

In Figure 6.5 the influence of steam on the permeation behavior of membrane M1 is given as function of time (t) at 623, 673 and 723 K. In the graph the permeation is given before, during and after feeding the membrane with the steam mixture. The three stages are represented in this graph; the hatched region represents the stage prior to the H_2O addition ($t < 0$), the next region ($t = 0$ to $t = 60$) represents the stage of H_2O addition to the feed, and the last one ($t > 60$) represent the stage after H_2O addition.

As can be seen that directly after the start of the steam addition, a sharp decrease in fluxes is observed at all three temperatures. A drop of ca. 50%, 43%, and 35% is observed at 723 K, 673 K, and 623 K, respectively. Afterwards, the flux in all series slowly increased until they reach steady fluxes.

A small distortion of the flux measuring at 723 K is visible, but this is caused by a change of the feed steam concentration. The time necessary to reach a steady flux decreased with increasing temperature.

After the steam addition is stopped, the H_2 flux increases sharply and then reaches stable values within several hours. Only in the series at 623 K a drop in the flux (from t = 59 to t = 63) is observed, but it is caused by a change in H_2 feed concentration. The sharp increase in flux of the membranes that previously worked with steam might be result of two processes: steam may clean the Pd surface or steam makes the Pd surface more active for H_2 dissociation. The above phenomena gives us a very important suggestion; prior to perform hydrogen separation, the membrane may be given a steam treatment to clean or activate its surface, thus obtaining even higher separation fluxes reported in section 6.4.1.

Based on above suggestion, several Pd membranes have been treated with steam, and used for separation. As expected, the measured fluxes were high and ca. 2 to 3 times higher than that of the membranes without steam treated. For instance, a flux of ca. 8 mol $H_2/m^2.s$ was measured though a 1000 nm pure Pd membrane at 723 K and 0.83 bar retentate hydrogen pressure (see Figure 6. 6). More interestingly, analyzing the hydrogen separation fluxes of the steam treated membranes (Figure 6.7) shows that the whole separation process

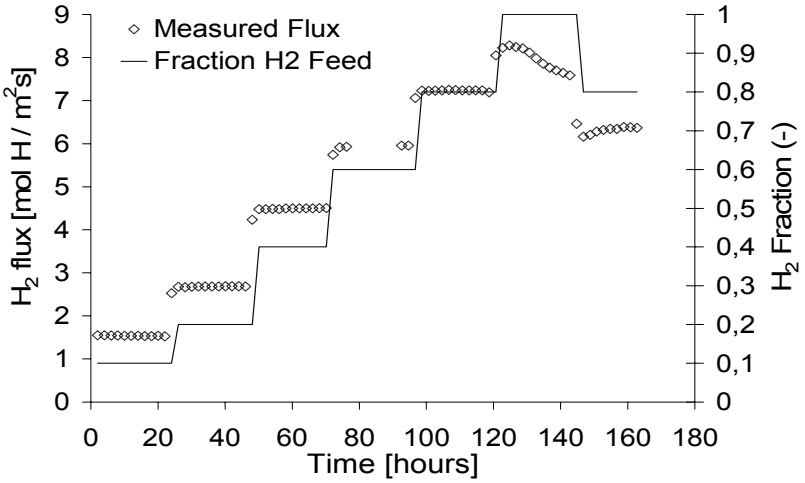

Figure 6.6*: Hydrogen flux of steam treated M1 membrane at 723 K. Retentate hydrogen pressures were varied from 0.1 to 1 bar.*

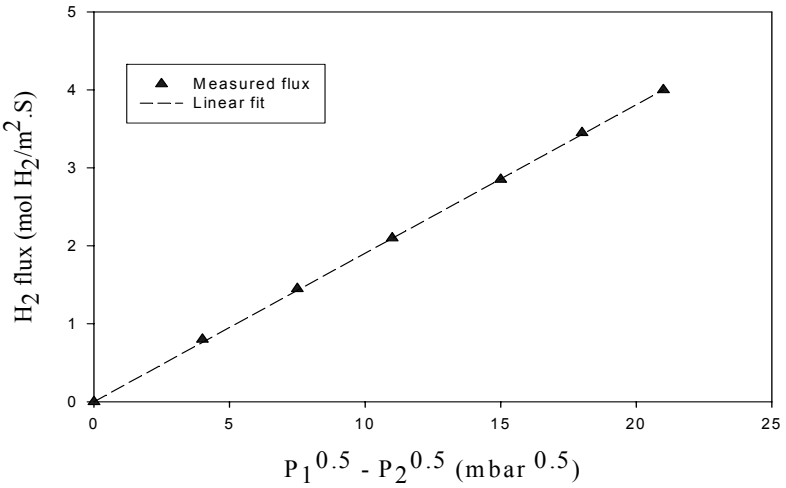

***Figure 6.7**: Hydrogen flux of steam treated M1 membrane as function of the retentate hydrogen pressure shows the diffusion through the membrane layer is the rate-limiting.*

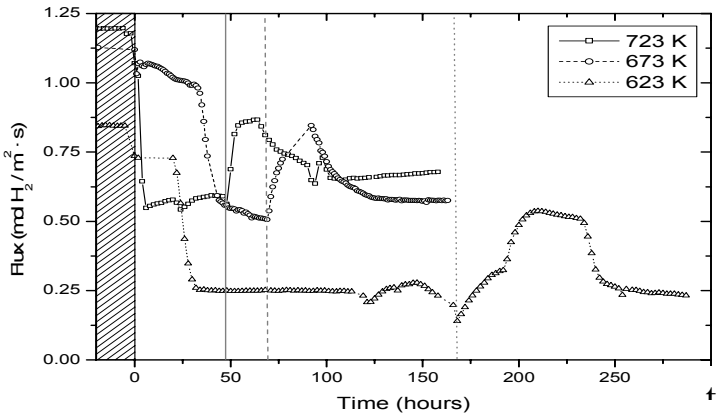

***Figure 6.8**: Influence of CO_2 on fluxes at 623, 673, and 723 K of the 1000 nm Pd on <110>-Si (M1 membrane). The hydrogen concentration was zero at 623 K from 120 to 166 hours, caused by an involuntary hydrogen valve shutdown.*

though these membranes was almost governed by the diffusion step ($n \approx 0.5$ in equation 5) although it was dominated by the surface reactions before ($n \approx 1$ in equation 5).

6.5.2. Influence of CO_2

Influence of CO_2 on the hydrogen permeation fluxes of Pd membrane at three temperatures of 623, 673, and 723 K are shown in Figure 6.8. Presentations of drawing areas are the same as in Figure 6.5.

It can be seen that the hydrogen flux of all three series drop after the CO_2 was added. The hydrogen flux of the 723 K series sharply drops just after the addition of CO_2, while the fluxes in series at 623 and 673 K show a large reduction after CO_2 was added for 20 and 30 hours, respectively. After these sharp drops, the hydrogen fluxes stabilize at values of 0.25, 0.51, 0.59 mol $H_2/m^2 \cdot s$ at 623, 673, and 723 K, respectively. Generally, after the addition of CO_2, the drops of ca. 44%, 45%, and 36% in fluxes are observed at 723 K, 673 K, and 623 K, respectively. However, after the CO_2 addition is stopped, the fluxes increase to their prior values, except the series at 723 K behaves a little difference. More details about the CO_2 influence on the hydrogen separation flux of the membrane have been reported elsewhere [33].

6.5.3. Influences of other gases

So far, the influence of steam and CO_2 on the hydrogen separation of the microfabricated membranes have been investigated and reported. In fact, hydrogen is commonly to be extracted from gas mixtures that not only contain CO_2, steam, but also CO, sulfur and chlorine. Therefore, the influence of these gases on the membrane behavior should be investigated as well [5-7,19,23]. Actually, the Pd-Cu membranes were developed, mainly aimed at testing the membrane resistance against the above poisoning gases. However, these tests have not been able to be carried out yet, due to a limitation of time and a limitation of the our measurement equipment and conditions.

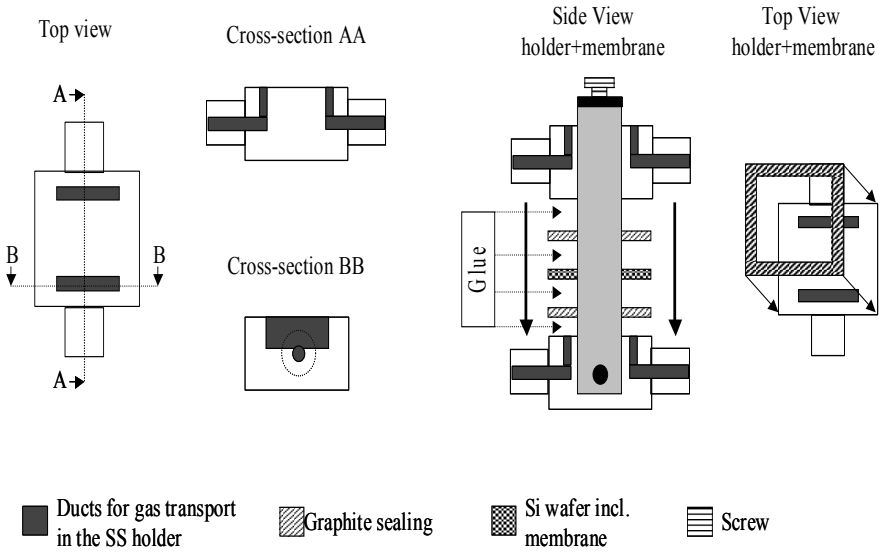

***Figure 6.9**: Schematic drawing (not on scale) of holder and of the module assemblage.*

6.6. Instability of membrane at high temperature

6.6.1. Membrane requirements to work at high temperature and the new packaging setup

In section 6.4.1 we have reported that the microfabricated Pd-based membranes showed good stability at operation temperature up to 723 K. For instance, one membrane was tested for ca. 1000 hours, but the measured results showed no significant reduction in the membrane flux or the membrane selectivity. Therefore it was concluded that the fabricated membranes can operate well at a range of temperatures up to 723 K.

It should be mentioned that although anodic bonding of the wafer membrane with glass cover helps to realize the very robust membrane module, a main limitation is that the membrane module, and therefore the membrane, can not be operated at temperatures higher than a softing point of glass of ca. 773 K.

However, in the membrane applications, one often desires to operate the membranes at higher temperature to obtain possibly higher separation fluxes. In

particular, a working at temperatures higher than 723 K is one of critical requirements for the Pd-based membranes when used as membrane reactors for (de) hydrogenation reactions, as these reactions often have to be carried out at 800 K or higher. For instance, in a dehydrogenation of methylbenzene to produce styrene:

$$C_6H_5 - CH_2 - CH_3 \Leftrightarrow C_6H_5 - CH_2 - CH_3 + H_2$$

Pd membranes may be employed for hydrogen removal to shift the thermodynamic (equilibrium) towards higher conversions.

To investigate a possibility to use the membranes at high temperature, several membranes without glass covers were directly packaged into the steel holder by a new packaging set-up (Figure 6.9), then tested for hydrogen separation at 823 K to 873 K.

The new module in Figure 6.9 consists of two stainless steel plates with Swagelok connections, two graphite layers, and the wafer membrane. Two stainless steel plates are pressed on the wafer membrane by screws to make the device gastight. The two graphite layers are used as sealing and tress-reducing medium. Details of the new packaging will be reported By Gielens [1]. However, the reliability of this new packaging procedure needs to be improved as the wafer membranes sometimes broke during packaging.

6.6.2. Separation results and instability of membrane at high temperature

The hydrogen flux through the membrane measured at high temperatures was very high. For example, a flux of ca. 10 mol $H_2/m^2.s$ was measured through a 900 nm Pd membrane at 873 K with retentate hydrogen pressure of only 0.2 bars. However, we observed that this high flux was unstable. More seriously, the membrane selectivity quickly and drastically dropped. The membrane selectivity could not even be detected after 7 hours of measurement.

6.6.3. Hole creation in membrane at high temperature

To reveal the reason that caused the loss of membrane selectivity, the surface morphology of the membranes before and after separation (at 873 K) was

investigated using scanning electron microscope (SEM), results are shown in Figure 6.10.

As can be seen that a pristine membrane has a smooth surface without any defect or hole (Figure 6.10.a). However, the surface morphology of the membranes has been drastically modified after separation; many holes are formed in the metal films (Figures 6.10. b, c and d). Such holes were obviously a reason for the complete loss of the membrane selectivity.

Because the thin metal membranes were used for hydrogen separation at relatively high temperatures, it can be assumed that there were annealing effects on them. And the formation of the holes on the annealed thin metal membranes has been commonly attributed for several reasons such as;

1) the growth of grains in thin metal film (crystallization process) to reduce its total surface areas, therefore reducing a total free energy inside the film [34-35,40]. This process forms "hillocks" and "voids" (or holes as called in this work) in the membrane [36-37].
2) the stress caused by the mismatch in thermal expansion coefficient between the films and supports [38-40]. For instance, thermal expansion coefficients are ≈ 10, 19, and 2.7-3.7, and 2.5 ppm/^{o}C for Pd, Ag, and SiN, and silicon substrate, respectively. It has been discussed that hillocks and voids are created in annealed thin films e.g., an annealed aluminum film, due to a stress relaxation [40].
3) For the hydrogen separation membrane, the hydrogen has additional effects that enhance the restructuring the metal films. For example, hydrogen is reported to induce a phase separation in several alloys, including Pd-Ag [29,41].

The grain growth in the annealed thin film has been described in detail by Bryden and Ying [34-35]. They also suggested that supersaturated Pd alloy membranes stabilize against grain growth. For example, the alloy of Pd-Y (30 wt% of Y) is stable in a hydrogen environment at temperatures up to 873 K [35].

We observed in all the deteriorative membrane samples that although the holes were created; the thin films were still free standing on the support. They were not detached or cracking from the support as reported by Bryden and Ying [34], and Liu et al. [35]. These researchers claimed that their membranes were delaminated from the support due to high stresses in their films. Based on the above observations and discussions we suppose that that the stresses in the

Pd or Pd-Ag films were not too high, therefore they should not be a main reason for the hole creation in the films.

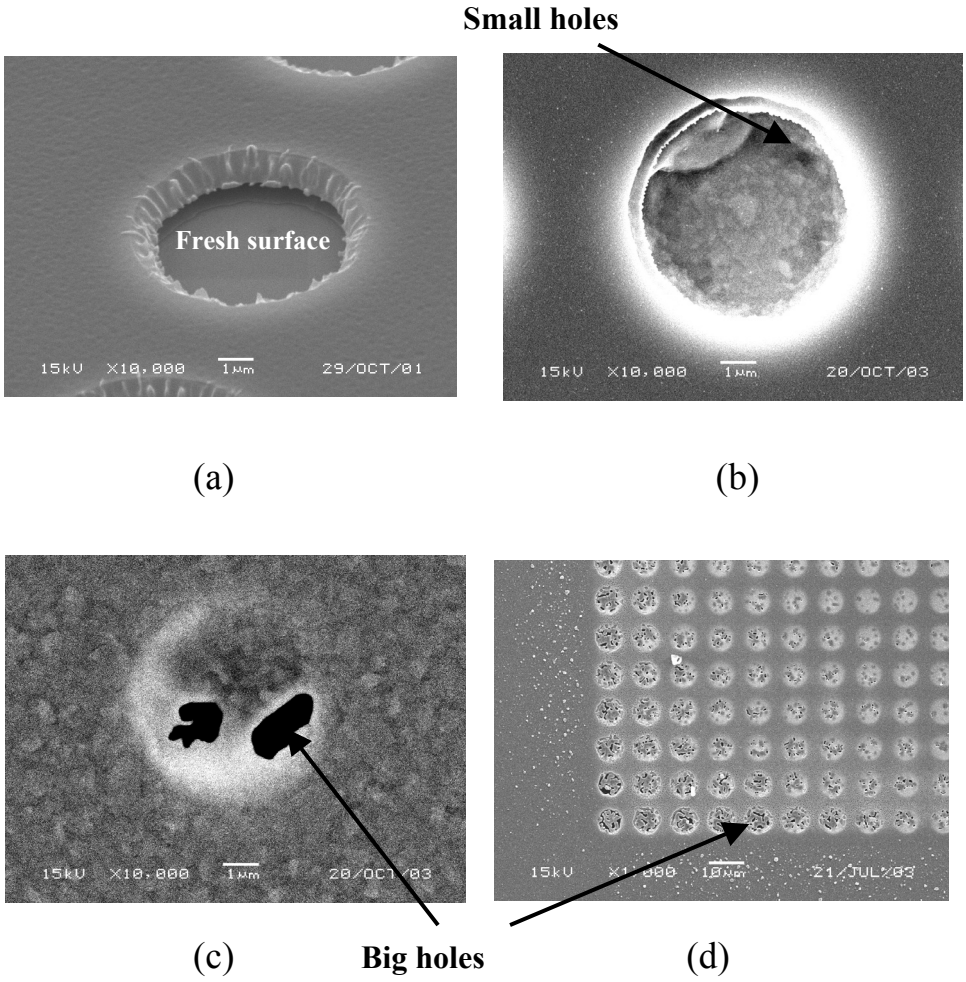

***Figure 6.10**: SEM images show morphologies of separation films on the supporting microsieve before and after performing hydrogen separation at 873 K for ca. 15 hours. (a) A pristine surface of 500 nm Pd as seen through the microsieve. (b) A after performed separation. (c) and (d) show 500 nm Pd-Ag membrane after separation.*

To investigate the influence of hydrogen onto the hole formation in the membrane at high temperature, two fresh Pd and Pd-Ag membranes with a thickness of 500 nm were prepared on the supporting microsieve, then annealed in a nitrogen environment at temperatures of 773 k and 823 K, each temperature for a period of 100 hours. Afterward, surface morphology of the annealed membranes was investigated by a high-resolution SEM. The results are presented in Figures 6.11.a-d. As shown, the surfaces of the annealed films are deteriorated in a similar fashion as those used for hydrogen separated. Grain size increased in membranes annealed at 773 K. They keep growing at higher temperature and eventually create the holes (voids) in the membranes at 873 K.

However, holes size and number of holes in the annealed films are smaller and less than those in the hydrogen separated films, although the annealing time (100 hours) was much longer than the separation time (15 hours). Apparently, hydrogen speeds up the structure rearrangement in the thin films.

Based on the above observations and discussion, we may conclude that the hole creation was mainly caused by the grain growth and an influence of hydrogen, which needs further investigation. The stress however has less influence.

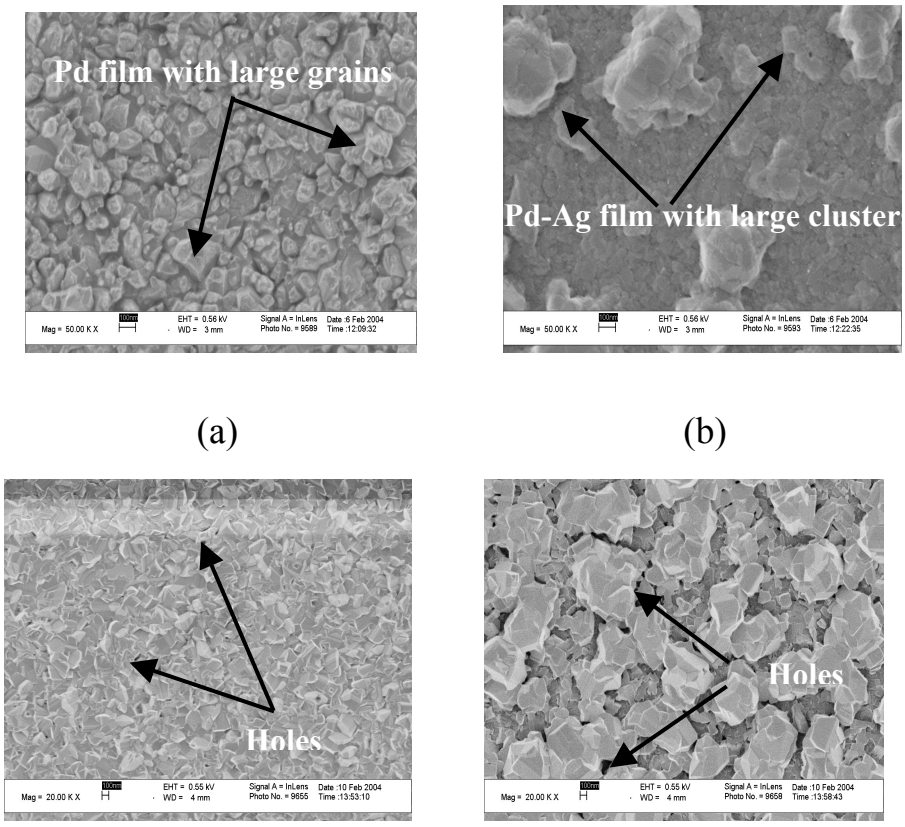

***Figure 6.11**: SEM images show morphologies of films after annealing. (a) Pd film at 773 K. (b) Pd-Ag film at 773 K. (c) Pd at 873 K. (d) Pd-Ag film at 873 K.*

6.7. Conclusions

The microfabricated membranes lead to high separation flux as well as high selectivity; fluxes up to 4 mol $H_2/m^2.s$ were measured with a minimal selectivity of 1500 for H_2/He. This flux is approximately one order of magnitude higher than the flux reported in the literature for Pd or Pd-based alloy membranes deposited on porous supports. Several advantages of the microfabricated

membranes used for hydrogen separation, a low mass transfer resistance, using thin membrane with high composition control were attributed for the reasons of obtaining high flux. In addition, the membrane showed excellent stability at temperatures up to 723 K.

The analysis of the experiments suggests that surface reactions were the limiting step on the whole hydrogen separation process.
The influences of steam and CO_2 on the hydrogen separation flux were studied. The flux was initially reduced from 35 to 50 % when steam or CO_2

were added. However, the flux recovered to the prior value when CO_2 was removed. Interestingly, membrane allowed higher flux after steam was removed. Separation by steam treated membrane turned out to be limited by diffusion. It was supposed that the steam cleans the membrane surface or makes the surface more active for dissociation of hydrogen molecules to hydrogen atoms. Nevertheless, more experiment results are needed to confirm as well as explain the steam effects.

Hydrogen separation at high temperature from 823 to 873 K was performed. The flux was initially high, but holes in the membranes appeared, so they completely lost their selectivity. The hole creation might be attributed for thermal grain growth, but pressure leads to more and large holes.

6.8. References

[1] F.C. Gielens, Ph.D thesis, University of Eindhoven (2004).
[2] F.A. Lewis, “The Palladium Hydrogen System”, Academic Press (1967).
[3] F.A. Lewis, “Hydrogen in Palladium and Palladium Alloys”, Int. J. Hydrogen Energy, 21, 461 (1996).
[4] J. Shu, B.P.A. Grandjean, A. VanNeste, J. Kaliaguine, “Catalytic Palladium-Based Membrane Reactors: review”, Can. J. Chem. Eng., 69, 233 (1991).
[5] R. Hughes, “Composite Palladium Membranes for Catalytic Membrane Reactors”, Membr. Techno., 131, 9 (2001).

[6] R. Dittmeyer, V. Hollein and K. Daub, "Membrane Reactors for Hydrogenation and Dehydrogenation Processes Based on Supported Palladium", J. Mole. Catal. A., 173, 135 (2001).

[7] T.L. Ward and T. Dao, "Model of Hydrogen Permeation Behavior in Palladium Membranes", J. Membr. Sci., 153, 211(1999).

[8] J.P. Collins and J.D. Way, "Preparation and Characterization of a Composite Palladium-Ceramic Membrane", Ind. Eng. Chem. Res., 32, 3006 (1993).

[9] V. Jayaraman, Y.S. Lin, "Synthesis and Hydrogen Permeation Properties of Ultrathin Palladium-Silver Alloy Membranes", J. Membr. Sci., 104, 251 (1995).

[10] R.C. Hurlbert, J.O. Konecny, "Diffusion of Hydrogen through Palladium", J. Chem. Phys., 34, 655 (1961).

[11] I. Ali-Khan, K.J. Dietz, F.G. Waelbroeck, P. Wienhold, "The Rate of Hydrogen Release out of Clean Metallic Surfaces", J. Nucl. Mater., 76-77, 337 (1978).

[12] A.B. Antoniazzi, A.A. Haasz, P.C. Stangeby, "The Effect of Adsorbed Carbon and Sulphur on Hydrogen Permeation Through Palladium", J. Nucl. Mater., 162-163, 1065 (1989).

[13] S. Yan, H. Maeda, K. Kusakabe, S. Morooka, "Thin Palladium Membrane Formed in Support Pores by Metal Organic Chemical Vapor Deposition Method and Application to Hydrogen Separation", Ind. Eng. Chem. Res., 33, 616 (1994).

[14] S. Uemiya, N. Sato, H. Ando, Y. Kude, T. Atsuda, E. Kikuchi, "Separation of Hydrogen through Palladium Thin Film Supported on a Porous Glass Tube", J. Membr. Sci., 56, 303 (1991).

[15] R.E. Buxbaum and A.B. Kinney, "Hydrogen Transport through Tubular Membranes of Palladium-Coated Tantalum and Niobium", Ind.Eng.Chem.Res., 35, 530 (1996).

[16] J.E. Kleiner, E.H. Sevilla, R.M. Cotts, "Diffusion of Hydrogen in α-Vanadium Hydride", Phys. Rev. B, 33, 6662 (1986).

[17] D.T. Peterson and C.L. Jensen, "Diffusion of Hydrogen in Niobium-Tantalum Alloys at 296 K", Metall. Trans. A, 11, 627 (1980).

[18] F.C. Gielens, H. D. Tong, C.J.M. Rijn, M.A.G. Vorstman, J.T.F. Keurentjes, "High-flux Palladium-Silver Alloy Membranes Fabricated by Microsystem Technology", Desalination 147, 417 (2002).

[19] Y.S. Lin, "Microporous and Dense Inorganic Membrane: Current Status and Prospective", Sep. Pur. Techno., 25, 39 (2001).

[20] G. Xomeritakis and Y.S. Lin, "CVD Synthesis and Gas Permeation Properties of Thin Palladium/Alumina membranes", AIChE. J., 44, 174 (1998).

[21] H.D. Tong, J.W. Ervin Berenschot, M.J. De Boer, J. G. E. Gardeniers, H. Wensink, H.V. Jansen, W. Nijdam, M.C. Elwenspoek, F.C. Gielens, and C.J.M. Rijn, "Microfabrication of Palladium–Silver Alloy Membranes for Hydrogen Separation", J. Microelectromech. Syst., 12, 622 (2003).

[22] A.J. Burggraaf and L. Cot (Eds), "Fundamentals of Inorganic Membrane Science and Technology", Elsevier, Amsterdam, 1996.

[23] A. Nijmeijer, "Hydrogen Selective-silica Membrane for Use in Membrane Steam Reforming", PhD. thesis, University of Twente (1999).

[24] F. Roa, J.D. Way., R.L. McCormick., S.N. Paglieri., "Preparation and Characterization of Pd-Cu Composite Membranes for Hydrogen Separation", J. Chem. Eng., 93, 11 (2003).

[25] E.J. Harbers and F.C. Gielen, "Optimization of Mass Transfer towards and from a Hydrogen Selective Palladium Membranes", Report, University of Eindhoven, (2001).

[26] V. Jayaraman and Y.S. Lin, "Synthesis and Hydrogen Permeation Properties of Ultrathin Palladium-Silver Alloy Membranes", J. Membr. Sci., 104, 251 (1995).

[27] B. McCool, G. Xomeritakis and Y.S. Lin, "Composition Control and Hydrogen Permeation Characteristics of Sputter Deposited Palladium-Silver Membranes", J. Membr. Sci., 161, 67 (1999).

[28] G. Xomeitakis and Y.S. Lin, "Fabrication of Thin Metallic Membranes by MOCVD and Sputtering", J. Membr. Sci., 133, 217 (1997).

[29] J. Shu, B.E.W. Bongondo, B.P.A. Grandjean and S. Kaliaguine," Surface Segregation of Pd-Ag Membrane upon Hydrogen Permeation," Surf. Sci., 291, 129 (1993).

[30] S. Uemiya, Y. Kude, K. Sugino, N. Sato, T. Matuda, E. Kikuchi, "A Palladium-Porous glass Composite Membrane for Hydrogen Separation", Chem. Lett., 10, 1687 (1988).

[31] K.J. Ali, E.J. Newson, D. Rippin, "Exceeding Equilibrium Conversion with a Catalytic Membrane Reactor for the Dehydrogenation of Methylcyclohexane", Chem. Eng. Sci, 49, 2129 (1994).

[32] R.M. Vos and H. Verweij, "High-Selectivity, High-Flux Silica Membranes for Gas Separation," Science, 279, 1710 (1998).

[33] F.C. Gielens, H. D. Tong, C.J.M. Rijn, M.A.G. Vorstman, J.T.F. Keurentjes, "Influences of Steam and CO_2 on the H_2 Flux of Thin Pd and Pd-Ag Membranes", submitted for publication in Journal of Membrane Science, January (2004).

[34] K.J. Bryden and J.Y. Ying, "Nanostructured Palladium Membrane Synthesis by Magnetron Sputtering", Mater. Scie. Eng A., 204, 140 (1995).

[35] K. J. Bryden and J. Y. Ying, "Thermal Stability and Hydrogen Absorption Characteristics of Palladium-Yttrium Nanoalloys", Acta Mater., 44, 3847 (1996).

[36] H. C. Kim, T. L. Alford, " Improvement of the Thermal Stability of Silver Metallization", J. Appl. Phys., 94, 5393 (2003).

[37] H. C. Kim, T. L. Alford, D. R. Allee, " Thickness Dependence on the Thermal Stability of Silver Thin Films", Appl. Phys. Lett., 81, 4287 (2002).

[38] C.B. Samantaray, A. Dhar, S.K. Ray, "Effects of Post-deposition Annealing on Microstructural and Optical Properties of Barium Strontium Titanate Thin Films Deposited by r.f Magnetron Sputtering", J. Mater. Sci., 12, 365 (2001).

[39] N.Y. Lee, T. Sekine, Y. Ito and K. Uchino, "Deposition Profile of RF-Magnetron-Sputtered $BaTiO_3$ Thin Films", Jpn. J. Appl. Phys. 33, 1484 (1994).

[40] M. Ohring, "The Material Science of Thin films", Academic Press (1991).

[41] R. Lüke, G. Schmitz, T. B. Flanagan and R. Kirchheim, "H-induced Phase Separation in Pd–Pt Alloys as Studied by High Resolution Electron Microscopy", J. Alloys Comp., 330-332, 219 (2002).

[42] L. Liu, Y. Wang, H. Gong, "Annealing Effects of Tantalum Films on Si and SiO_2/Si Substrates in Various Vacuums", J. Appl. Phys., 90, 416 (2001).

[43] S.E. Nam and K.H. Lee, "Hydrogen Separation by Pd Alloy Composite Membrane: Introduction of Diffusion Barrier", J. Membr. Sci., 192, 177 (2001).

[44] S.V. Karnik, M.K. Hatalis and M.V. Kothare, "Towards a Palladium Micro-Membrane for the Water Gas Shift Reaction: Microfabrication

Approach and Hydrogen Purification Results", J. Microelectromech. Syst., 1, 93 (2003).

[45] H.T. Hoang, H.D. Tong, F.C. Gielens, H.V. Jansen, M.C. Elwenspoek, "Fabrication and Characterization of Dual Sputtered Pd–Cu Alloy Films for Hydrogen Separation Membranes", Materials Letters, 58, 525 (2004).

Chapter 7

Conclusions and future research

Abstract

In this final chapter an overview will be given of the most important experimental results obtained in the research presented in this thesis. Then, basis concepts are provided for several future research proposals, including palladium (Pd)-based membrane reactors for (de) hydrogenations, silver (Ag)-based membranes for oxygen separation, and a nanosieve shadow mask for pattern transfer of nanodots, and a nanoslit-mask for patterning (metal) nanowires.

7.1. Conclusions

Chapter 1: Introduction

A short description was given to explain why Pd-based membranes have been extensively studied and used as hydrogen selective membranes in hydrogen separation and in (de) hydrogenation reactions. Also, current and potential applications of pure hydrogen were reported. These applications of pure hydrogen have required the development of methods to extract hydrogen from gas mixtures.

Using Pd-based membranes to separate hydrogen from gas mixtures is a promising technology because it enables a high hydrogen separation flux and a high selectivity for hydrogen over the other gases. Then, the two main types of the conventional Pd-based membranes: self-supporting membranes; and composite type structures were briefly described, pointing out several limitations of these existing membrane types.

Finally, the main goal of this thesis was pointed out: exploring techniques of microfabrication technology to make thin and defect-free Pd-based membranes for hydrogen separation and membrane reactor for (de) hydrogenations.

Chapter 2: Membranes on a <110> silicon wafer

An innovative process for the microfabrication of Pd and Pd-Ag alloy membranes on a <110>-Si frame was developed. Dual sputtering was used to synthesize Pd-Ag alloy films having a thickness between 700 and 1000 nm containing 23 wt% Ag. The films were deposited on the unetched side of the <110> silicon support, and etched free in a final step. This approach is the key point to obtain thin and defect-free membranes.

From the fabrication point of view, the membranes were fabricated by a relatively simple process; the process utilizes only two masks, KOH etching of <110>-Si, and thin film sputter deposition. Anodic bonding of thick glass plates (containing powder blasted flow channels) to both sides of the silicon substrate was used to package the membranes and create a robust module. This was important because the robust membrane module allowed it to be integrated easily into a membrane holder to have gas-tight connections to the outer world.

The mechanical strength of the membrane was found to be adequate; pressures of up to 4 bars at room temperature did not break the 1000 nm Pd-Ag

membrane. However, the fabrication of membranes thinner than 700 nm while maintaining sufficient strength is difficult using the technology presented in this chapter. 700 nm Pd-Ag membrane obtained a high separation flux of ca. 3.6 mol $H_2/m^2.s$ with a minimal selectivity of 1500 for H_2/He at 450 ^oC and 0.83 bar H_2 retentate pressure.

Based on the above results, it is concluded that micron thick and defect-free Pd-based membranes can be fabricated.

Chapter 3: Membranes on a supporting microsieve

Another successful process was developed to fabricate Pd-based membranes with thickness down to 100 nm. The technique uses an additional silicon nitride (SiN) microsieve support to enhance the mechanical strength of the membranes. Again, the deposition of the Pd-based films on a dense and planar support makes defect-free thin membranes possible.

From the fabrication point of view, the fabrication process developed in this chapter is more complicated than that presented in chapter 2 because it requires the use of the SiN microsieve. In addition, this film can only be patterned by dry etching, leading to low fabrication throughput. However, the advantage of this technology is that it allows the fabrication of very thin and strong membranes. For instance, 100 nm thick Pd-Ag membranes can withstand a pressure difference over 2 bars.

The microfabricated membranes obtained high separation fluxes; 500 nm Pd-Ag membrane achieved fluxes of up to 4 mol H_2/m^2s with a minimal selectivity of 1500 for H_2/He. The measurement results show that the surface processes control the hydrogen transport through the membrane. This fact explains why the flux is not much higher than that reported in chapter 2. Based on the fabrication and measurement results, it is concluded that the microsieve technology allows us to fabricate very thin but strong membranes.

Chapter 4: A silicon nitride nanosieve membrane

Nanosieve membranes with a pore diameter below 10 nm are fabricated in an ultrathin micromachined silicon nitride membrane. In this new membrane type, the technology introduced in chapter 3 is adapted to form a nanosieve membrane supported by the microsieve.

The nanosieve membrane possesses adequate mechanical strength, possible high separation flux, and high chemical and thermal stability.

Although the developed nanosieve membranes could not be used in hydrogen separation application, they have a great potential to be used in many applications in different sectors, ranging from as absolute sterile filtration (bacteria as well as viruses), size-exclusion-based separations, templates for nanosensors, and nano shadow masks etc. Therefore, a further research on this membrane is strongly recommended.

Chapter 5: Preparation of Pd-Ag alloy films by a dual sputtering technique

A dual sputtering procedure is developed to synthesize Pd-Ag alloy films with the high composition control. Crack-free Pd-Ag alloy films with high density (non-porous), smooth surface, and fine polycrystalline structures etc. are obtained. These films are very useful to achieve high hydrogen separation fluxes and with high selectivity.

The results suggest that dual sputtering may be a powerful technique to synthesize other alloy films with accurate compositions for different applications.

Chapter 6: Hydrogen separation of the microfabicated membranes

The microfabricated membranes lead to high separation flux as well as high selectivity; fluxes up to 4 mol $H_2/m^2.s$ were measured with a minimal selectivity of 1500 for H_2/He. This flux is approximately one order of magnitude higher than the flux reported in the literature for Pd or Pd-based alloy membranes deposited on porous supports. Several advantages of the microfabricated membranes e.g., a low mass transfer resistance of the supports and a high composition control of the separation film are attributed as the reasons of obtaining such high fluxes. In addition, the membranes show excellent stability at temperatures up to 723 K.

The analysis of the experiments suggests that surface reactions are the limiting step on the whole hydrogen separation process.

The influences of steam and carbon dioxide (CO_2) on the hydrogen separation flux were studied. The fluxes are initially reduced from 35 to 50 % when steam or CO_2 is added. However, the flux recovered to the prior value when CO_2 is removed. Interestingly, the membrane shows a higher flux after the

steam is removed. Separation by steam treated membrane turned out to be limited by diffusion. It is supposed that the steam cleans the membrane surface or makes the surface more active for dissociation of hydrogen molecules to hydrogen atoms. Nevertheless, more experimental data is needed to confirm as well as to explain the steam effects. The investigation of other important poisoning gases like sulfurous and chlorine containing gases on the membrane behavior needs further research.

Hydrogen separation at high temperature from 823 to 873 K is performed. The flux is initially high, but holes in the membranes appear, so they completely lose their selectivity. The hole creation might be attributed for the thermal grain growth, but stress and hydrogen lead to more and large holes. The use of alloy materials that can stabilize against the grain growth is recommended in fabrication of membrane for high temperature applications.

7.2. Future research

7.2.1. Palladium-based membrane reactors

Up to now the application of the developed Pd membranes has been mainly investigated and discussed with respect to hydrogen separation, but the Pd-based membranes can be used as membrane reactors for (de) hydrogenations as well [1-4]. By selectively adding or removing hydrogen from a reaction, the steady-state concentration of reactants and products can be shifted to a more favorable equilibrium conversion [5]. For instance, by continuous adding hydrogen through a Pd membrane in to a membrane reactor Niwa et al. converted a ca. 90% of benzene to a high-value chemical of phenol, compared to the closed-system equilibrium conversion of less than 5% [6]. Moreover, this synthesis process was carried out at relatively low temperatures (150 to 250^{o}C) and at atmospheric pressure.

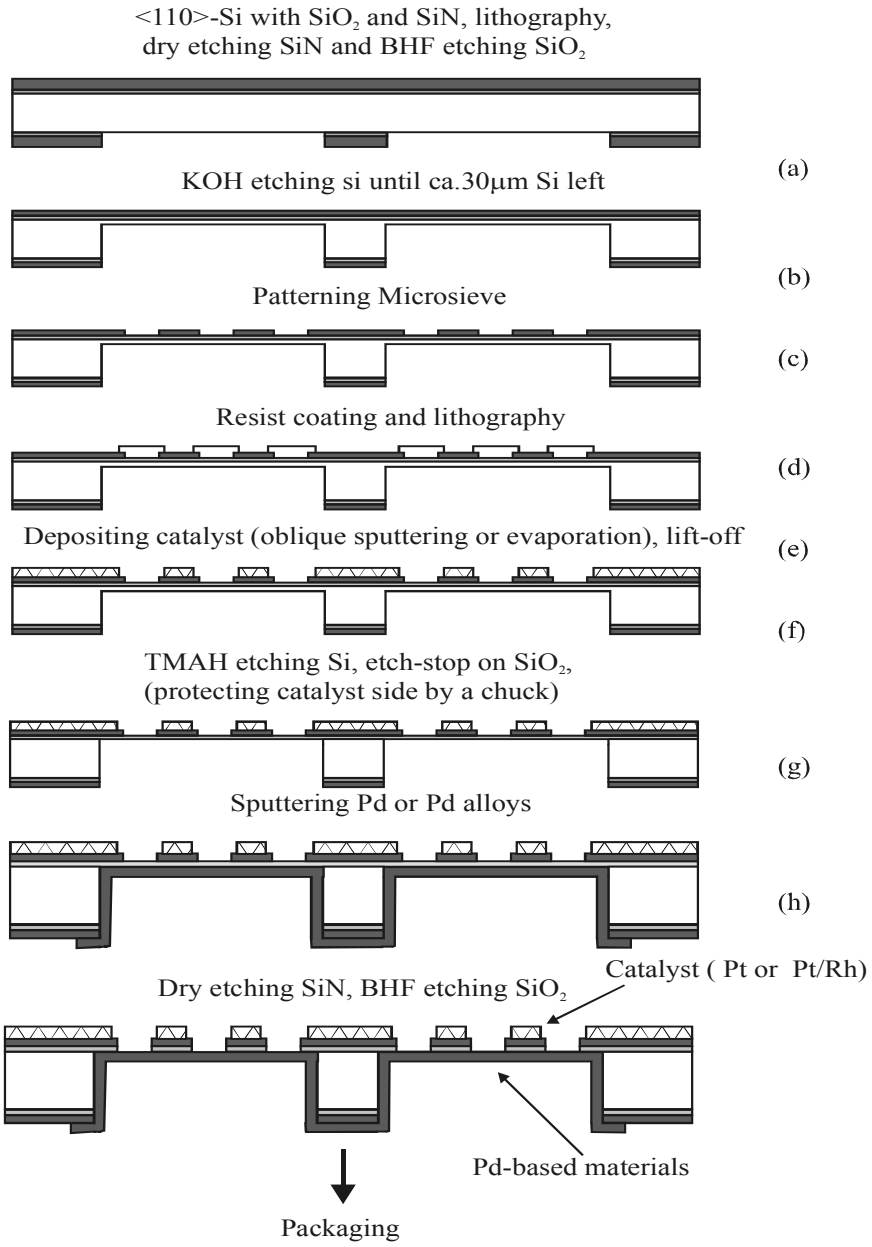

***Figure 7.1**: A process development for a membrane reactor.*

For many reactions, the presence of catalyst(s) within a system is required. Therefore, a membrane reactor is suggested as presented in Figure 7.1. This process scheme does not directly depend on the intended application of the reactor, and is rather similar to that for the microsieve supporting membrane (chapter 3). Nevertheless, there are some notes;

1) In any reaction, the use of catalysts with highly porous structures is desirable, because the porous catalyst has a large contact area, thus increasing the contact between the catalyst and chemicals. We recommend using of an oblique-angle sputtering, or an oblique-angle evaporation [7-10] to deposit the catalyst (Figure 7.1.d), as these techniques can realize the catalyst films with highly porous structures.

2) The use of a tetramethylammonium hydroxide solution (TMAH) for the second silicon removal is recommended (Figure 7.1.e), because TMAH normally does not attack metals [11], and may not poison the catalyst properties. Using a chuck to cover the catalyst side during this step is another option.

3) Because certain Pd-alloys are poisoned by certain gases [12], choosing the right type of alloy for a specific gas mixture is important. For instance Pd-Cu membranes are reported to have a high resistance against sulfurous containing gases [13-14]. Actually, Pd-Cu alloy membranes containing Cu contents between 23 to 40wt% were synthesized in this project [14]. Although the Pd-Cu membranes were tested with respect to the hydrogen separation, testing them with sulfurous containing gases was not conducted due to the limitation of time in the project.

4) Depending on reaction conditions, especially operating temperature, the reactor can be packaged (Figure 7.1.h) with polymers [15], glasses [16-17], or directly inside a stainless steel holder. Packaging the reactor with polymer is simple and cheap, but the device can not work at high temperature, while a glass covered reactor is only able to operate at temperatures below ca. 773 K. If the reactor (without bonding with glass plates) can be directly packaged into the stainless steel holder (Figure 6.9), it will be able to operate at high temperatures, which is one of the important conditions for several reactions to be taken. Actually, several membranes were directly packaged into the stainless steel holder for testing membrane at high temperatures (see section 6.6 chapter 6), but we found out that the membranes were broken quite often. Because it is very important to make reactor that can work at high temperature, a further

research on this subject is highly recommended. Also, it is important to use membrane materials that can stabilize against grain growth (section 6.6).

7.2.2. Silver-based membranes for oxygen separation

In a number of industrial processes, the separation of oxygen from gas mixtures plays an important role [18]. Normally, oxygen is separated from air by distillation at high pressures and low temperature [19]. However, the low energy efficiency of this cryogenic air separation process and the safety risks, which are caused by the presence of pressurized pure oxygen in the system, are major disadvantages.

Alternative ways to separate oxygen from a gas stream are using pressure swing adsorption [20], porous (polymeric and ceramic) membranes [21], and dense membranes [18,22-24]. Among these methods, the use of dense membranes [18,22-24] is a promising technology because it can give high-purity oxygen.

Dense membranes for oxygen separation are commonly based on inorganic oxide ceramics, e.g., mixed-ionic-electronic conducting Perovskites [18,22]. In the last decade, extensive research has been conducted to deposit Perovskite-based films on porous supports, preferably of the same material to avoid compatibility problem, thus forming the membranes for oxygen separation. In addition, this membrane has many applications, including the partial oxidation of light hydrocarbons, e.g., natural gas to value-added products, waste reduction and recovery [18,21]. Unfortunately, inorganic oxide ceramics normally have a coefficient of thermal expansion that is ca. one order of magnitude higher than that of the silicon, so the films of these materials on the silicon-based supports cracks at modest temperature [25]. Therefore, it would be very difficult to obtain defect-free Perovskite-based membranes on the silicon-based supports developed in this thesis.

Another material long known for its permeability to oxygen is silver (Ag). Permeability of oxygen through Ag membranes was first investigated by Johnson and Larose in 1924 [26], then followed by several research groups [27-29]. A mechanism of oxygen permeation through the Ag membrane is similar to that of hydrogen permeation through Pd membrane; in brief: molecular oxygen (O_2) adsorbs on the surface of the Ag surface, dissociates into oxygen atoms (O), then O atom diffuses through the bulk metals, and finally recombines to form oxygen molecules on other side of the membrane.

However, in all the above experiments [26-29], the used membranes were relatively thick Ag plates (200 μm or greater). This membrane thickness considerably limits the oxygen separation flux through the membrane because the flux is inversely proportional with the membrane thickness [27]. Based on our experiences with the development of Pd-based membranes for hydrogen separation in this thesis, we suggest to use the technology developed in this thesis to make thin and defect-free Ag membranes for oxygen separation. In principle, the processes presented in chapters 2 and 3 are both suitable to fabricate the Ag membrane. In addition, Ag alloy membranes should be used, as it has been reported that alloying Ag membrane with several transition metals such as Pt, Pd, Cu, Zn etc. helps to increase both permeability and thermal stability of the membrane [30].

In fact, several membranes of pure Ag, Ag-10 wt% Pd, and Ag-10 wt% Cu with the thickness around 500 nm were made in the supporting microsieves. After fabrication, these membranes were heated up to temperatures of 773 K, and there was no observation of films peeling off from the microsieve support. However, testing membranes for oxygen separation has not been performed yet. Because of the particular interest on the development of dense membrane for oxygen separation, we suggest a further research on this subject.

7.2.3. Nanosieve shadow mask for pattern transfers

7.2.3.1. Dry etching through a nanosieve shadow mask to produce nanosieve membrane

In chapter 4, the SiN nanosieve membrane has been introduced having great potential in several applications in different sectors. For instance, several research groups have interest in the nanosieve membrane with pores size around 20 nm for research in nano-biotechnology etc.
However, the technology to make the nanosieve membrane is time consuming and therefore (very) expensive, mainly due to the use of Focused Ion Beam Etching. Here we suppose a new method that may allow us to fabricate low-cost nanosieve membranes. The principle is shown in Figure 7.2, in which the nanosieve membrane of chapter 4 is used as a shadow mask to transfer its pores to a second SiN membrane by means of dry etching. Note that the transferred pores can be reduced in size by coating them with a second LPCVD SiN layer.

Because of the interest we suggest a further research on this subject.

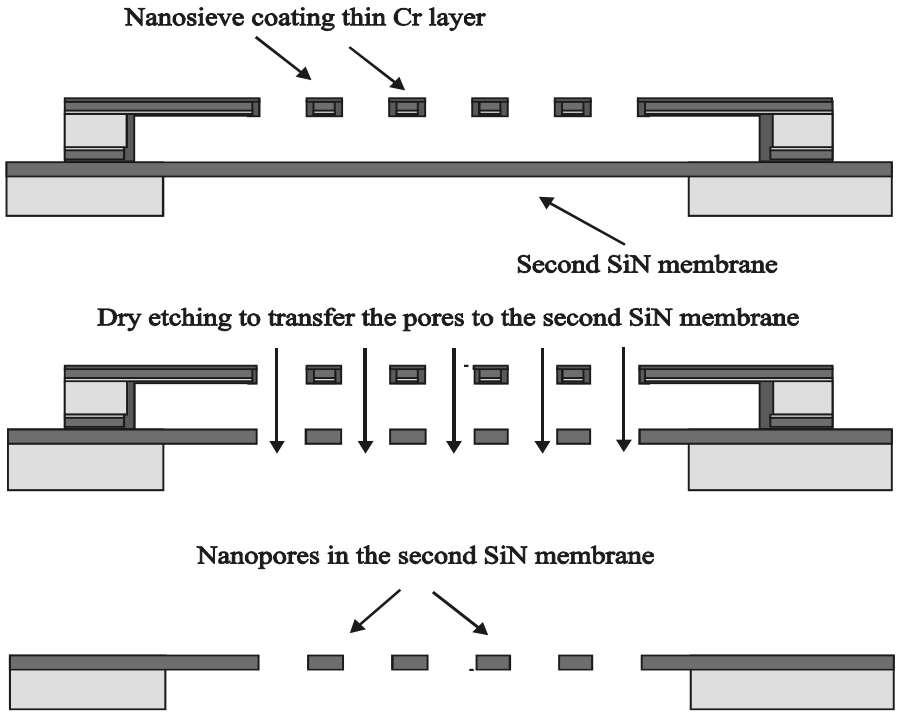

***Figure 7.2**: A nanosieve shadow mask etching.*

7.2.3.2. Nanosieve shadow mask for pattern transfer of nanodots

In the past decade, a variety of new patterning technologies have emerged, which attempt to create nanoscale structures [33-38]. Among these nanoscale structures, dot arrays patterned on the nanometer scale - *nanodots* hold promise for many applications, such as photonic devices [39], DNA or protein electrophoresis [40-41], magnetic data storage, and catalysts [42]. Semiconductor quantum dots have been prepared by several techniques such as molecular beam epitaxy [43], metal organic chemical vapor deposition [44-45], and electron beam lithography [46]. An ordered array of multiple dots has also been formed by way of alumina membranes as evaporation masks [47-48], but feature sizes are still larger than 50 nm. Also, nanosieve membranes with sieve size down to 100 nm have been fabricated by laser interference, and used as evaporation masks for patterning nanodots by the Transducer Science and Technology Group [49].

Generally, the nanodots have been studied at sizes down to 20 to 30 nm although the studying of smaller dots may reveal completely new phenomena. It is probably due to the fact that the fabrication of nanodots with sizes below 20 nm has been remained difficult.

We suggest using the nanosieve membrane of chapter 4 as shadow masks for patterning nanodots with dot sizes down to a few nm.

7.2.4. Nanoslit mask for patterning (metal) nanowires

Recent studies of the electrical and magnetic properties of metal nanowires smaller than 100 nm in diameter have revealed a variety of fascinating properties. For example, gold nanowires smaller than the mean free path of an electron exhibit a depressed conductivity caused by classical boundary scattering [50]. The conductance and yield strength of atomic-scale gold wires are both quantized [51-53]. The shot noise in metal nanowires is suppressed [54] while the thermoelectric figure of merit is enhanced [55-56]. The conductivity of gold nanowires immersed in liquids is reduced by the presence in the liquid of adsorbates such as thiols [57]. These studies suggest that metal nanowires might form the basis for chemical sensors. Bismuth nanowires can have a magnetoresistance of up to 44000 % [58-60]. Finally, arrays of fractured Pd nanowires can function as hydrogen gas nanosensors [61].

Collectively, these exciting results provide motivation for the development of new methods for preparing metal nanowires [62]. Moreover, the synthetic method that produces nanowires that are predisposed to manipulation is of particular interest [62]. We suggest a shadow mask method to produce the nanowires: sputtering (or evaporation) through a nanomembrane with nanoslit structures to form nanowires on a second substrate (see Figure 7.3). In this method the nanoslits in the nanomembrane are aligned to an IC controlling circuit in another silicon wafer, thus obtaining nanowires that are predisposed to manipulation. A strong point of this method is that it enables a wafer scale connection between the nanowires and electronics. In addition, the SiN shadow mask can be treated in several aggressive chemicals to remove “clogging metals” after several sputtering/evaporation runs, thus allowing the shadow mask to be reused.

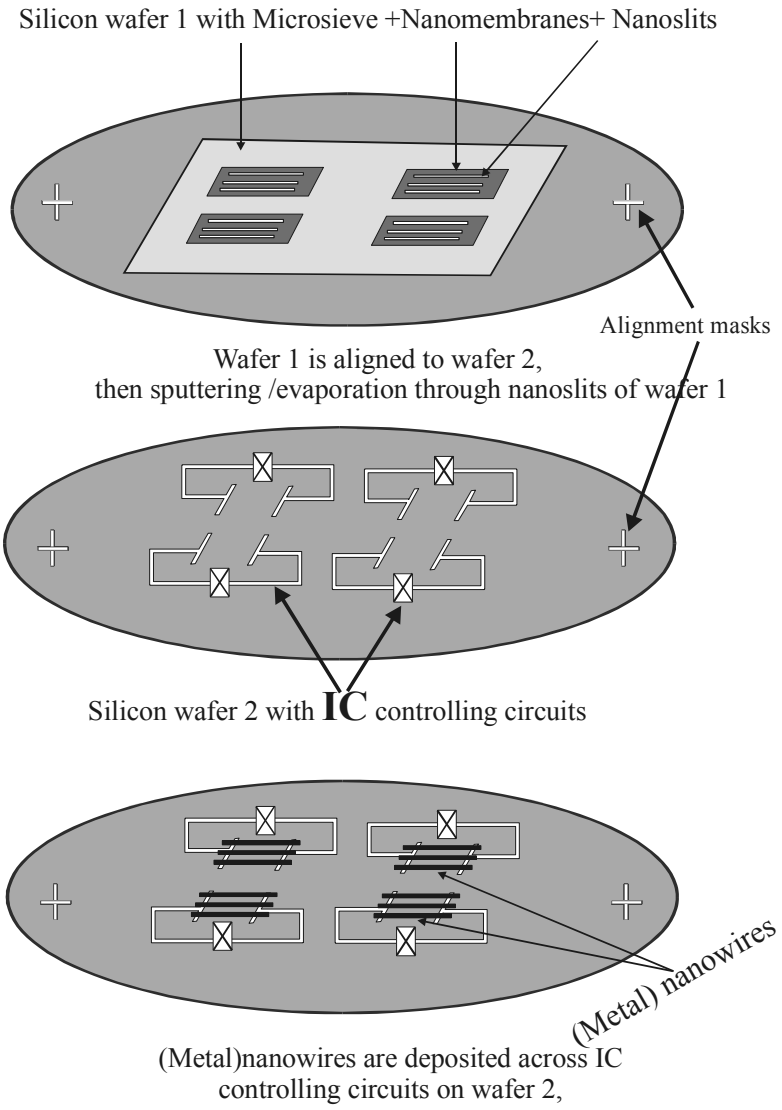

***Figure 7.3**: A principle of patterning metal nanowires through a nanoslit mask.*

7.3. References

[1] C.J.M.van Rijn, "Nano and Micro Engineered Membrane Technology", Elsevier (2004.).

[2] R. Hughes, "Composite Palladium Membranes for Catalytic Membrane Reactors", Membr. Techno., 131, 9 (2001).

[3] N. Toh, AIChe J., 33, 1576 (1987).

[4] H. Weyten, J. Luyten, K. Keizerb, L. Willems, R. Leysen, "Membrane Performance: The Key Issues for Dehydrogenation Reactions in a Catalytic Membrane Reactor", Catal. Today, 56, 3 (2000).

[5] R. Dittmeyer, V. Hollein and K. Daub, "Membrane Reactors for Hydrogenation and Dehydrogenation Processes Based on Supported Palladium", J. Mole. Catal. A., 173, 135 (2001).

[6] S.I. Niwa, M. Eswaramoorthy, J. Nair, A. Raj, N. Itoh, H. Shoji, T. Namba, F. Mizukami, "A One-Step Conversion of Benzene to Phenol with a Palladium Membrane", Science, 295, 105 (2002).

[7] D.L. Bellac, G.A. Niklasson, and C.G. Granqvist, "Angular-Selective Optical Transmittance of Highly Transparent Al-Oxide-Based Films Made by Oblique-Angle Sputtering", J. Appl. Phys., 78, 2894 (1995).

[8] L. Abelmann, P. Berge, J.C. Lodder, and T.J.A. Popma, "Oblique Evaporation of $Co_{80}Ni_{20}$ Part I: Fixed Angle of Vapour Incidence", J. Magn. Soc. Jpn.,18, 291 (1994).

[9] J.A. Thornton, "High Rate Thick Film Growth", Ann. Rev. Mater. Sci., 7, 239 (1977).

[10] M. Ohring, "The Material Science of Thin films", Academic Press (1991).

[11] M.C. Elwenspoek and H.V.Jansen, "Silicon Micromachining", Cambridge, 1999.

[12] F.L. Chen, Y. Kinari, Y. Nakayama, Y. Sakamoto, "Hydrogen Permeation Through Palladium-Based Alloys Membranes in Mixtures of 10% Methane and Ethylene in the Hydrogen", Int J. Hydrogen Energy, 21, 555 (1996).

[13] F. Roa, J.D. Way., R.L. McCormick., S.N. Paglieri., "Preparation and Characterization of Pd-Cu Composite Membranes for Hydrogen Separation", J. Chem. Eng., 93, 11 (2003).

[14] H.T. Hoang, H.D. Tong, F.C. Gielens, H.V. Jansen, M.C. Elwenspoek, "Fabrication and Characterization of Dual Sputtered Pd–Cu Alloy Films

for Hydrogen Separation Membranes", Materials Letters, 58, 525 (2004).

[15] A.J. Frank, K.F. Jensen, M.A. Schmidt, "Palladium Based Membranes for Hydrogen Separation and Hydrogenation/Dehydrogenation", Proc. IEEE. MEMS 99, 382 (1999).

[16] S.V. Karnik, M.K. Hatalis and M.V. Kothare, "Towards a Palladium Micro-Membrane for the Water Gas Shift Reaction: Microfabrication Approach and Hydrogen Purification Results", J. Microelectromech. Syst., 1, 93 (2003).

[17] H.D. Tong, J.W. Ervin Berenschot, M.J. De Boer, J. G. E. Gardeniers, H. Wensink, H.V. Jansen, W. Nijdam, M.C. Elwenspoek, F.C. Gielens, and C.J.M. Rijn, "Microfabrication of Palladium–Silver Alloy Membranes for Hydrogen Separation", J. Microelectromech. Syst., 12, 622 (2003).

[18] H.J.M. Bouwmeester and A.C. Burggraaf, Chapter 10, pp.435-515, "Fundamentals of Inorganic Membrane Science and Technology", Edit. By A.C. Burggraaf and L. Cot, Elsevier: Amsterdam (1996).

[19] I.P. Usyukin, " Plant and Machinery for the Separation of Air by Low Temperatures Methods", Pergamon Press (1965).

[20] M.D. Ruthven, "Pressure Swing Adsorption", VCH Publishers (1993).

[21] A.R. Smith and J. Klosek, "A Review of Air Separation Technologies and Their Integration with Energy Conversion Processes", Fuel Processing Technology, 70, 115 (2001).

[22] H.J.M. Bouwmeester, "Dense Ceramic Membrane for Methane Conversion", Catal. Today., 82, 141 (2003).

[23] C.S. Chen, S.J. Feng, S. ran, D.C. Zhu, W. Liu, H.J.M. Bouwmeester, "Conversion of Methane to Syngas by a Membrane-Based Oxidation-Reforming Process", Angew. Chem. Int. Ed., 42, 5196 (2003).

[24] Edward A.F. Span, "Oxygen-Permeable Perovskite Thin-Film Membranes by Pulsed Laser Deposition", PhD. Thesis, University of Twente (2001).

[25] Private Communication with Edward A.F. Span (2002).

[26] F.M.G. Johnson and P. Larose, "The Diffusion of Oxygen Through Silver" (1924).

[27] V.M. Gryaznov, S.G. Gulyanova, S. Kanizius, "Diffusion of Oxygen Through a Silver Membrane", Russian J. Phys. Chem., 47, 1517 (1973).

[28] R.A. Outlaw, W.K. Peregoy, G.B. Hoflund, "Permeation of Oxygen Through High Purity, Large Grain Silver", NASA: Hampton, VA 23665-5255, 1(1987).

[29] R.A. Outlaw, S.N. Sankaran, G.B. Hoflund, "Oxygen-Transport Through High-Purity, Large-Grain Silver", J. Mater. Res., 3, 1378 (1988).

[30] J. Bergwerff, "The Interaction of Oxygen with Silver: A Survey on the Molecular Processes in the Passage of O_2 Through a Silver Membrane", Internal Report, Catalyst Group, Chemical Department, Utrecht University (2002).

[31] M.J. De Boer, J.G.E. Gardeniers, H.V. Jansen, M.J. Gilde, G. Roelofs, J.N. Sasserath, and M.C. Elwenspoek, "Guidelines for Etching Silicon MEMS Structures Using Fluorine High Density Plasmas at Cryogenic Temperatures," J. Micromech. Syst., 11, 385 (2002).

[32] H.V. Jansen, "Plasma Etching in Microtechnology", PhD Thesis, University of Twente (1996).

[33] Y. Xia, G.M. Whitesides, "Soft Lithography", Angew. Chem., Int. Ed., 37, 550 (1998).

[34] K. Lee, S. Park, C.A. Mirkin, J.C. Smith, M. Mrksich, "Protein Nanoarrays Generated by Dip-Pen Nanolithography", Science 295, 1702 (2002).

[35] G.M. Wallraff, W.D. Hinsberg, "Lithographic Imaging Techniques for the Formation of Nanoscopic Features", Chem. Rev., 99, 1801, (1999).

[36] S.I. Stupp, V. LeBonheur, K. Walker, L. Li, K. Huggins, M. Keser, A. Amstutz, " Supramolecular Materials: Self-Organized Nanostructures", Science 276, 384(1997).

[37] C.R. Martin, "Nanomaterials: A Membrane-based Synthetic Approach", Science 266, 1961(1994).

[38] S.S. Wong, E. Joselevich, A.T. Woolley, C.L. Cheung, C.M. Lieber, "Covalently Functionalized Nanotubes as Nanometre-sized Probes in Chemistry and Biology", Nature 394, 52 (1998).

[39] B.R. Chalamala, B.E. Gnade, "Fed up with Fat Tubes", IEEE Spectrosc., 35, 42(1998).

[40] W.D. Volkmuth, R.H. Austin, "DNA Electrophoresis in Microlithographic Arrays", Nature 358, 600 (1992).

[41] W.D. Volkmuth, T. Duke, M.Wu, R.H. Austin, A. Szabo, "DNA Electrodufusion in a 2D Array of Posts", Phys. Rev. Lett., 72, 2117(1994).

[42] R.M. Bright, D.G. Ealter, M.D. Musick, M.A. Jackson, K.J. Allison, M.J. Natan, "Chemical and Electochemical Ag Deposition onto Preformed Au Colloid Monolayers: Approches to Uniformly sized Surface Features with Ag-like Optical Properties", Langmuir, 12, 812(1996).

[43] Q. Xie, A. Madhukar, P. Chen, N.P. Kobayashi, "Vertically Self-organized InAs Quantum Box Islands on GaAs(100)", Phys. Rev. Lett., 75, 2542 (1995).

[44] R.R. Li, P.D. Dapkus, M.E. Thompson, W.G. Jeong, C.P. Harrison, M. Chaikin, R. Register, D.H. Adamson, "Dense Arrays of Ordered GaAs Nanostructures by Selective Area Growth on Substrates Patterned by Block Copolymer Lithography", App. Phys. Lett., 76, 1689(2000).

[45] F.M. Heinrichsdorff, A.O. Kosogov, P. Werner, "Room-Temperature Continuous-Wave Lasing from Stacked InAs/GaAs Quantum Dots Grown by Metal Organic Chemical Vapor Deposition", Appl. Phys. Lett., 71, 22(1997).

[46] T. Ishikawa, S. Kohmoto, K. Asakawa, "Site Control of Self-organized InAs Dots on GaAs by In Situ Electron-beam Lithography and Molecular-beam Epitaxy", Appl. Phys. Lett., 73, 1712 (1998).

[47] H. Masuda, K. Yasui, K. Nishio, " Fabrication of Ordered Arrays of Multiple Nanodots using Anodic Porous Alumina as an Evaporation Mask", Adv. Mater.,12, 1031 (2000).

[48] H. Masuda and K. Fukuda, "Ordered Metal Nanohole Arrays Made by a Two-step Replication of Honeycomb Structures of Anodic Alumina ", Science 268, 1466 (1995).

[49] C.J.M. van Rijn, G.J. Veldhuis and S. Kuiper, "Nanosieves with microsystem technology for microfiltration applications", Nanotechnology, p. 343 (1998).

[50] C. Durkan, M. E. Welland, "Size Effects in the Electrical Resistivity of Polycrystalline Nanowires", Phys. Rev. B, 61, 14215 (2000).

[51] J. M. Krans, C. J. Muller, I. K. Yanson, T. C. M. Govaert, R. Hesper, J. M. Vanruitenbeek, "One-Atom Point Contacts", Phys. Rev. B, 48, 14721 (1993).

[52] C. J. Muller, J. M. Krans, T.N. Todorov, M.A. Reed, "Quantization Effects in the Conductance of Metallic Contacts at Room Temperature", Phys. Rev. B, 53, 1022 (1996).

[53] J. I. Pascual, J. Mendez, J. G. Herrero, A.M. Baro , N. Garcia, U. Landman, W. D. Luedtke, E. N. Bogachek, H. P. Cheng, Science, 267, 1793 (1995).

[54] M. Henny, S. Oberholzer, C. Strunk, C. Schnenberger, "1/3-Shot-Noise Suppression in Diffusive Nanowires", Phys. Rev. B, 59, 2871 (1999).

[55] O. Rabina, Y. M. Lin, M. S. Dresselhaus, "Anomalously High Thermoelectric Figure of Merit in $Bi_{1-x}Sb_x$ Nanowires by Carrier Pocket Alignment", App. Phys. Lett., 79, 81(2001).

[56] X. Sun, Z. Zhang, M. S. Dresselhaus, "Theoretical Modeling of Thermoelectricity in Bi Nanowires", App. Phys. Lett., 74, 4005 (1999).

[57] A. Bogozi, O. Lam, H. X. He, C. Z. Li, N. J. Tao, L. A. Nagahara, I. Amlani, R. Tsui, "Molecular Adsorption onto Metallic Quantum Wires", J. Am. Chem. Soc., 123, 4585 (2001).

[58] F. Y. Yang, G. J. Strijkers, K. Hong, D. H. Reich, P. C. Searson, C. L. Chien, "Large Magnetoresistance and Finite-Size Effect in Electrodeposited Bismuth Lines", J. Appl. Phys., 89, 7206 (2001).

[59] C. L. Chien, F. Y. Yang, K. Liu, D. H. Reich, P. C. Searson, "Very Large Magnetoresistance in Electrodeposited Single-Crystal Bi Thin Films", J. Appl. Phys., 87, 4659 (2000).

[60] K. Liu, C.L. Chien, P.C. Searson, Y.Z. Kui, "Giant Positive Magnetoresistance in Arrays of Semi-Metallic Bismuth Nanowires", IEEE. Trans. Magn., 34, 1093 (1998).

[61] F. Favier, E. C. Walter, M. P. Zach, T. Benter, R. M. Penner, "Hydrogen Sensors and Switches from Electrodeposited Palladium Mesowire Arrays" Science, 293, 2227 (2001).

[62] E.C. Walter, M.P. Zach, F. Favier, B.J. Murray, K. Inazu, J.C. Hemminger, and R.M. Penner, "Metal Nanowire Arrays by Electrodeposition", J. Chem. Phys. Chem., 4, 131 (2003).

Publications

Journal papers

1. **Hien D. Tong,** H.V. Jansen, J.W. Berenschot, M.J. De Boer, J. G. E. Gardeniers, H. Wensink, W. Nijdam, M.C. Elwenspoek, F.C. Gielens, and C.J.M. van Rijn, "Microfabrication of Palladium–Silver Alloy Membranes for Hydrogen Separation", *Journal of Microelectromechanical System*, vol., 12, pp. 622-630, 2003, (chapter 2, microfabrication).
2. **Hien D. Tong**, F.C. Gielens, H.V. Jansen, J. G. E. Gardeniers, C.J.M. van Rijn, M.C. Elwenspoek, "Microfabrication of Palladium-Silver Alloy Membrane Module for Hydrogen Separation", *Submitted* for publication in *Journal of American Institute of Chemical Engineering*, December 2003, (chapters 2+6).
3. **Hien D. Tong**, F.C. Gielens, H.V. Jansen, J. G. E. Gardeniers, W. Nijdam, C.J.M. van Rijn, M.C. Elwenspoek, "Microfabricated Palladium-Silver Alloy Membranes and their Application in Hydrogen Separation", *Industrial and Engineering Chemistry Research*, (in press, 2004), (chapter 3).
4. **Hien D. Tong**, F.C. Gielens, H.V. Jansen, J. G. E. Gardeniers, J.W. Berenschot, M.J. De Boer, C.J.M. van Rijn, M.C. Elwenspoek, " Microsieve Supporting Palladium–Silver Alloy Membranes and Their Application to Hydrogen Separation", Accepted for publication in *Journal of Microelectromechanical System*, 2004 (chapters 1+3+6).
5. **Hien D. Tong**, H.V. Jansen, J.W. Berenschot, V.J. Gadgil, C.G. Bostan, C.J.M. van Rijn, M.C. Elwenspoek, "A Silicone Nitride Nanosieve Membrane", *Nanoletters*, vol., 4, pp. 283-287, 2004 (chapter 4).
6. **Hien D. Tong**, F.C. Gielens, H.V. Jansen, J. G. E. Gardeniers, M.C. Elwenspoek, "Preparation and Characterization of a Dual Sputtered Pd-Ag Alloy Film and Its Application in Hydrogen Separation Membrane", *Submitted* for publication in *Journal of Thin Solid Films*, January, 2004 (chapter 5, Pd-Ag membrane).
7. H.T. Hoang, **Hien D. Tong**, F.C. Gielens, H.V. Jansen, M.C. Elwenspoek, "Fabrication and Characterization of Dual Sputtered Pd–Cu Alloy Films for Hydrogen Separation Membranes", *Materials Letters*, 58, pp. 525-528, 2004 (chapter 5, Pd-Cu membrane).

8. F.C. Gielens, **Hien D. Tong**, C.J.M. Rijn, M.A.G. Vorstman, J.T.F. Keurentjes, "High-flux Palladium-Silver Alloy Membranes Fabricated by Microsystem Technology", *Desalination***,** 147, pp. 417-420, 2002 (chapter 6).
9. F.C. Gielens, **Hien D. Tong**, C.J.M. van Rijn, M.A.G. Vorstman, J.T.F. Keurentjes, "Microsystem Technology for High-Flux Hydrogen Separation membranes", Accepted for publication in *Journal of Membrane Science*, 2004 (chapter 6).
10. F.C. Gielens, **Hien D. Tong**, C.J.M. Rijn, M.A.G. Vorstman, J.T.F. Keurentjes, "Influences of Steam and CO_2 on the H_2 Flux of Thin Pd and Pd-Ag Membranes", *Submitted* for publication in *Journal of Membrane Science*, January, 2004 (chapter 6).

Conference papers

11. **Hien D. Tong**, F.C. Gielens, J.W. Berenschot, M.J. De Boer, J. G. E. Gardeniers, H.V. Jansen, W. Nijdam, C.J.M. van Rijn, M.C. Elwenspoek, " Fabrication and Characterization of MEMS Based Wafer-Scale Palladium-Silver Alloy Membrane for Hydrogen Separation and Hydrogenation/Dehydrogenation Reactions", Proc. of the 15th IEEE International Conference on Micro Electro Mechanical Systems, MEMS 2002, pp. 268-271 (chapter 2).
12. **Hien D. Tong**, F.C. Gielens, J.W. Berenschot, M.J. De Boer, J. G. E. Gardeniers, H.V. Jansen, W. Nijdam, C.J.M. van Rijn, M.C. Elwenspoek, "Hydrogen Separation Module based on Wafer Scale Micromachined Palladium-Silver Alloy Membranes", Proc. of IEEE Transducers 2003, pp. 1742-1745 (chapter 3).
13. **Hien D. Tong**, F.C. Gielens, H.T. Hoang, H.T, J.G.E. Gardeniers, H.V. Jansen, W. Nijdam, C.J.M. van Rijn, M.C. Elwenspoek, "Thin, Strong and Defect Free Microfabricated Palladium Composite Membranes for Hydrogen Separation", Proc. of International Conference on Microreaction Technology (IMRET 7), pp.343-345, 2003 (chapters 2+3).
14. **Hien D. Tong**, F.C. Gielens, H.T. Hoang, H.T, H.V. Jansen, M.C. Elwenspoek, "Preparation of a Dual Sputtering PD-Cu Alloy Film and Its Application in Hydrogen Separation", Proc. of MME Conference, 2003, pp. 127-130 (chapter 5).
15. **Hien D. Tong**, F.C. Gielens, .J.W. Berenschot, M.J. De Boer, J. G. E. Gardeniers, H.V. Jansen, W. Nijdam, C.J.M. van Rijn, M.C. Elwenspoek

"Micromachined Palladium-Silver Alloy Membranes for Hydrogen Separation", SeSens Conference, pp. 688-691, 2002.
16. F.C. Gielens, **Hien D. Tong**, C.J.M. van Rijn, M.A.G. Vorstman, J.T.F. Keurentjes, " High Flux Palladium-Silver Alloy Membranes Fabricated by Microsystem Technology", Oral presentation at International Congress on Membrane Science (ICOM), 2002 (chapters 2 +3+6).
17. F.C. Gielens, **Hien D. Tong**, C.J.M. van Rijn, M.A.G. Vorstman, J.T.F. Keurentjes; "High Flux Hydrogen Selective Palladium and Palladium-Silver Membranes Fabricated by Microsystem Technology", Oral presentation at International Conference on Inorganic Membrane (ICIM), 2002 (chapter 3+6).
18. F.C. Gielens, **Hien D. Tong**, M.A.G. Vorstman, J.T.F. Keurentjes " Influence of CO_2 and Steam on High-flux H_2 Selective Pd Membranes Manufactured with Microsystem Technology", Proc. of International Conference on Microreaction Technology (IMRET 7), pp. 170-172, 2003 (chapter 6).

Other publications

19. **Hien D. Tong**, R.A.F. Zwijze, J.W. Berenschot, R.J. Wiegerink, G.J.M. Krijnen, M.C. Elwenspoek, "Platinum Patterning by a Modified Lift-off Technique and Its Application in a Silicon Load Cell", *Sensors and Materials*, vol. 13, pp. 235-246 (2001).
20. **Hien D. Tong**, C. D. Nguyen, H.N. Vu: " Electrochemical Etch Stop of P-N Junction Silicon in KOH Solution", *Journal of Viet Nam Physics Communication*, vol., 8, pp.171-176 (1998).
21. **Hien D. Tong**, R.A.F. Zwijze, J.W. Berenschot, R.J. Wiegerink, G.J.M. Krijnen, M.C. Elwenspoek, "Characterization of Platinum Lift-off Technique", Proceeding of SeSens Conference, The Netherlands, pp. 697-702, 2000.
22. R.A.F. Zwijze, R.J. Wiegerink, G.J.M. Krijnen, **Hien D. Tong**, M.C. Elwenspoek, "Design and Realization of a Miniature Capacitive Silicon Force Sensor for Loads up to 500 kg", Proc. of 2000 IMECE MEMS Symposium of the ASME International, 2000.

Acknowledgements

There are many people to thank for their support and encouragement, without which my Ph.D. at the University of Twente would have not been possible.

First of all, I would like to thank my promotor, Prof. Dr. Miko Elwenspoek, who provided the chance for me to work on the project, which resulted in this thesis. Miko, I thank you very much for your general guidance, encouragement, and continuous support during my Ph.D. research.

Next, I wish to thank the assistant-promotor, Dr. ir. Henri Jansen. Henri, thank you very much for your enthusiastic guidance, for the numerous fruitful discussions, and critical reading and correcting of the thesis manuscript.

I also wish to thank my former assistant-promotor, Dr. Han Gardeniers, for his guidance in the first period of the project as well as his continuous support afterwards.

As the research described in this thesis is a result of a corporation between the two research groups; the Transducers Science and Technology Group of the University of Twente; and the Process Development Group of the University of Eindhoven, I deeply express my thanks to the second research team in Eindhoven, headed by Prof. Dr. Ir. Jos T.F. Keurentjes. Jos and Marius, thank you very much for your formulation and managing the project in Eindhoven. Frank, I enjoy very much our collaborations during the past four years; I could not express my thanks to you for the work you have done in our corporation research.

I thank Meint de Boer and Erwin Berenschot for their technical help. Meint and Erwin, I highly appreciate your expertise in developing a new device process as well as solving my device process problems.

I would like to express my thanks to Dr. ir. Cees J.M Van Rijn and Wietze Nijdam from Aquamarijn for their project formulation and their help in and out of my research during the past four years.

I thank several researchers at the university of Twente; Jisk Holleman and Tom Aarnink (SC), Frederic Mertins (IMS), Ben Mentink (Aqamarijn), Cazimir Bostan, Gabriel Sengo, and Anton Hollink (IOMS)… for their kind help, research corporation, or friendship during the time I stay at Twente.

I address my acknowledgements to the Dutch Technology Foundation (STW) for mainly financial support, and to ABB LUMMUS GLOBAL INC., DSM and Aquamarijn for their contributions.

I would like to express my appreciation to the members of the Graduation Committee for their presents and comments.

Before I started the "Membrane project", I worked with a "Silicon load-cell team". Together with Gijs Krijnen, Remco Wiegerink, and Robert Zwijze, I was involved in the design and fabrication of the silicon load cell. I shall specially thank the team members for their guidance and kind help, particularly in the first period when I studied in The Netherlands.

To all (former) members of the Transducers Science and Technology Group (MICMEC); MiKo Elwenspoek, Gijs Krijnen, Han Gardeniers, Henri Jansen, Remco Wiegerink, Theo Lammerink, Meint de Boer, Erwin Berenschot, Dick Ekkelkamp, Henk van Wolferen, Remco Sanders, Judith Beld, Ingrid Boers, Rik Deboer, Roald Tiggelaar, Joost van Honschoten, Toon Kuijpers, Jeroen Haneveld, Saravanan, Szabolcs Deladi, Edin Sarajlic, Luis J. Fernandez, Boudewijn de Jong, Nguyen Quoc Duy, Laura Vargas, Hoang Thi Hanh, Imran Fazak, Vitaly Svetovoy, Niels Tas, John van Baar, Hen Wensink, Marcel Dijkstra, Marko Blom, Willem Tjerkstra, Stephan Schlautmann, Theo Veenstra, Mink Hoexum, Edwin Oosterbroek, Pele Leussink, Jasper Nijdam, Robert Zwijze, Stein Kuiper, Zakaria Moktadir, Florian Lim…: Thank you very much ***ALL MICMECERS*** for your creating and an enjoyable working environment. I shall never forget a funny atmosphere at the MICMEC coffee corner.

The (former) staff in MESA$^+$ Lab. and CMO Lab. are acknowledged for their technical support; Bert Otter, Gerard Roelofs, Johnny Sanderink, Eddy Ruiter, Huib van Vossen, Arie Koy, Hans Mertens, Samantha Geerdink, Rene Wolf, Peter Linders, Marion Groen, Albert van den Berg, Enrico Keim, Mark Smithers, and Vishwas Gadgil.

Before doing Ph.D. at the University of Twente, I had studied at the International Training Institute for Materials Science (ITIMS), Hanoi, Viet Nam. I would like to express my deep gratitude to Prof. Dr. Nguyen Duc Chien and Dr. Vu Ngoc Hung, who were my former supervisors during my early research at ITIMS. The constant support from them as well as from other members of the ITIMS; Prof. Dr. Than Duc Hien, Prof. Dr. Nguyen Phu Thuy… during my study in the Netherlands is greatly appreciated.

To my Vietnamese friends in Twente, Amsterdam, Delft, and around the world; Ha-Hanh-Hoang Anh, Hieu-Lam-Trung, Viet-Nga-Minh Anh, Phuong-Ha-Hung, Kim-Van Anh, Giang-Chi, Duy-Chi, Thang-Mai, Viet Anh, Tu, Kieu An, Long, Kien, Hoa, Vinh, Toan, Duong, Huy, Chinh, Khuong, Hung, Dung, Duc, Bao, Nghiep, Cuong, Hai, Thai, Minh, Loan, Ha, Tuan…: Thank you all for your friendship and care during the years.

I wish to express my gratitude to my mother, sister, and brother-in-law for their understanding, and all my relatives in Vietnam for their love and care.

My most grateful worlds are expressed to my parents, my sister and brother for their whole life support and love that they have given me.

Last but certainly not least, I thank my wife Quynh Nhu for her patience love and sacrifices, which she has done for me since the years; and my daughter Quynh Anh - a little busy maker - for the joys she has given me.

Enschede, 20 April 2004

Tong Duy Hien

Biography

Tong Duy Hien was born in Thai Binh, Vietnam on January 30th, 1973**.** He received his first Engineering Degree in Chemical Engineering from Hanoi University of Technology in 1995.

In 1997 he received his M.Sc. Degree in Materials Science at Hanoi International Training Institute for Materials Science (ITIMS). His M.Sc thesis dealt with a fabrication of pressure sensors by MEMS. After graduation he worked as a research scientist at ITIMS till March 1999.

Since April 2000, he has worked at the Transducers Science and Technology Group in MESA^{+} Research Institute, University of Twente, The Netherlands, where he completed his Ph.D. research. He has successfully developed microfabicated-based methods to fabricate new membranes for gas and liquid separations.